LACUSTRINE EVIDENCE FROM MOTHER GOOSE LAKE OF HOLOCENE GEOTHERMAL ACTIVITY AT MOUNT CHIGINAGAK, ALASKA PENINSULA

BY: CHRISTOPHER MICHAEL KASSEL

A Thesis

Submitted in Partial Fulfillment

of the Requirements for the Degree of

Master of Science

in Geology

Northern Arizona University

May 2009

Approved:

_____

Darrell S. Kaufman, Ph.D., Chair

_____

Michael Ort, Ph.D.

_____

Roderic A. Parnell Jr., Ph.D.

_____

Mary Reid, Ph.D.

ABSTRACT

LACUSTRINE EVIDENCE FROM MOTHER GOOSE LAKE OF HOLOCENE GEOTHERMAL ACTIVITY AT MOUNT CHIGINAGAK, ALASKA PENINSULA

CHRISTOPHER MICHAEL KASSEL

Geochemical properties of sediment and water from Mother Goose Lake, Alaska Peninsula, were used to reconstruct the major late Holocene geothermal events of Mt. Chiginagak, an ice-capped volcano within the headwaters of the lake. In 2005, geothermal activity melted most of the glacier cover at the summit of the volcano, which generated an acidified crater lake that spilled into Mother Goose Lake, 18 km to the northwest. The slurry pH of Mother Goose Lake sediment deposited during this event was similar to the overlying acidified water (~pH 3), indicating that slurry pH reflects the pH of the lake at the time of deposition. Acidification events can also affect the physical properties and the elemental composition of sediment deposited during the acidification. To characterize the composition of the lake two years following the acidification, 22 water samples and five water profiles were analyzed for temperature, pH, conductivity, oxidation-reduction (redox) potential, and total, ferric and ferrous iron contents. Mother Goose Lake is well-mixed, oxidized, fresh and approaching neutral pH, except in small, cold, acidic, conductive, reduced interflows near the inflow. Twelve sediment cores were collected to determine if the lake had experienced previous geothermally-induced acidifications. A surface core (MG06-1B) and a percussion core (MG07-6) were selected

for detailed chemical analyses based on their mostly laminated, uniquely undisturbed stratigraphy and were dated using $^{239+240}$Pu and ^{14}C methods. The sediment structure, color, magnetic susceptibility (MS), locations of tephra, loss on ignition (31 samples), bulk density (31 samples), concentration of active iron (31 triplicate samples by flame atomic adsorption spectrometry (FAAS)), bulk elemental chemistry (22 samples by FAAS), grain-surface chemistry (34 samples by electron dispersive spectroscopy (EDS)), and slurry pH (494 samples) were analyzed. Only slurry pH and the grain-surface concentration of S show differences between sediment deposited during the 2005 acidification and sediment deposited during presumably typical conditions. The majority of the sediment is of 5YR or 10YR Munsell colors. Magnetic susceptibility typically is less than 100-200 x 10^{-6} SI, except for tephra. Active iron varies between 1.2 and 9.1%. EDS indicates S is most abundant on sediment deposited during 2005. Slurry pH ranges from 3.24 to 6.67 and is the most feasible method of producing a high-resolution record (~6 year contiguous sample spacing) of acidifications in Mother Goose Lake. However, redox reactions were shown to slightly affect slurry pH. Therefore, equal parts of coexisting reduced and oxidized sediment were included in each sample, producing slurry pH values approximately equal to lake water values. Because only a geothermal event can overcome the bicarbonate buffering capacity of the lake, periods when slurry pH was below pH 4.4 indicate geothermally-induced acidification events. Based on slurry pH, at least seven such events have impacted the lake over the last ~3800 years, including the event in 2005. Only one of these seven pH-indicated events was associated with one of the 54 tephra; consequently, most events were probably initiated by non-explosive geothermal activity of Mt. Chiginagak.

ACKNOWLEDGMENTS

I can‘t possibly adequately thank everyone who helped me during this project. Thank you to my advisor, Darrell Kaufman, and committee, Michael Ort, Rod Parnell, and Mary Reid, for support and guidance during this project. My advisor, Darrell Kaufman, and committee member Rod Parnell were especially helpful. Darrell Kaufman was always available for discussions and to make sure that my project was on track. Rod Parnell provided guidance on many geochemical aspects of this project. Both Darrell and Rod, in addition to Heidi Roop, Janet Schaefer (Alaska Volcano Observatory and Alaska Department of Geological and Geophysical Surveys), and Kristi Wallace (Alaska Volcano Observatory) provided amazing field support at Mother Goose Lake. Without their assistance, this project would not have been possible. Janet Schaefer was also instrumental in providing funding. I was very privileged to follow in her, and others‘, steps while working in the shadow of Mt. Chiginagak.

Principal funding for this project was provided by the Alaskan Volcano Observatory and the Alaska Department of Geological and Geophysical Surveys. Additional funding was granted by a Geological Society of America Graduate Research Grant, a Tom and Rose Bedwell Earth Physics Scholarship, and a Friday Lunch Clubbe Award.

I am grateful to my family and friends for helping to make graduate school a more enjoyable experience. My dad, mom, and sister have always been there for me and helped me through many trying times. I can‘t begin to describe how much my fiancée, Megan Beach, has done for me. To all of my friends, thank you. Joanne Best, Chris Bory, Megan Green, Eric Helfrich, Chris Oaks, Steve Rice, Heidi Roop, Rory San

Fillippo, Caleb Schiff, Sheena Styger, and Jari Willing are just a few of the friends with whom I shared many good times during graduate school. Thanks to the Alaska field crews that included Tom Daigle, Eric Helfrich, Kasey Kathan, Darrell Kaufman, Nick McKay, Rod Parnell, Heidi Roop, Janet Schaefer, Caleb Schiff, and Kristi Wallace for fun in Alaska. I am also indebted to John Garver, Don Rodbell, and others at Union College for their friendship and for introducing me to geology.

TABLE OF CONTENTS

LIST OF TABLES

LIST OF FIGURES

CHAPTER 1

INTRODUCTION

Active volcanoes influence the composition of water and sediment in their catchments through processes ranging from eruptions to the passive emission of heat and vapors and subsequent interaction with the surrounding landscape. These processes typically result in local hazards, especially when water is involved. A hazard specific to snow- and ice-capped volcanoes is a geothermal event that generates abundant melt water. This can lead to lahars and floods (e.g. Major and Newhall, 1989), and in some cases, volcanic gases can acidify water throughout the drainage. Although most ice-capped volcanoes are remote from densely populated areas, reconstructing their geothermal history is imperative to evaluating their hazards.

Lakes near volcanoes serve as sedimentary reservoirs that capture erupted particles and are influenced chemically by volcanoes in their watershed. Lacustrine sediment, collected by coring, has been used to deduce histories of volcanic activity from nearby volcanoes by analyzing the stratigraphy of volcanic products. The sediment can be dated by several geochronological methods, potentially producing a detailed, well-dated, and continuous record of the activity of nearby, and sometimes distant, volcanoes.

In this study, the past geothermal activity of ice-capped Mt. Chiginagak, an active stratovolcano on the Alaska Peninsula, was reconstructed by studying the sediment of nearby (~18 km distant) Mother Goose Lake (Figure 1). Mt. Chiginagak is the focus of an on-going hazard assessment by the Alaska Volcano Observatory (AVO). Previous research by Schaefer et al. (2008a) summarized the chemical and hydrological properties of a crater-lake overflow in the summer of 2005 caused by increased geothermal activity.

The 2005 acidification event serves as a case study for the impact of acidified melt water from Mt. Chiginagak in Mother Goose Lake. This event acidified a drainage that includes several creeks, Mother Goose Lake, and its outflow (Figure 2). The frequency of these events prior to 2005 was unknown because they do not leave lasting geological evidence on the volcano. A small lahar on the summit glacier was the only deposition in 2005. No evidence of previous lahars was found. Furthermore, it is not known if all previous events produce an overflow of melt water that exits the crater.

The objective of this study is to reconstruct the history of large acidic hydrologic discharges from Mt. Chiginagak. This was accomplished by: (1) determining the influence of geothermal activity on the water and sediment in Mother Goose Lake, (2) using standard lake sediment coring procedures to recover sediment from Mother Goose Lake, (3) dating the cores, (4) analyzing physical and geochemical properties of the sediment potentially related to geothermal activity and subsequent acidification, and (5) constructing a summary of the timing of past geothermal events. A new method of determining the occurrence of past acidification events in lakes was developed using slurry pH techniques.

Study area

The study area is strongly influenced by volcanism. The subduction of the Pacific plate under Alaska drives volcanism along the Aleutian Arc, including the Alaska Peninsula (Figure 1; Kienle et al., 1981). Ice-capped Mt. Chiginagak is located on the Alaska Peninsula ~ 300 km southwest of Anchorage, Alaska (Figure 1). Mt. Chiginagak is classified as a historically active, minimally monitored, high-threat volcano by the U.S.

Geological Survey (Miller et al., 1998; Ewert et al., 2005). Mt. Chiginagak is surrounded by Quaternary to Permian sedimentary and igneous rocks (Detterman et al., 1983). Its summit rises to 2135 masl, with the upper ~1 km covered in snow and ice. A crater glacier is drained by Indecision Creek on the southern side of the volcano (Figure 3), which is a tributary to Volcano Creek, the major inflow to Mother Goose Lake. Indecision Creek flows through yellow, orange, and red hydrothermally altered lava flows and breccias on the flank of the volcano (Schaefer et al., 2008a).

Mt. Chiginagak has not had a confirmed major historical eruption, but it is hydrothermally and fumarolically active. Mt. Chiginagak has been reported to have had elevated hydrothermal or fumarolic activity in 1852 (Coats, 1950; Powers, 1958; Kisslinger, 1983), 1929 (Jaggar, 1932; Simkin and Siebert, 1994; Miller et al., 1998), 1971 (Miller et al., 1998), 1997 (McGimsey and Wallace, 1999; McGimsey et al., 2007), 2000 (Neal et al., 2004), and 2005 (McGimsey et al., 2007; Schaefer et al., 2008a), with potential minor eruptions in 1929 and 1971 (Jaggar, 1932; Simkin and Siebert, 1994; Miller et al., 1998). The fumarole field on the north flank of Mt. Chiginagak was emitting 200-300 tons per day of SO_2 in 1998 (Schaefer et al., 2008a).

Mother Goose Lake is an ~0.5 km^3, 28 km^2, up to 50-m-deep, well-mixed lake. It occupies a bifurcated trough formed by or enhanced by Pleistocene glacial erosion This erosion is interpreted based on the extent of Pleistocene glacial coverage, the location of the lake, and the <25,000 yr age of the moraine damming the lake (Detterman et al., 1987, Manley and Kaufman, 2002). The major inflow to Mother Goose Lake from Mt. Chiginagak has avulsed at least once between Indecision and Volcano Creeks (Detterman et al., 1983; Schaefer et al., 2008a).

Geothermal activity is known to have melted glacier ice in Mt. Chiginagak's crater at least once (Schaefer et al. 2008a). In early May 2005, ~3.8 x 10^6 m^3 of hydrothermally influenced acidic water streamed out of a lake that formed in Mt. Chiginagak's crater and flowed 27 km down Indecision and Volcano Creeks to Mother Goose Lake, and subsequently into the King Salmon River to the Bering Sea (Figures 1 and 2). Accompanying the acidic overflow from the crater lake were a ~14,500 m^3 lahar and acidic and metal-rich aerosols that damaged 29 km^2 of vegetation along Indecision Creek up to 150 m above stream level. The entire volume of Mother Goose Lake (~0.5 km^3) was acidified to a pH of 3 or less, and by July 2005, a foamy yellowish orange coating, most likely iron hydroxides and colloids, had precipitated along shorelines.

The combination of low pH and high concentrations of toxins was severe enough that salmon have not spawned in the drainage since 2005. After the 2005 event, the pH of water in Mother Goose Lake drainage has slowly increased, but in 2007 was still below levels typical of ecologically healthy lakes (e.g. Burgner et al., 1969). In 2005, sulfate concentrations in surface waters in upper Indecision Creek reached 506 mg/l and 128 mg/l in Mother Goose Lake. Sulfate concentrations were at least 12,800 mg/l in the crater lake when it overflowed (Schaefer et al., 2008a). The pH of the crater lake has never been measured. High concentrations of Al, S, and Fe in the water of Mother Goose Lake drainage are a consequence of the partial neutralization, by aluminoslicate minerals, of metal-laden, low-pH aerosols and water that exited the crater lake in May 2005 (Schaefer et al., 2008).

Background

Aqueous chemistry of acid rock drainage

Most literature regarding the impact of acidification on watersheds is based on the effects of acid mine drainage, which is similar to geothermal acidification. Oxidation of, and percolation of water through, sulfide mine tailings produces sulfate-rich acidic water, which should impact watersheds similarly to the sulfate-rich acidic water that drained from the crater of Mt. Chiginagak in the past, which is further described in Schaefer et al. (2008a).

To understand how elevated geothermal activity at Mt. Chiginagak affects Mother Goose Lake, one must first describe the formation of the aqueous ions involved in transporting and depositing evidence of the event in the lake. Acid rock drainage (ARD) has a low, in some cases negative, pH. A major source of ARD is volcanic discharge (e.g. Sriwana et al., 1998; Armienta et al., 2008; Varekamp, 2008). Volcanic lakes can contain mostly meteoric circum-neutral water to hyper-acidic brines (Varekamp et al., 2000). The variations arise from the degree of influence of volcanic gases and fluids. The primary gases that interact with water in a crater to generate acidity and dissolved or suspended species are SO_2, HCl, and HF (Equations 1-3).

$$3SO_{2(g)} + 3H_2O_{(g)} \Leftrightarrow 2HSO_4^-{}_{(aq)} + 2H^+_{(aq)} + S_{(s)} + H_2O_{(l)} \quad (1a)$$

$$2O_2 + 3SO_{2(g)} + 3H_2O_{(g)} \Leftrightarrow 3HSO_4^-{}_{(aq)} + H^+_{(aq)} + H_2O_{(l)} \quad (1b)$$

$$HCl_{(g)} + H_2O_{(g)} \Leftrightarrow Cl^-_{(aq)} + H^+_{(aq)} + H_2O_{(l)} \quad (2)$$

$$HF_{(g)} + H_2O_{(g)} \Leftrightarrow F^-_{(aq)} + H^+_{(aq)} + H_2O_{(l)} \quad (3)$$

Dissolved species can be magmatic in origin or liberated from water-rock interactions and the subsequent creation of secondary minerals. Secondary species include sulfate

salts and silica (Varekamp et al., 2000). Generally, the ratio of magmatic to secondary species is high for volcanoes with shallow magma bodies and is lower for those with deeper magma bodies, and thus more extensive hydrothermal systems (Giggenbach, 1974; Sigurdsson, 1977; Christenson and Wood, 1993).

Because the extent and depth of Mt. Chiginagak's hydrothermal system is unknown, this study does not focus on secondary minerals. However, during an acidic discharge from Mt. Chiginagak, dissolved H^+, Cl^-, F^-, and suspended S would be transported to Mother Goose Lake through Volcano and Indecision Creeks (Equations 1-3). Along the way, acidic water-rock interaction would liberate Al and Fe species, which would then be oxidized and neutralized due to lake mixing and interaction with bicarbonate and aluminosilicates, causing the deposition of Al and Fe hydroxides and sulfates. Immiscible S would be deposited as detritus. Cl^- and F^- behave conservatively and would likely flush out of the lake (e.g. Varekamp, 2008). H^+ would have partially flushed out of the lake or been neutralized by water-rock interactions, but some would be adsorbed and absorbed onto and into sediment.

Lacustrine sediment as an archive of previous acidification events

Evidence for past lacustrine acidification can be preserved in the sediment that accumulates in lakes, including the pH and the concentration of metals and sulfides in affected sediment and pore water (e.g. Herlihy and Mills, 1985; Ryan and Kahler, 1987; Young and Harvey, 1992; Varekamp, 2008). The pH of sediment analyzed using conventional soil-pH techniques (sediment slurry) is a proxy for the pH of the overlying water at the time of deposition (e.g. Ryan and Kahler, 1987). Acidity is the most

abundant primary product of these reactions (Equations 1-3) and therefore probably the most robust proxy of geothermal activity. Acidified water entering a lake acidifies the pore water at the sediment-water interface. The acidic water is first buffered by the alkalinity of the lake; reactions with minerals, such as kaolinite and smectite, and bacteria in the sediment, further buffer the acidity. These processes result in a pore-water $[H^+]$, and thus sediment-slurry $[H^+]$, that can be several orders of magnitude lower than the $[H^+]$ of the water entering the lake (e.g. Herlihy and Mills, 1986; Sherlock et al., 1995; Stumm and Morgan, 1996). Thus, the pH of sediment slurries reflects the pH of water at the time of sediment deposition, but the acidification signal can be muted by the buffering capacity of the lake water and sediment. Furthermore, seasonal variations in melting snow and ice can dilute acidity in lakes.

Interpreting slurry pH is complicated by oxidation/reduction reactions that occur after burial and in the laboratory after splitting cores. After sediment is buried, it undergoes reduction, which generates alkalinity caused by bacterially mediated reactions with sulfates (e.g. Herlihy and Mills, 1985; Küsel et al., 2001). Furthermore, once a core is split and exposed to air, it begins to oxidize in an environment with much more oxygen than the sediment-water interface. Oxidation of reduced iron releases acidity and lowers the pH of the sediment below the pH of the sediment-water interface. Using slurry pH to reconstruct the pH of the lake requires that the sediment be sampled appropriately to account for the oxidation/reduction reactions that the sediment has undergone since deposition.

Detrital S can be generated, like H+, directly by the interaction of volcanic gases with water (Equations 1-3). Therefore, the concentration of elemental S in Mother Goose

Lake sediment is potentially a robust proxy of geothermal activity. Other forms of S are not as robust proxies. For example, acid-volatile sulfides comprise a fraction of sulfides that is sensitive to changing pH in lacustrine sediment (e.g. Herlihy and Mills, 1985). Acid-volatile sulfides are defined as sulfides that are extractable with cold hydrochloric acid and are primarily represented in sediment as mackinawite and greigite (Leonard et al., 1993). Because of the ease with which these sulfides are oxidized and destroyed, sediment containing them must be kept anoxic and measured immediately after coring (Herlihy and Mills, 1985). Therefore, this potentially useful technique is not appropriate for this study. Other sulfides take much longer to oxidize than acid-volatile sulfides, and elemental S should be relatively stable in lacustrine sediment, making their concentrations better proxies of geothermal activity.

Al and Fe are liberated in secondary reactions of acidity with silicate minerals, and therefore are less robust proxies of geothermal events than primary H^+ and S. However, Al and Fe concentrations in sediment are still potentially useful proxies of geothermal activity. Deposition of acid-sensitive transition metals in sediments decreases in low pH conditions (e.g. Herlihy and Mills, 1985; Fillpek et al., 1987; Ferris et al., 1989; Sriwana et al., 1998). Low pH increases the solubility of select minerals and elements, and lowers the metal-binding ability of microbes that remove metals from solution (e.g. Ferris et al., 1989). Thus, at low pH, precipitation of transition metal is reduced in lakes, whereas at neutral pH values transition metals are more likely to precipitate. As pH rises, transition metals typically precipitate as metal oxyhydroxides, such as amorphous ferric oxyhydroxides and, to a lesser extent, reduced metal sulfides such as Cu_2S and MoS_2 (e.g. Lindsay, 1979). Active iron is an operationally defined

fraction of iron that includes organically bound, colloidal, and other amorphous iron oxides (Chao and Zhou, 1983). Dissolved Fe will precipitate in these forms as the solution containing iron is neutralized. Therefore, active iron is the selective extraction that best targets Fe precipitation caused by rising pH in lake sediment after acidification by ARD.

The lithology of the source area for lacustrine sediment can potentially be inferred from bulk-sediment geochemistry. The majority of the drainage basin for Mother Goose Lake is underlain by sedimentary (including some volcaniclastic) and igneous rocks (Figure 2; Detterman et al., 1983). During geothermally induced melt events, the lake may receive a greater proportion of igneous rocks and secondary volcanic minerals from freshly deposited lahars and crater-lake discharge, and this change should be reflected in the bulk geochemistry of lake sediment. The magnetic susceptibility (MS) (ratio of induced to applied magnetic fields) of sediment is also affected by the source of sediment because of changes in the amount of magnetic minerals (Verosub and Roberts, 1995).

More selective than bulk-sediment geochemistry, and potentially more informative than MS, energy dispersive spectrometry (EDS) provides a semi-quantitative measurement of elemental concentrations in grain exteriors or coatings. ARD minerals rich in transition metals and sulfur may form grain coatings after pH increases (e.g. Varekamp, 2008). EDS can be used to estimate the concentration of pH-sensitive transition metals and S species along transects of sediment core subsamples. However, EDS cannot confidently distinguish if sulfur is present as elemental S, sulfates, or sulfides. A further complication with EDS, and any other elemental analysis, is that transition metals and sulfate/sulfide species are affected not only by pH but also by

oxidation/reduction conditions in the sediment (e.g. Stumm and Morgan, 1996). Therefore, estimates of both the pH and Eh of the water column and the sediment-water interface at the time of deposition are needed to fully understand the dissolution and precipitation of transition metals and sulfate/sulfide species in lacustrine chemical systems.

CHAPTER 2

METHODS

Mother Goose Lake water chemistry

Building on the work of Schaeffer et al. (2008a), water samples were collected and depth profiles were measured in Mother Goose Lake in the summer of 2007. Water collection sites (Figure 4) focused on areas strongly affected by acidified inflow, and at sediment core sites near depocenters, where the general state of the entire lake is better represented.

Water samples were taken from the surface and at depth. Surface samples were either collected in ~3.5 l containers or by pumping from the lake with a peristaltic pump. They were then analyzed and bottled. Samples from depth were collected from water trapped above the surface sediment in gravity cores, or with a Van Dorn water sampler. After setting aside enough water for iron analysis, the water temperature, pH, and conductivity were recorded within 30 min of collection. Iron concentrations as Fe^{2+} and total Fe were measured by the colorimetric 1,10-phenanthroline method within 12 hr of collection, allowing the calculation of Fe^{3+} concentrations by subtraction (Loeppert and Inskeep, 1996).

Water profiles of oxidation-reduction potential, pH, conductivity, and temperature were also recorded. Profiles were measured with an In Situ Inc. Troll 9500 multi-parameter water quality instrument or with a YSI model 6820 multi-parameter monitor. The profiles did not always reach the base of the water column because of limited cable length. Water samples were taken from depths that exhibited large shifts in water properties.

Sediment geochronology and physical characteristics

Sediment cores and geochronology

Water depth was measured across several tracks in Mother Goose Lake with a Lowrance sonar unit in 2006 and 2007, and the profiles were compiled into a bathymetric map (Schaefer et al., 2008b). To reconstruct the sedimentological and chemical history of Mother Goose Lake, sediment cores were taken from six sites in the lake (Figure 5). Cores were taken from depocenters both proximal and distal to the acidic inflow from Volcano Creek.

Five percussion cores and six accompanying surface gravity cores were recovered in water ranging from 31.7 to 48.1 m deep from the two subbasins of Mother Goose Lake during the summer of 2007 (Table 1; Figure 5). In addition, two short cores were recovered in 2006 by Kristi Wallace and Janet Schaefer (Alaska Volcano Observatory). Cores from both years were shipped to Northern Arizona University for cold storage and analysis in the Sedimentary Records of Environmental Change Laboratory.

Organic material from percussion cores MG07-2 and -6 was separated by soaking sediment samples that appeared organic-rich in deionized water, sieving the wet sediment at 150 μm, and then picking and drying the vegetation macrofossils. The material was then analyzed for ^{14}C by the Keck Carbon Cycle AMS Facility at the University of California at Irvine (Table 2). The ages were calibrated to calendar years with CALIB v5.0.1 using the IntCal04 calibration series (Stuiver and Reimer, 1993). After instantaneously deposited tephra thicknesses were subtracted from the sediment depths, an age model for MG07-6 was constructed based on the methodology of Heegaard et al. (2005).

The $^{239+240}$Pu content of samples from surface gravity cores MG06-1B and MG07-12B was measured with an inductively coupled mass spectrometer at Northern Arizona University following the procedure of Ketterer et al. (2002). Pu data were used to locate the 1963-1964 peak [$^{239+240}$Pu] from the fallout from nuclear testing. The surface ages and the depth of the peak [$^{239+240}$Pu] were used to develop an age model for gravity cores as outlined in Ketterer et al. (2002).

Physical properties of Mother Goose Lake sediment

Sediment color, sedimentary structures, magnetic susceptibility, bulk density, and loss on ignition were measured in selected cores. All cores were split and photographed along with Munsell soil color charts within 2 hr of splitting, with constant exposure, lighting, and white-balance settings for each section. The short lapse between splitting and photographing minimized oxidation of the sediment, which allowed accurate color classification of the sediment, although variations in reflected light altered the appearance of some core sections. Sedimentary structures, including massive units, laminated units, and obviously disturbed stratigraphy, were described for all cores. Magnetic susceptibility (MS) was logged along all split core axes at 5 mm intervals using a Bartington MS2 meter with a MS2E surface probe. The locations of tephras in cores containing sediment that appeared largely undisturbed were also recorded. The most prominent tephras were also photographed under a reflected light microscope.

Tephras were classified based on the certainty that they are tephras, without petrographic microscope evaluation. High MS, the presence of visual tephra grains (medium ash to fine lapilli), and color shifts were used to classify the extent to which

each layer could confidently be recognized as tephra. The designations ‗A', ‗B', and ‗C' were used to qualitatively indicate certain, probable, and possible tephras, respectively, based on the above attributes. A tephra was classified as certain if tephra grains comprise ~90% or more of the sample. Probable and possible tephra are composed of ~50% and ~70% or more tephra grains, respectively. Magnetic susceptibility and color shifts were primarily used to locate and confirm potential intermediate to mafic tephra.

Bulk density and loss on ignition were measured for sediment samples selected at random throughout MG07-6. Bulk density was measured by weighing samples both before and after drying at 60°C for 12 hr. Loss on ignition was calculated as the percent of mass lost from the dried samples after they were heated to 550°C for 5 hr.

Sediment geochemistry

Elemental composition of sediment

Elemental abundances were analyzed in sediment cores using flame atomic adsorption spectrometry (FAAS) of samples prepared by whole-sediment dissolution and active iron selective dissolution. In addition, slabs of raw sediment were analyzed by energy dispersive spectrometry (EDS). FAAS analyses were conducted in the Colorado Plateau Analytical Laboratory, and EDS analyses were conducted in the Geology Scanning Electron Microscope Laboratory, both at Northern Arizona University.

Bulk composition of sediment Thirty ~0.1 g samples were taken from cores MG06-1A and -1B, nine from MG06-1A, and 21 from MG06-1B. Five randomly selected replicate samples, seven USGS or National Institute of Standards & Technology

standards, and four blank samples were also analyzed and are reported in the Results section. Samples were weighed to the nearest 0.0001 g and then dry-ashed at 600°C for 74 hr. The dry-ashed samples were placed into 45 or 50 ml plastic centrifuge tubes. One milliliter each of reagent grade 70% HNO_3 and reagent grade 43% HF and 4 g of 100% H_3BO_3 were added to each centrifuge tube. Tubes were diluted with distilled deionized water to 45 or 50 ml, and heated in a microwave oven for 2 min in groups of five. The digest solution was diluted with digest matrix and matrix modifiers to concentrations needed for metal analyses by FAAS. The dissolutions were complete except for one fine-sand-sized particle in standard Andesite AGV-1. The concentrations of Cu, Fe, K, Mg, Mn, Na, Ni, and Zn were measured three times for each solution. Ca was not measured because it is present in matrix the modifiers used. Concentrations were reported as mg/kg in the original sediment.

Energy dispersive spectroscopy Two slabs were removed from MG06-1B, 0.00-2.16 cm and 21.50-23.18 cm, using aluminum trays slid into and out of the sediment, exposing grain exteriors. These slab depths were chosen because the upper slab should contain the known 2005 event, and the sediment in the lower slab was inferred to have been deposited during a period when no known acidification occurred. The slabs were placed in a scanning electron microscope (SEM) and brought to a low vacuum (~30-70 Pa). The pressure was difficult to keep constant because of the constant evaporation of water from the sediment. The SEM was set to a 10 mm working distance. Transects composed of 1.250 mm long x 0.900 mm wide patches aligned side by side were completed down-core along each slab of sediment by accumulating an EDS spectrum for

100 s at each patch. Si, S, Al, Fe, Na, Ca, K, Mg, Ti, P, and Mn concentrations were estimated for each patch of sediment.

Active iron content Active iron is a functional definition of amorphous iron oxides found in soil and sediment (Chao and Zhou, 1983; Loeppert and Inskeep, 1996; Drever, 1997). It is mostly composed of ferrihydrite ($Fe(OH)_3$) and ferrihydrite-like minerals (Loeppert and Inskeep, 1996; Drever, 1997). The standard procedure for the selective dissolution of active iron in sediment and soil is dissolution in the dark with 0.175 M $(NH_4)_2C_2O_4$—0.100 M $H_2C_2O_4$ taken to pH 3 with HCl (acidified ammonium oxalate), also known as Tamm‘s reagent (Chao and Zhou, 1983; Loeppert and Inskeep, 1996).

Active iron was analyzed on samples from the same location as those analyzed for bulk density in the upper portion of MG06-1B and throughout MG07-6. Three 500-mg aliquots were taken from several grams of sediment that were homogenized in a 50-ml centrifuge tube on a vortex mixer for 1 min from MG06-1B. Three subsamples were taken straight from the core in MG07-6 to quantify the degree of homogeneity at each depth. Samples were not dried or ground, as described in Loeppert and Inskeep (1996), to prevent changes in the mineral form of iron. Instead, the bulk density of each sample depth was used to calculate the mass of dry sediment in each moist sample. The remainder of the dissolution and measurement procedure followed Loeppert and Inskeep‘s (1996) acid ammonium oxalate in the darkness-Tamm‘s reagent procedure, using FAAS, with a slightly different ratio of ammonium oxalate to sample. Twenty milliliters of Tamm‘s reagent were added to each sample, rather than 30 ml, lowering the

concentration of oxalate in the solution to prevent clogging of the burner head during analysis by FAAS. Samples were stored in the dark and analyzed within one day of dissolution to impede iron precipitation due to the decomposition of oxalate (Borggaard, 1988). Concentrations were reported as mg/kg in the original sediment.

Sediment slurry pH

Reconstructions of lake pH from sediment have used many techniques, such as micro pH electrode measurements (e.g. Conkling and Blanchar, 1989), pH of extracted pore water (e.g. Siever et al., 1961), diatom and chrysophyte taxa abundances (e.g. Charles and Smol, 1988), plant pigment ratios (e.g. Guilizzoni et al., 1992), and sediment slurry pH (e.g. Ryan and Kahler, 1987). For soils, the pH of sediment slurries is accepted as the standard method of estimating the pH (Thomas, 1996). Sediment slurries are similar to pore-water measurements because of the ~~–b~~uffering" effect discussed by Davis (1943) (see Discussion below). The concentration of diatoms in Mother Goose Lake sediment is not sufficient to facilitate an accurate reconstruction of lake pH (A.P. Wolfe, University of Alberta, personal communication, November 30, 2006.).

Slurry pH values were measured on 1-cm-thick adjacent intervals along the axes of MG06-1B and MG07-6. Desiccation and complete oxidation of parts of MG06-1B following prolonged storage rendered some of the core unusable. The procedure used to measure slurry pH was modified from Thomas (1996). The sediment was not dried prior to measurement to minimize changes in the mineral assemblage that affect the activity of H^+. Instead of 10 g each of water and sediment, 5 g were used because sample material was limited. Also, the slurry pH was measured in separate 50-ml centrifuge tubes for

each sample instead of reusing beakers, reducing potential contamination between samples and speeding analysis. The sediment was sampled from the interior of the core, avoiding the edges that could be contaminated from the coring process. Slurries were stirred for 2 min on a vortex mixer. After 10 min of settling, a model 9157BN Thermo Orion glass Ag/AgCl pH triode, attached to a calibrated (pH 4.00 and 7.00 buffers) Orion Research Inc. model 250A pH meter, was inserted into the sediment slurry. The triode was positioned so that the exterior case surrounding the bulb touched the bottom of the centrifuge tube. The slurry pH was recorded when the meter automatically determined that the value was stable, or after 2.5 min, whichever was longer. Between samples, the pH electrode was rinsed with deionized water, checked for offset from either the pH 4.00 or the pH 7.00 buffer, and rinsed with deionized water before measuring the next sample. If the meter misread a standard buffer by more than 0.05 pH units, it was recalibrated before measuring the next sample. During analyses, a 5-min period between checks and recalibrations in standard buffers, with the sediment pH reading taken at 2.5 min, ensured that the drift of the meter at the time of sample measurement was half of the difference between the first and second standard measurements, assuming linear drift.

When an electrode touches sediment, pH readings can be different than a reading in only the solution (e.g. Olsen and Robbins, 1971), but it is generally accepted that such pH reading anomolies are a problem for calomel electrodes, not Ag/AgCl glass electrodes such as the one used in this study (Coleman et al., 1951; Marshall, 1964; Swoboda and Kunze, 1968; Olsen and Robbins, 1971; Thomas, 1996). Furthermore, the electrode was always placed the same depth into the slurry.

Replicate measurements were not conducted because of limited material. To assess the analytical precision of pH measurements, the slurry pH of 15 aliquots from 255 g (dry weight) of homogenized sediment from core MG07-2 were measured. Approximately equal amounts of oxidized and reduced sediment were removed from the core MG07-6, dried at 64°C for 12 hr, and then ground to pass through a 250 μm sieve. This sediment was mixed for 10 min as a dry powder, rehydrated to the consistency of sediment from MG07-6, and then mixed again for 15 min before aliquots were analyzed for slurry pH.

Oxidation and reduction reactions in the sediment column and laboratory can alter the pH of the samples from the pH at the time of deposition, so the slurry pH samples were taken ensuring both reduced and oxidized sediment were included. Samples for slurry pH analyses were taken making sure to include approximately half reduced and half oxidized sediment. This mixture was chosen because the effect of the oxidation and reduction conditions on pH can be countered by sampling sediment with an average oxidation reduction potential (ORP) similar to the ORP of the sediment-water interface at the time of deposition. The optimum ratio of oxidized-to-reduced sediment is dependent on the form(s) of metal hydroxide produced, the concentration of Fe and Al, and the concentration of sulfates and sulfides. Because all of these variables are not known for any part of Mother Goose Lake or its drainage, slurry pH samples were estimated to be best composed of half fully-oxidized and half fully-reduced sediment. This approach was checked by comparing the slurry pH at the top of the core to the pH of the water in the lake at the time of deposition.

The extent to which the samples used to measure slurry pH deviated from a theoretical sample comprising exactly half reduced and half oxidized sediment was determined. This "oxidation-state uncertainty" was determined by analyzing the slurry pH of eight 2-cm-thick samples separated into reduced and oxidized subsamples, based on color, from the archive half of MG07-6 (Figure 6). The samples were taken from a contiguous section of core because, although the depth to which the oxidized front had penetrated the core varied by core section because of holes in some of the plastic core wraps, the degree of oxidation and reduction appeared similar throughout the entire core, based on color differences. Because the same mass was taken for each subsample, the depth of oxidation does not matter, only the degree that samples were oxidized. The oxidation-state uncertainty was estimated as the difference between the average $[H^+]$ of the samples from the main slurry pH dataset and the average $[H^+]$of the separate reduced and oxidized subsamples from the same depth (Equation 4).

$$[([H^+]_{\text{main data set depth 0-1}} + [H^+]_{\text{main data set depth 1-2}})/2] - [([H^+]_{\text{100\% oxidized depth 0-2}} + [H^+]_{\text{100\% reduced depth 0-2}})/2] \quad (4)$$

The oxidation-state uncertainty was estimated as the average of the eight replicate groups plus one standard deviation.

CHAPTER 3

RESULTS

Mother Goose Lake water chemistry

Like other nearby lakes with long fetches, Mother Goose Lake is probably well mixed most of the year (Burgner et al., 1969). Previous analyses, and those in this study, show that Mother Goose Lake is generally well mixed (Figure 7, Schaefer et al., 2008a). A weak thermocline and chemocline form at the mouth of Volcano Creek at times when the discharge of the creek is high, but the majority of the lake is thermally and chemically unstratified with a conductivity of ~200 µs/cm and a temperature of ~15ºC (Table 3; Figure 7). Water from Volcano Creek entering the lake in the summer of 2007, probably with much lower discharge than during the 2005 overflow event, generated an interflow that was both reduced and acidified at a site ~1.7 km from the inflow (Table 3; Figures 4 and 7). By the summer of 2007, most of Mother Goose Lake water was less acidic than in 2005 (pH of ~4.5 vs. ~3), and almost iron-free except for the interflows and at the Volcano Creek inlet, which was still rich in reduced iron (~57 ppm) and more acidic (pH of ~3.5) (Tables 3 and 4; Figure 8; Schaefer et al., 2008a). Nearby Needle Lake (Figure 4) had a pH of ~7.3, based on one surface water analysis in 2007.

Sediment physical properties

The length of the 12 sediment cores from the six core sites ranges from 46.0 cm, for the shortest surface gravity core, to 558.5 cm for the longest percussion core (Table 1). Sediment from Mother Goose Lake, including the sediment deposited in 2005, is

mostly laminated, but sparse nonlaminated layers include massive and normally graded units (Figure 9). Most discrete units, based on color or grain size, are tens of centimeters thick, whereas beds are millimeter to centimeter scale. Grain size typically is silty with some clay- and sand-rich beds. The sediment in the upper several centimeters of MG06-1B is uniquely composed of primarily high chroma and value 10YR Munsell colors. The majority of sediment has Munsell colors of medium to low chroma and value 10YR, 5YR, and 5Y hues(Table 5; Appendix 1).

Cores MG07-10, MG07-11, and MG07-12 contain abundant massive layers, extremely tilted or folded layers, and erosive contacts (Figures 9 and 10). These core sites are near steeply sloping bathymetry, whereas MG07-6 is surrounded by the flattest bathymetry of any of the core sites (Figure 5). Because of the disturbed stratigraphy and unconformities, MG07-10, MG07-11, and MG07-12 and their associated gravity cores, with the exception of MG07-12B, were described for structures and color only. The disturbed stratigraphy also hampered correlation among sites across the lake. It was not possible to tie stratigraphically any of the long cores to surface cores.

Sediment geochronology

Only cores MG06-1A and 1B, and MG07-2, -6, and -12B appeared to be relatively undisturbed and thus suitable for dating. MG06-1A was not dated because it is from the same site as MG06-1B, which is longer, and thus includes older sediment.

Radiocarbon ages on core MG07-6 were used to generate an age-depth model following the spline-fitting procedure of Heegaard et al. (2005). Tephra beds were subtracted from depths because they were instantaneously deposited. The seven

radiocarbon ages (Table 2), excluding one outlier, were fit using a k value of 5 (Figure 9). The outlier was excluded because it is older than the next two lower ages and made of terrestrial macrofossils that were probably sitting on the landscape for a prolonged period before being washed into the lake. The ages indicate the last ~670 years of sediment are missing from the top of this ~3800-year-old record. Because the age of the upper sediment in MG07-6 is 622 (±154) years old, the surface core MG06-1B and the percussion core MG07-6 do not overlap temporally, resulting in an ~550 year gap in the stratigraphic sequence. The ^{14}C ages from core MG07-2 overlap with each other, or are stratigraphically reversed (Figures 5 and 12).

Pu inventories were obtained for gravity cores MG06-1B and MG07-12B (Table 4). Assuming that the peak [Pu] at 52 cm depth was deposited in 1963 and the surface of the core was deposited in 2006, the Pu profile from MG06-1B indicates that there is an average sedimentation rate of ~1.2 cm/yr, yielding an age ~120 years at the base of the core (Figure 11). In contrast, the results for MG07-12B show that only the uppermost 1 cm contains detectable Pu. The lack of detectable Pu below this level indicates either erosion of the upper sediment or dilution by either older sediment or volcanogenic, Pu-free, sediment.

The age-depth relationships in MG07-2 and MG07-12B indicate that the sediment in these cores is disturbed (Table 4; Figures 12 and 13). Steep bathymetry near the core sites likely encouraged turbid underflows or subaqueous landslides that modified previously deposited sediment and created normal grading or massive sediment structure. The uppermost 1 cm of sediment in MG07-12B could have been deposited over older and Pu-free sediment exposed in the erosional zone of a subaqueous slope failure, or

reworked older sediment. Site MG07-6 is probably relatively undisturbed because it is surrounded by gently sloping bathymetry (Figure 5). Only cores MG06-1A and B, and MG07-6 are suitable for detailed analysis.

Magnetic susceptibility and tephra

Sediment MS is most strongly influenced by the concentration of iron-bearing minerals and grain size, and is often used to aid in locating tephra in lacustrine sediment (e.g. Nowaczyk, 2001). Most of the 52 tephras in MG07-6 (19 "A", 10 "B", and 23 "C" tephra) and 2 "A" tephra in MG06-1B are composed of glass that is opaque to translucent under reflected light, and mafic minerals, commonly with vesicles (Appendix 3). The average thickness is 0.80 ± 1.1 cm. Most tephra is composed of fine sand-sized grains. One notable exception is a coarse-grained (up to 7 mm c-axis) pumiceous 8.5-cm-thick tephra deposited 3454 ± 283 cal yr BP in MG07-6. In Mother Goose Lake cores, tephras generally coincide with MS peaks above the ~100-200 x 10^{-6} SI background of the ambient sediment (Table 6; Figure 12; Appendix 3). Some broader peaks coincide with massive layers that do not include tephra (Figure 12).

Loss on ignition and bulk density

The bulk density of lake sediment varies with water content and composition; loss on ignition (LOI) measures the mass of bulk volatile matter (burns or vaporizes at 550 °C), such as organic material, in the sediment (Dean, 1974). Bulk density of sediment from Mother Goose Lake ranges, without a first-order trend with respect to depth, from 0.41 to 0.90 g/cm^3, and LOI from 6.7 to 9.0%, also without a first-order trend with

respect to depth (Table 7; Figures 14 and 15). The material lost on ignition in Mother Goose Lake sediment likely includes sulfides and sulfates formed from volcanic gases (e.g. Sriwana et al., 1998).

Sediment geochemistry

Elemental composition of sediment

Bulk composition Base-cation concentrations measured by FAAS in core MG06-1B (K, Mg, Na) follow the same general trends, and vary inversely to the acid cation Fe (Table 8; Figures 16-18). The concentrations of individual base cations vary between 8 and 25 mg/kg. Fe reaches its highest concentration (64 mg/kg) in the top of MG06-1B, but the lowest concentration (43 mg/kg) is one cm below (Table 8; Figure 17). Ni and Mn exhibit similar trends to each other, with relatively stable concentrations that decrease in the uppermost 2 cm. Zn concentrations are highly variable, but also decrease in the uppermost sediment. Cu is below detection limits. Except for Ni, the differences between replicate samples are within analytical error (~10%), on average (Table 9). Ni concentrations were near the detection limit, possibly explaining the highly variable readings on replicates (Table 9). The standards used to check the completeness of the sediment dissolution each differed in their resistance to dissolution (Table 9). In contrast the sediment samples had similar compositions, and therefore similar behavior during the dissolution process. This is confirmed by the well-reproduced results from replicate samples (Table 9).

Surface composition by energy dispersive spectroscopy Elemental concentrations measured by EDS are reported as weight percent element (Table 10). The most abundant element is Si (20.9% from 0.00-2.16 cm, and 20.8% from 21.50-23.18 cm), followed by Al and Fe (6.5% and 3.3%, and 7.3% and 4.6% in the upper slab and lower slab, respectively). The other analyzed elements each make up less than 2% of the total abundance on average. The analyzed elements add up to only 36.3 and 37.7% in the upper and lower slabs, respectively. The majority of the remainder of the weight is most likely oxygen, based on charge balance. The average concentrations of all acid and base cations (expressed as ratios to Si to eliminate closed-array bias) are within one standard deviation of each other in the two sample depths, except for Ca and Al (Figure 19). Ca and Al are more concentrated in the lower sediment than in the upper sediment, whereas S concentrations are higher in the upper sediment (Figure 19). The transects do not reveal any first-order trends by depth within the slabs except for a slight increase in S with depth in the 0.00 – 2.16 cm slab (Figure 20).

Active-iron content Active iron is best generalized as ferrihydrite ($Fe(OH)_3$), a poorly crystalline hydrous ferric oxide that is approximately synonymous with amorphous $Fe(OH)_3$ (Chao and Zhou, 1983; Drever, 1997). Ferrihydrite is aqueous in reduced, low-pH conditions, and precipitates in oxidizing environments as pH increases (Figure 8). Active iron concentration shows no down-core trend in either core, but in MG07-6 remains higher than in MG06-1B (Table 7; Figures 21 and 22). The average active-iron concentration in MG06-1B is 13,455 ±2,004 mg/kg (n = 8), compared with 57,886 ± 16,618 mg/kg (n = 23) in core MG07-6.

Sediment slurry pH

The analytical error in slurry pH readings should be less than 0.05 pH units. The drift test confirmed this. The difference after 5 min was always less than 0.1 pH units, giving a maximum analytical error of 0.05 pH units. This is confirmed by the replicate analysis of 15 aliquots from MG07-2, which have a standard deviation of 0.04 pH units at pH 4.53.

The oxidation-state uncertainty for the slurry pH measurements, as calculated using Equation 4, is $\pm$ 2.1 x 10^{-5} mol H^+ (a difference of 0.02, 0.58, and 2.20 pH units at the minimum (3.24), average (5.26), and maximum (6.67) pH values, respectively, in MG06-1B and MG07-6 (n = 494)) (Tables 11 and 12; Figure 23). The analytical error in slurry pH measurements is 0.05 pH units, which represents a different amount of H^+ depending on the pH, so it was converted to moles of H^+ from the average slurry pH in MG06-1B and MG07-6. This is $\pm$ 3.03 x 10^{-7} mol H^+, which is two orders of magnitude less than the oxidation-state uncertainty and negligible relative to the more important uncertainty that results from variations in sediment oxidization. The oxidation-state uncertainty is shown for data tabulated as [H^+].

Slurry pH values vary between 3.24 and 6.14 in MG06-1B and between 3.89 and 6.67 in MG07-6 (Table 12). The average and median slurry pH values in MG06-1B are 5.37 $\pm$ 0.71 and 5.60 (n = 21), and 5.25 $\pm$ 0.54 and 5.29 (n = 473) in MG07-6. The slurry pH values are slightly negatively skewed for MG06-1B and approximately normally distributed for MG07-6 sediment. For a log scale to be normally distributed, there must be a strong skewness to the data on a linear scale. The skewness is caused by acidifications with much higher [H+] than average, such as the last ~2 years of sediment

in MG06-1B. A general first-order trend with depth through MG07-6 first rises until about 250-cm-deep, and then decreases to about 400-cm-deep before starting to increase to the base of the core (Figure 24). This trend results in the last ~1,100 years of sediment in MG07-6 being generally more acidic than the rest of the sediment. Superimposed over this first-order trend is a high degree of smaller-scale variability that includes several depressions of one or more pH units that occur in clusters of less than 10 data points. Most of the slurry pH values are above ~4.4-4.6. Approximately 60% of tephra deposits in Mother Goose Lake sediment coincide with low slurry pH spikes, while the thickest tephra coincides with a high pH spike.

CHAPTER 4

DISCUSSION

When analyzed in conjunction with the modern water data and the strongest indicator of past pH (slurry pH), at the time of deposition no other proxies seem to be strongly influenced by the pH of the lake. It was hoped that a multi-proxy approach would produce a more robust estimate of the frequency of acidification events, but slurry pH alone can still produce an estimate. Although slurry pH is not a measurement of the actual pH of the water at the time of sediment deposition, it is the best proxy because it is a measurement of the pH of a solution that is only slightly different from the lake water at the time of sediment deposition. All other proxies are only potentially influenced by pH do not measure pH directly, and are subject to additional post-depositional changes.

Mother Goose Lake water chemistry

Mother Goose Lake was not acidified for some time prior to the 2005 geothermal event. Salmon spawned in the lake annually (Schaefer et al., 2008a). Major sockeye salmon nurseries in southwestern Alaska have pH values between 7 and 8 (Burgner et al., 1969), although salmon do spawn in water with pH values as low as ~5.5 (e.g. Fromm, 1979; Ikuta et al., 2004). The previously viable salmon nursery indicates that the pH of Mother Goose Lake is normally higher than ~5.5. When Mother Goose Lake is not acidified, inflow from Volcano Creek likely results in spatially focused deposition of ARD minerals at the inflow where mineral acids are rapidly neutralized and reduced aqueous species, such as Fe, are oxidized by lake water (Table 3; Figures 4 and 6). All of the lake water and surface sediment is probably reduced after large crater-lake overflow

events. This assumption is supported by presence of a small lens of reduced water at the top of Profile C (Figure 7), which is at the mouth of Volcano Creek. This lens must expand across the lake during times of high discharge from the crater of Mt. Chiginagak. Approximately uniform acidic and reducing conditions throughout the lake would allow ARD minerals to evenly mix in the lake. Once the lake begins to recover to typical circum-neutral and oxidized conditions, ARD minerals should precipitate first in oxidized zones near neutral inflows, and then flocculation should sweep towards the acidic inflow (Figure 8), as was observed in 2005 (Schaefer et al., 2008a). Uniform conditions in the lake should then uniformly affect pore water pH in surface sediments.

Sediment physical characteristics

Sediment color

The oxidation of Mother Goose Lake after the input of aqueous ARD minerals during previous acidification events should have resulted in the deposition of brightly colored oxidized sediment, based on the effects of the 2005 event. However, the bright 10YR colors at the top of MG06-1B are not seen elsewhere in MG06-1B or MG07-6. If these colors became muted over time from reduction due to burial, they have become indistinguishable from the majority of the other layers (Table 5; Appendix 1). Color does not indicate the presence of any acidifications other than the 2005 event. Poorly crystalline iron oxyhydroxides/sulfates change from bright 10YR colors to duller colors as they transform into more crystalline minerals with time (i.e. Schroth and Parnell, 2005), eliminating strong color differences with surrounding sediment.

Magnetic susceptibility and tephra

High MS values in thick massive and normally graded layers suggest pulses of terrigenous sediments from floods or earthquakes (e.g. Karlin and Abella, 1992; Wolfe et al., 2006), while thinner dark layers with high MS are typically tephras that presumably contain mafic glass and minerals. The tephras probably originate mostly from nearby volcanoes, which include Mt. Chiginagak (~19 km distant), Yantarni Volcano (~20 km distant), Mt. Kialagvik (~34 km distant), and Mt. Aniakchak (~60 km distant). The morphologically unique (coarse pumice), unusually thick (~8.5 cm), 3454 ± 283 cal yr BP tephra in MG07-6 may have erupted from Mt. Aniakchak during its caldera-forming eruption, which occurred 3350-3815 cal yr BP (Begét et al., 1992; Waythomas and Neal, 1998). Mother Goose Lake is on the eastern edge of fallout from the caldera-forming Aniakchak tephra (Miller and Smith, 1987; Begét et al., 1992; Dreher et al., 2005). The Aniakchak tephra is present on the landscape ~4 km northwest of Mother Goose Lake as a buried ~13-cm-thick deposit of lapilli fallout (Riehle et al., 1999). Geochemical analyses are needed to confirm the correlation between the Mother Goose tephra and the caldera-forming tephra from Mt. Aniakchak. Confirming the origin of the tephra would strengthen the age model for Mother Goose Lake sediment.

Loss on ignition and bulk density

LOI and bulk density did not indicate any past geothermal events at Mt. Chiginagak that influenced Mother Goose Lake. Bulk density is only useful to determine original weights of samples from dry weights for elemental analyses. LOI could potentially be used as a measure of the abundance of volatile chemical species deposited

after a melt event (e.g. Sriwana et al., 1998). However, the organic content of sediment may be positively correlated with the pH of a lake at the time of deposition (Davis at al., 1985), because plants generally thrive in neutral conditions but die and decompose in prolonged acidic conditions. These two processes operate in opposition to each other. The poor correlation between LOI and slurry pH ($r^2 = 0.002$, $p = 0.84$ $n = 22$) suggests that LOI is influenced by both competing processes and can not be used to reconstruct the occurrence of geothermal events at Mt. Chiginagak.

Sediment geochemistry

Elemental composition of sediment

The three methods of quantifying elemental abundances in Mother Goose Lake cores (bulk chemistry by FAAS analysis, surface composition by EDS analysis, and active iron content by FAAS analysis) each reveal a different aspect of the influence of acidified and reduced water on the sediment composition.

Bulk-sediment composition The bulk-sediment analyses are analytically sound, but the extraction method was selective enough that the compositions in the sediment are relative. The data are inconclusive as to whether bulk composition of the lake sediment was altered by acidification events. Furthermore, the lack of a first-order trend with respect to depth suggests no change in the provenance of the sediment deposited during acidic conditions from sediment deposited during normal, circum-neutral and oxidized, conditions (Figures 16 and 17). The slight decrease in the concentrations of Ni and Mn at the top of MG07-6 (Table 8) could be due to a change in source area, but it is a minor

feature in the concentration trends and should not be used as a robust indicator of provenance.

Surface composition by energy dispersive spectroscopy Based on the Pu age model that indicates an average sedimentation rate of ~1.2 cm/yr in MG06-1B, the upper ~2.4 cm of sediment were deposited during the 2005 crater-lake overflow event, and in 2006. Acid-cation concentrations (Fe and Al) were expected to be higher in and on the sediment associated with the acidification event (0.00-2.16 cm), which should have been associated with a large influx of iron and, presumably, aluminum, as in 2005, whereas base-cation concentrations (Na, Ca, Mg, K) were expected to be higher below this level (21.50-23.18 cm). However, both Al/Si and Ca/Si ratios are higher in the lower sediment (Table 10), indicating acid and base cations did not vary inversely and that acid cations did not dominate during the acidification event while base cations dominated during ‗normal' conditions.

The higher concentrations of S in the upper slab (Figure 20) may reflect the deposition of elemental S, adsorption of sulfates/sulfides, or the onset of neutralization and reduction of the buried sediment, resulting in precipitation of sulfates such as iron sulfate. All are expected for the upper sediment, which was deposited during 2005 to 2006. Detrital elemental S could have been generated by the interaction of volcanic SO_2 with water (Equation 1). Increasing pH would also result in a peak in S concentration, as both the sulfur and metal sulfides precipitated, the latter by combining with transition metals, such as Fe, followed by a decrease in S concentration with time as the dissolved S

reservoir in the lake was depleted (e.g. Herlihy and Mills, 1985), similar to the trend in the upper slab (Figure 20).

On the other hand, oxidation/reduction conditions could have been the main control on the deposition of S rather than the production of S from gas or changing pH (e.g. Küsel et al., 2001). If S was present as dissolved sulfides, such as H_2S, during the overflow event, progressive oxidation of the water from lake mixing could have oxidized sulfides to sulfates, precipitating solid sulfur at the sediment-water interface (e.g. Herlihy and Mills, 1985). As the sediment deposited during the event was buried, it was reduced, converting sulfates to sulfides, which are soluble in reduced environments, unless combined with metals. This would initially increase the concentration of S incorporated into freshly deposited sediment, followed by a decrease in the concentration of S in the sediment, similar to the trend in the upper slab (Figure 20). Interpreting the S concentration in the sediment is hampered by the unknown history of oxidation/reduction conditions in the sediment, which influences the migration of S as changing oxidation/reduction conditions force S between aqueous and mineral phases (e.g. Herlihy and Mills, 1985; Williamson and Parnell, 1994). Without a better understanding of the pH and oxidation/reduction history of the lake and sediment, a comprehensive understanding of the controls on S concentration is not possible, reducing its utility as an indicator of acidification events in Mother Goose Lake.

Active-iron content As Mother Goose Lake recovers from acidic and reducing conditions, the oxidation/reduction state and pH should favor the deposition of ferrihydrite (oxidized and circum-neutral). The lack of an upwardly decreasing trend in

the concentration of active iron during and immediately after 2005 indicates that active iron was not leached by the acidification and was not sensitive to the acidification (Figure 21). Bacteria also affect the concentration of ferrihydrite in sediment (e.g. Ferris et al., 1989). The poor correlation between sediment slurry pH and active-iron content (r^2 = 0.06, p = 0.27, n = 22) indicates that pH is not the main control on the concentration of active iron. Instead, availability of Fe, or oxidation/reduction conditions might be the strongest influence on the concentration of active iron. Because there is no independent record of oxidation/reduction conditions from Mother Goose Lake, the degree of oxidation/reduction-controlled mobilization and deposition of active iron cannot be assessed. Additionally, oxidation/reduction conditions likely change as sediment is buried, and as the influence of the lake water is overshadowed by bacterially mediated oxidation/reduction reactions that are influenced by the availability of sulfates, CO_2, or acetate (e.g. Jørgensen and Fenchel, 1974; Jørgensen, 1977; Herlihy and Mills, 1985; Ward and Winfrey, 1985; Whiticar et al., 1986). Furthermore, most of the errors in measurement overlap, making even the trends in the data difficult to determine (Figures 21 and 22). The utility of active iron as an indicator of acidification events is limited, except to show that the oxidation/reduction conditions in the sediment have varied, probably because of burial.

Sediment slurry pH

Identifying the past input of water from large geothermal events at Mt. Chiginagak into Mother Goose Lake requires reconstructing changes in the pH of Mother Goose Lake. The bulk and selectively extracted concentrations of elements in the

sediment cannot be used as unequivocal evidence of geothermal events because past pH and oxidation/reduction conditions are both needed to interpret the concentration of those solid species. Even if the past oxidation/reduction conditions were estimated, the errors from reconstructing them would add to the errors in measurement, most likely rendering the data useless for reconstructing past acidifications. Although oxidation/reduction conditions can influence sediment slurry pH values (Equations 5 and 6), slurry pH is the best proxy of geothermal events because it is a direct measure of pH. Slurry pH measurements are also simpler and faster than any other measurement, facilitating the construction of a high-resolution record of acidifications. However, some precautions must be taken when interpreting slurry pH values as well. Processes in the lake water, sediment, and in the laboratory can influence slurry pH.

Effects of lake-water alkalinity on pH The presence of carbonates is a major control on the pH of natural water (e.g. Stumm and Morgan, 1996; Drever, 1997). To lower the pH of water below 4.4, all of the bicarbonate must first be effectively consumed (Figure 25). When adding acid at a constant rate to a circum-neutral, buffered lake, the activity of H^+ will increase approximately linearly until a pH of ~5 is reached. Around a pH of 5, the activity of H^+ will increase slower until effectively all of the bicarbonate is consumed at pH 4.4, then the activity of H^+ will start to increase again at the initial, higher, rate (Figure 25). Although the carbonate buffering capacity of Mother Goose Lake has never been measured, the carbonate buffering capacity of nearby Painter Creek (Figure 4) was measured in 2005 as 20 mg/l as bicarbonate (Schaefer et al., 2008a). Painter Creek flows through bedrock similar to the inflows to Mother Goose

Lake, and therefore should have a similar carbonate buffering capacity. However, the carbonate buffering capacity of Mother Goose Lake might typically be higher than Painter Creek because of the input from bicarbonate-rich springs on the northern flank of Mt. Chiginagak, which contained 388 mg/l bicarbonate in 2005 (Schaefer et al., 2008a).

Because the acid neutralizing capacity of water includes chemical species other than bicarbonate, the total alkalinity of surface water is best described by Equation 5 (Morel and Hering, 1993):

$$\text{Alkalinity} = [OH^-] + [HCO_3^-] + 2[CO_3^{2-}] + [NH_3] + [HS^-] + 2[S^{2-}] + [HSiO_3^-] + 2[SiO_3^{2-}] + [B(OH)_4^-] + [\text{Organic}^-] + [HPO_4^{2-}] + 2[PO_4^{3-}] - [H_3PO_4] - [H^+] \quad (5).$$

The concentration of most noncarbonate species is generally low in natural fresh water (e.g. Sherlock et al., 1995; Stumm and Morgan, 1996). Although only $[PO_4^{3-}]$ has been measured in Mother Goose Lake water (Schaefer et al., 2008a), it, and probably the concentration of other contributors to alkalinity, was negligible.

Effects of tephra fall on pH Tephra grains can add acidity to lakes into which they fall (Stewart et al., 2006). Cation-exchange sites on tephra are occupied by H^+, because of the influence of mineral acids such as H_2SO_4, HCl, and HF in volcanic plumes, and Ca, Mg, and other metals (Schiffman and Southard, 1996; Witham et al., 2005; Stewart et al., 2006). When tephra falls on a lake, mineral acid coatings can be released and adsorbed H^+ can be exchanged (Stewart et al., 2006).

The effect of acidified tephra falling in Mother Goose Lake was evaluated to determine whether tephra could overcome the bicarbonate buffering in Mother Goose Lake. The average density of tephra deposits in the lake was assumed to be between 600

and 700 kg/m^3, which is the range of ash fall deposit densities (including air-filled pore space) given in Pyle (2000). The cation-exchange capacity was generously assumed to be between 300 and 600 meq/kg, which is the range for palagonitized glass given in Schiffman and Southard (1996). Fresh tephra has a much lower cation-exchange capacity. The volume of the lake was assumed to be between 0.43 km^3, based on a volume calculation (triangular irregular network) using ESRI ArcGIS™, and 0.50 km^3, based on the work of Schaefer et al. (2008a). Minimum, average, and maximum meq HCO_3^-/l needed to neutralize the resulting acidity from the total dissociation of H^+ from tephra in a 0- to 8.5-cm-thick layer were calculated based on these inputs (Figure 26). The probable carbonate-buffering capacity of Mother Goose Lake (>0.5 meq/l HCO_3^- based on the capacity of Painter Creek and the hot springs on Mt. Chiginagak) indicates that it is not possible for even the total dissociation of H^+ from the thickest tephra that lowered the pH of the lake with H^+ in all of its cation-exchange sites (unlikely) to lower the pH below 4.4, except in the maximum meq HCO_3^-/l required scenario. The thickest pure tephra in Mother Goose Lake sediment that coincides with a drop in slurry pH is 1.5 cm thick. The thickest tephra, which unexpectedly coincides with an *increase* in slurry pH from ~4.5 to ~5.7, is 8.5 cm thick (Figure 24). This calculation overestimates the effect of tephra acidification because, not only does it assume H^+ saturation of palagonitized glass and total dissociation, it assumes an equal distribution of tephra over the lake, whereas the tephra thicknesses are based on sediment from a depocenter and should be thicker than the lake-wide average.

Effects of redox conditions on slurry pH As shown by the slurry pH oxidation-state uncertainty estimate, diagenetic and in-laboratory oxidation/reduction reactions alter slurry pH values. Oxidation/reduction reactions can change the pH of sediment. Reduction of sulfates leads to the bacterial production of HCO_3^-, lowering the activity of H^+ (e.g. Herlihy and Mills, 1985; Küsel et al., 2001; Equation 6).

$$SO_4^{2-}{}_{(aq)} + 2C_{(s)} + 2H_2O_{(l)} \Leftrightarrow H_2S_{(aq)} + 2HCO_3^-{}_{(aq)} \quad (6)$$

Oxidizing aqueous Fe (II) to produce ferrihydrite releases acidity according to the hydrolysis equation Equation 7.

$$Fe^{2+}{}_{(aq)} + 3H_2O_{(l)} \Leftrightarrow Fe(OH)_{3(aq)} + 3H^+{}_{(aq)} + e^- \quad (7)$$

Similar reactions occur to form aluminum hydroxides.

The oxidation state of the sediment, and therefore the proportion of oxidized versus reduced sediment that comprises each sample, is probably the second largest control on the slurry pH, after the pH of the water at the time of deposition. The core face was more oxidized at the time of analysis than the sediment-water interface because the core face had been exposed to air (ORP = ~750 mv at pH 6; ~900 mv at pH 4), whereas the sediment-water interface at site MG07-6 had an ORP of ~500 mv in 2007 (Figure 7). The validity of using approximately half reduced and oxidized sediment is supported by the similarity of the slurry pH of sediment deposited in 2005 and 2006 (3.2) (Table 12) and the pH of Mother Goose Lake in 2005 (~2.9-3.1) and 2006 (~4.1) (Schaefer et al., 2008a). The average lake $[H^+]$ for those years is 5.53×10^{-4} (pH 2.25) the sediment slurry $[H^+]$ for those years is 5.75×10^{-4} (pH 2.24). The calculated uncertainty (2.1×10^{-5} mol H^+) matches the empirical uncertainty for the 2005 and 2006 sediment compared to the 2005 and 2006 lake water (2.2×10^{-5} mol H^+). The 2005/2006

error is probably inflated because the sediment does not perfectly encapsulate all of the 2005 and 2006 sediment.

The pore water in the sediment cores started to oxidize once the cores were split, although oxidization probably occurred fastest while samples were disaggregated during slurry pH analysis. Therefore, acidity was produced. The amount of acidity produced can be quantified by calculating the moles of Fe^{2+} that could have been oxidized and multiplying that by three to obtain the moles of H+ produced by oxidation and formation of $Fe(OH)_3$ (Equation 7). The inorganic rate constant of precipitation for $Fe(OH)_3$ has been experimentally defined as 2.4×10^{-7} M/s when [Fe] = 0.28 mg/l and pH = 6 (Pham et al., 2006). The concentration of Fe was 0.6 mg/l above the sediment-water interface at core site MG07-6 in 2007 (Table 3) and because the ‗normal' pH of Mother Goose Lake is within the range for salmon spawning (>5.5), the conditions used by Pham et al. (2006) are similar to those that should ‗normally' exist in Mother Goose Lake. The inorganic rate is the best rate to use because the main Fe-oxidizing bacteria, *Thiobacillus ferrooxidans*, grows only in acidic water and prefers pH values between 1.5 and 6.0, with optimal conditions for growth at pH 2.0 (Leduc and Ferroni, 1994). Although the rate constant for inorganic precipitation of $Fe(OH)_3$ is high enough to produce a large amount of acidity in the time that it took to analyze the slurry pH, the low concentration of Fe^{2+} in the pore water limited the production of acidity. If all of this Fe^{2+} precipitated as $Fe(OH)_3$, than only 3.21×10^{-8} mol of H^+ would have been produced. Therefore, the precipitation of $Fe(OH)_3$ from the pore water in Mother Goose Lake sediment during slurry pH analysis was two or more orders of magnitude less than the amount already in the pore water. As discussed in the oxidation-state uncertainty explanation in Chapter 2,

oxidation of the sediment after core splitting can also contribute to acidification, probably through the production of ferrihydrite.

If the sediment contained pyritic minerals, oxidizing conditions would produce H_2SO_4, lowering the slurry pH according to Equation 8:

$$FeS_{2(s)} + 2H_2O_{(l)} + 3O_{2(g)} \Leftrightarrow Fe^{2+}(aq) + 2H_2SO_{4(aq)} \quad (8)$$

Pyrite has not been detected by visual inspection of Mother Goose Lake sediment, but the high concentration of S in the uppermost sediment in MG06-1B may reflect sulfates created by the oxidation of sulfides. However, even the potentially high production of acidity in the uppermost sediment due to the oxidation of sulfides did not result in a slurry pH lower than the pH of the lake (Table 12). Therefore, oxidation of pyritic minerals probably does not appreciably influence the slurry pH values.

Effects of sediment buffering on slurry pH In sediment with pH below ~4, dissolution reactions, such as the dissolution of kaolinite (Equation 9), consume the available H^+ until all clays have been dissolved to the point of Al saturation (Coleman and Craig, 1961; May et al., 1986).

$$Al_2SiO_5(OH)_{4(s)} + 6H^+_{(aq)} \Leftrightarrow 2Al^{3+}_{(aq)} + 2Si(OH)_{4(aq)} + H_2O_{(l)} \quad (9)$$

Slurry pH values between ~2 and 3 require a constant supply of mineral acids, such as H_2SO_4, to force the dissolution and alteration of other silicate minerals (Thomas, 1996). This requirement could explain why all slurry pH values are above 3 in Mother Goose Lake sediment.

Because the weathering of primary minerals by acidity consumes H^+ (e.g. Equation 9) in a closed acidified system, $[H^+]$ will decrease with time until completely

consumed, or until all of the dissolvable minerals are dissolved. If the former was a slow process, slurry pH should increase with time and therefore, depth downcore. However, this process is rapid and therefore downcore trends are not expected. For example, May et al. (1986) found that the experimental dissolution of kaolinite at pH 4 took ~3.4 years to reach equilibrium, but only a day for dissolution to be ―clearly evident". Any consumption of H^+ by the dissolution of clay minerals was effectively instantaneous compared with the mean sample spacing in this study of 6.4 years in core MG07-6 (Table 12). Based on a student's t-test, slurry pH is significantly lower ($p = 1.4 \times 10^{-69}$) below 2.8 m in the 5.07-m-long core MG07-6 (Table 12). This suggests that one or more of the following pertains: (1) slurry pH values do not increase with time following burial, (2) acid is being supplied to the sediment column post-depositionally, (3) the lower part of the core is more oxidized, or (4) Mt. Chiginagak was more active during the time the lower sediment was deposited. The first and last explanations are most probable because there is no structural evidence of upward flow of acidified liquids in the lower sediment (although this would be difficult to detect) and the degree of oxidation is similar above and below 2.8 m based on visual inspection.

Effects of diffusion on slurry pH Slurry pH could also be influenced by the diffusion of acids and bases through the sediment pore water. Some diffusion likely has taken place because the sediment is permeable and saturated. The relative degree of diffusion of H^+ could be estimated by comparing selectivity coefficients of clays. If clays select H^+ for their exchange sites more than other cations, H^+ should not diffuse far through the pore water because much of it will be adsorbed by clays, lowering the

concentration gradient and creating hydrogen clays. Unfortunately, the selectivity coefficient of H^+ replacing Na^+ (the most abundant cation in Mother Goose Lake water (Schaefer et al., 2008a)) is difficult to determine for clays, and its sign is disputed (e.g. Gilbert and Laudelout, 1965; Foscolos and Barshad, 1969).

On the other hand, the peaks and troughs in slurry pH are sharply preserved, and values range over 3 pH units, from about the pH value of the acidified water in 2005 (3.2 in slurry vs. ~3.0 in lake water) to almost neutral (6.7), although the upper error in measuring the pH at circum-neutral pH values is about 2 pH units. The water in Mother Goose Lake has probably not been much more basic than pH ~6.7 because of the potential for nearly constant input of small amounts of slightly acidified hydrothermal water from Mt. Chiginagak (Table 12). The preservation of large local variation in the slurry pH record (e.g. up to 4.5×10^{-4} M H^+ difference between the upper two samples in MG06-1B and 7.94×10^{-5} M H^+ difference between 65 and 66 cm centered depth in MG07-6) indicates that diffusion of H^+ probably had a minor effect on the slurry pH record. If diffusion was prevalent, the peaks and troughs would be smoothed into rounder multipoint highs and lows, which is not the case.

Some of the sharp differences in $[H^+]$ could reflect post-depositional oxidation/reduction reactions that impacted adjacent sediment differently. The assessment of oxidation-state uncertainty indicates that the average uncertainty is 2.10×10^{-5} M H^+ (Table 11). Therefore, this effect cannot account for the full range of the abrupt shifts in slurry pH.

Other effects on slurry pH Because slurry pH was analyzed using moist sediment, the water content of each sample affected the ratio of sediment to water. Higher water contents decrease the slurry pH values for a given sample. However, because of several feedbacks, the influence on pH is small, about a 0.05 pH unit change for a 100% increase in the ratio of water to sediment, based on the data of Davis (1943). Although pH is a measure of the activity of H^+ in a solution, diluting acidic sediment results in an increase in the dissociation of H^+ from sediment grain surfaces and an increase in the hydrolysis of Al^{3+} (Thomas, 1996). The hydrolysis of Al^{3+} (and Fe^{3+}) adds to the acidity of a solution during dilution by increasing H^+ activity and decreasing OH^- activity (Equations 10-13):

$$Al(H_2O)_6^{3+}{}_{(aq)} \Leftrightarrow Al(H_2O)_5OH^{2+}{}_{(aq)} + H^+{}_{(aq)} \quad (10)$$

$$Al^{3+}{}_{(aq)} + 3OH^-{}_{(aq)} \Leftrightarrow Al(OH)_{3(aq)} \quad (11)$$

$$Al(OH)^{2+}{}_{(aq)} + 2OH^-{}_{(aq)} \Leftrightarrow Al(OH)_{3(aq)} \quad (12)$$

$$Al(OH)_2^+{}_{(aq)} + OH^-{}_{(aq)} \Leftrightarrow Al(OH)_{3(aq)} \quad (13)$$

The combination of dilution, H^+ dissociation, and Al hydrolysis results in ~~b~~uffering" the slurry pH over the range of dilutions used in this study (Davis, 1943; Thomas, 1996).

Salt content can also alter slurry pH values (Thomas, 1996). High salt content results in lower pH values due to the displacement of Al^{3+} from exchange complexes and an increase in the hydrolysis of Al (Ragland and Coleman, 1960). Because the salt content of sediment was not measured in this study, the degree of acidification due to salt can not be quantified. However, the salt content in freshwater Mother Goose Lake sediment is likely neither high nor variable, based on the measurements of dissolved Na and Ca presented in Schaefer et al. (2008a).

Large hydrologic discharges from Mt. Chiginagak and subsequent acidifications of Mother Goose Lake

To acidify water below a pH of 4.4 requires that its bicarbonate-buffering capacity be exceeded. Furthermore, silicate dissolution and alteration consume H^+ around and below pH 4. Bicarbonate and silicate buffering result in threshold pH values that can be used to distinguish between minor and major impacts on the pH of lake water. Sulfate reduction also consumes H^+ and increases the slurry pH of sediment once it is buried. Because the amount of pH increase due to sulfate reduction is unknown, it is not possible to calculate the amount of H^+ needed to lower sediment slurry pH values below 4.4 or 4.0.

The 2005 overflow and acidification as a reference

The 2005 event provides an example of the effect of acidified discharge on slurry pH that can be applied to the rest of the sedimentary sequence. Because Mt. Chiginagak is the only known source of acidity that can overcome the bicarbonate and clay-mineral dissolution buffers, slurry pH values below these buffer pH values indicate times when Mother Goose Lake was acidified by geothermal activity of Mt. Chiginagak similar to the summer of 2005. This assumes that volcanic gases melt and acidify the snow and ice in the crater of Mt. Chiginagak and that the resulting lake spills out of the crater, as in 2005, which may not happen with every geothermal event.

Aerosol plumes, such as the 1998 plume reported by Schaefer et al. (2008a), can also deliver acidity to the lake (e.g. Fulignati et al., 2002; Schiffman et al., 2006). For the acidity to be deposited, the plume must contact the ground or precipitation must result in

wet deposition (e.g. Fulignati et al., 2002), otherwise the hot plume will dissipate into the atmosphere. It is unlikely that a plume from Mt. Chiginagak would intersect Indecision or Volcano Creeks or Mother Goose Lake ~1600 to 2100 m below its summit. If a plume contacted the snow and ice around the peak, the acidified water produced would flow into the crater lake, or into the snow and ice around the peak. Regardless of whether the ice in the crater was melted, melting around the summit alone could result in abundant acidified discharge similar to the 2005 formation of the crater lake and melting of the crater rim ice plug, if a similar flux of heat and acidic gases were vented. In 1929, there may have been a minor acidification event caused by a plume from Mt. Chiginagak (Jaggar, 1932, Simkin and Siebert, 1994; Miller et al., 1998). The elevated fumarolic activity reported in 1929 coincides with a slight decrease in pH to 4.79 in MG06-1B for the year 1926 ±0.9 (there is no measurement from 1929 sediment) (Table 12), which is not low enough to indicate a major event, but provides evidence that the activity of fumaroles may affect the pH of Mother Goose Lake.

Frequency and nature of major acidifications of Mother Goose Lake

Approach to estimating the number of past acidification events Because of the myriad processes that influence slurry pH, such as the influence of oxidation in the laboratory, it is not an exact record of the pH of Mother Goose Lake. Furthermore, Herlihy and Mills (1986) suggest that the pH of lake water may be as much as 2 pH units lower than the pH of sediment pore water at the sediment-water interface. In contrast, the slurry pH of Mother Goose Lake sediment from 2005 and 2006 was only 0.01 pH units higher than the pH of the water at the time of sediment deposition (Schaefer et al., 2008a;

Table 12), suggesting that the slurry pH of Mother Goose Lake sediment is a close approximation of the pH of the lake at the time of sediment deposition. Unfortunately, 2005-2006 is the only direct tie between historical and sediment records. Considering the complicated relation between slurry pH and lake pH, I assume only that, to lower the slurry pH of the sediment below the cut off of bicarbonate buffering (4.4), the lake was most likely at least as acidic as pH 4.4. This criterion probably underestimates the number of major acidification events. Minor events are not unequivocally identifiable in the slurry pH record because they do not overcome the buffering systems in the lake and sediment. For example, any melting due to a hot plume of volcanic aerosols would be diluted by the large volume of snow and ice on Mt. Chiginagak or by the water in the creeks that transport the acidity, as happened in 2005. Only a large event can acidify the lake after this dilution.

In addition to the conservative $[H^+]$ cutoff, gaps in the recovered sediment lead to an underestimate of the number of acidification events. The largest gap is the ~570 years between cores MG06-1B and MG07-6. In addition, three gaps between core segments of core MG07-6 represent about 160 years total. One gap of 8 years in core MG07-6 is within a core section where not enough sediment was available for slurry pH analyses.

If Mother Goose Lake was stratified at the time of acidification, it is possible that an acidified discharge from Mt. Chiginagak would not be recorded in the sediment across the lake. Acidic water could pass over a core site and exit the lake as an overflow or an interflow if the lake was stratified and denser than the melt water. This is unlikely because Mother Goose Lake has a long fetch and, except for near the mouth of Volcano Creek, water profiles from the summer of 2007 show that the lake was well mixed

(Figure 7). Although the reduced, acidic, and saline inflow formed ephemeral overflows and interflows, they dissipated into the lake, leaving the lake well mixed (Figure 7). The lake was also well mixed following the 2005 event (Schaefer et al., 2008a).

However, the major inflow of water from the crater of Mt. Chiginagak has probably fluctuated between deltas as Volcano Creek and Indecision Creek avulse, which has happened at least once since 1983 (Detterman et al., 1983; Schaefer et al., 2008a). Because of the strongly bifurcated bathymetry of Mother Goose Lake (Figure 5), underflows may be more likely to enter separate subbasins, depending on the location of the inflow. However, there is no evidence of underflows in the water profiles, they would probably dissipate like the overflows and interflows (Figure 7). Therefore, overflows, interflows, and underflows have probably not reduced the number of events recorded by the sediment.

A geothermal event at Mt. Chiginagak cannot cause the acidification of Mother Goose Lake without water to carry the acid. While seasonal variations in snow and ice melting may dilute or concentrate the signal slightly, the maritime climate of Mt. Chiginagak probably provides enough water from precipitation and melting to prevent the kind of seasonal variation that would be found in a continental setting. There is no way to account for any seasonal variation both because of the short historical record of precipitation and temperature and the limited precision of the geochronology of the cores. However, Mt. Chiginagak has probably been glaciated over the last ~3800 years, based on limited climate reconstructions along the Gulf of Alaska and Aleutian Islands summarized by Calkin (1988). Therefore, it is unlikely that a single geothermal event would melt all of the ice and snow in the headwaters of Mother Goose Lake. There

should always have been a source of water to transport acidity to Mother Goose Lake. For example, even after the 2005 event, which was registered in the sediment as the lowest slurry pH, and melted almost all of the ice within the crater, ice and snow remained in the headwaters of Indecision Creek (Table 12; Schaefer et al., 2008a).

It generally takes about six residence times for an acidified lake to chemically recover to a steady state (Varekamp, 2003). Six residence times of Mother Goose Lake is about 16 years (Table 13). This estimate is based on the average precipitation at Port Heiden (the closest long-term weather station to Mother Goose Lake (~83 km distant)) spread over the entire drainage basin compared to the volume of the lake. This may be an overestimation of the residence time because it assumes pure mixing and does not account for the higher terrain around Mother Goose Lake where precipitation rates are higher than at Port Heiden. On the other hand, assuming 100% runoff underestimates the residence time because it assumes no water is evapotranspirated and thus overestimates the inflow discharge, roughly countering the elevation-dependent precipitation gradient. The residence time could have been more or less than 16 years if precipitation rates were different in the past, but 16 years seems to be a reasonable estimate of the recovery period of Mother Goose Lake.

Given the average resolution of the slurry pH record (~6.4 years per sample) and the persistence of pH below 4.4 in Mother Goose Lake for 16 years or less, the slurry pH timeseries should record the recovery of Mother Goose Lake between acidification events. If the sediment is acidified for more than about 16 years, it probably reflects either continuous acidification of Mother Goose Lake or multiple discrete inputs of acid. Prolonged acidification could result from an input of meteoric water to the crater lake

when it is still acidic, causing it to overflow, or from multiple events occurring within a short interval of time.

Classification of major acidic hydrologic discharges Because no other slurry pH value is as acidic as the uppermost samples from 2005 and 2006, the 2005 event appears to be unique in the last ~3800 years (Figure 27). However, clay dissolution may not have been completed in this sediment when it was sampled in 2006, so the $[H^+]$ may have decreased slightly over the following few years. But, the 2005 peak $[H^+]$ would most likely still be well above the rest of the peaks in $[H^+]$. To define the slurry $[H^+]$ that constitutes an acidification event, I used the cutoff for the bicarbonate-buffering system (3.98×10^{-5} M H^+, pH 4.4). I classified an acidification event as "highly likely" if the measured slurry $[H^+]$ value minus the oxidation-state uncertainty (2.1×10^{-5} M H^+) was higher than 3.98×10^{-5} M. An event was classified as "likely" for intervals where the measured slurry $[H^+]$ was higher than 3.98×10^{-5} M, and as "possible" for intervals where the slurry $[H^+]$ plus the oxidation-state uncertainty was higher than 3.98×10^{-5} M. Acidifications were considered to represent separate geothermal events only if the slurry $[H^+]$ values were separated by an interval with slurry $[H^+]$ below the cutoff for at least the time it takes the lake to recover (16 years). If the lake was below the slurry $[H^+]$ cutoff for less than 16 years, then it is possible that the crater only needed to be refilled by snowmelt to re-acidify weakly buffered Mother Goose Lake. The number and timing of acidified hydrologic discharges from Mt. Chiginagak defined by these three categories (highly likely, likely, and possible) are summarized in Tables 12 and 14. Over the last

3815 ± 349 years, the slurry pH shows seven highly likely, 12 likely, and 28 possible geothermal events.

Relationship between volcanic activity and acidifications The acidification of Mother Goose Lake could result from only geothermal activity, as in 2005, or from the explosive eruption of Mt. Chiginagak. As discussed above, tephra alone can not acidify Mother Goose Lake. However, an eruption of Mt. Chiginagak accompanied by meltwater would likely acidify Mother Goose Lake. To estimate the number of acidification events that were associated with eruptions, the locations of tephras were compared with the slurry pH record. I considered an acidification to coincide with an eruption if tephras were deposited at the base of a low pH interval, or anytime during the 16 years it takes Mother Goose Lake to recover. Tephras classed as A, B, and C were counted. On the basis of this criterion, only one ―highly likely" event, four ―likely" events, and 11 ―possible" events coincide with a tephra eruption (Tables 6 and 14). This is less than one third of the acidification events. Tephra beds that correlate with acidifications most likely came from Mt. Chiginagak, providing the first tephra-based estimate of the minimum eruptive frequency of the volcano (~1 eruption every 350 years based on ―possible" events that correlate with tephra) .

The most conservative estimate of the frequency of geothermal events is based on the number of ―highly likely" acidifications. Seven geothermal events over ~3074 years (3812 years minus the gaps) represents an average frequency of one event every 439 years. These events were the most similar to the 2005 event based on the slurry pH values, although nowhere in the record does $[H^+]$ decrease to the extent of the 2005

event. The impact of the ―likely" and ―possible" events on Mother Goose Lake was probably minor compared to the seven ―highly likely" events.

CHAPTER 5

SUMMARY AND CONCLUSIONS

This study used the chemical properties of the water in Mother Goose Lake and the sediment deposited in the lake to reconstruct changes in the pH of the lake during the last 3800 years. This record, together with a catalog of 54 tephra falls (Table 6), aids in the on-going hazard assessment of Mt. Chiginagak. One of the 54 tephra in the cores is probably from the caldera-forming eruption of Mt. Aniakchak. Approximately 60% of tephras coincide with very slight decreases in slurry pH values. In 2007, Mother Goose Lake was still acidified from a crater-lake overflow that was initiated in the summer of 2005 (Table 12), and acidic water with abundant dissolved Fe was still entering the Mother Goose Lake through Volcano Creek (Table 3). Because the lake water is generally more neutral and oxidized than the creek, ARD minerals were rapidly precipitated at the mouth of the river (Schaefer et al., 2008a).

Twelve sediment cores were recovered in 2006 and 2007 from Mother Goose Lake (Table 1). Most of the sediment was determined to be disturbed after the cores were split, photographed, described, and the MS was measured. Cores MG06-1B (100.5 cm long) and MG07-6 (508.0 cm long) were selected for further analyses based on their undisturbed, mostly laminated, stratigraphy (Table 1; Figure 12). These two cores are from different subbasins (Figure 5).

$^{239+240}$Pu profiles were measured on two surface cores (MG06-1B and MG07-12), and ^{14}C ages were analyzed on vegetation macrofossils from two longer percussion cores (MG07-2 and MG07-6). Only the uppermost 1 cm of MG07-12 contains detectable

$^{239+240}$Pu (Table 4), indicating that the sediment is disturbed. Likewise, the seven ^{14}C ages from MG07-2 do not show a downcore progression (Figure 10), indicative of pervasive reworking. The $^{239+240}$Pu profile from surface core MG06-1B shows that the peak in atmospheric fallout during 1963-1964 occurs at 52 cm depth (Figure 11), therefore this core contains ~120 years of sediment. The seven ^{14}C ages from core MG07-6 show a regular downcore progression with one outlier (Figure 9). The age model for this core goes back ~3800 years, but the upper ~675 years are missing, so it does not overlap with core MG06-1B.

The sedimentology of the cores did not aid in identifying past acidification events. Sediment deposited during the 2005 acidification event is laminated, as is sediment deposited during periods known to be free of large acidification events (Figure 12), and therefore sedimentology could not be used as an indicator of acidification events. Although the Munsell color of the sediment deposited during the 2005 event is primarily high chroma and value 10YR colors (Table 5), the colors probably change to less-oxidized colors following burial. The MS of the cores was useful to locate tephra beds, but like LOI and bulk density, is controlled by factors other than the pH of the lake. Changes in sedimentary structures, sediment color, MS, LOI, and bulk density do not appear to correlate with acidification events (Tables 5 and 7; Figure 28).

Elemental concentrations in the sediment were measured by EDS with a scanning electron microscope and by bulk and selective dissolution and FAAS. The results show that the elemental composition of sediment varies independently of the pH of Mother Goose Lake, as indicated by slurry pH values. The concentration of S on sediment grains in the uppermost sediment increased along with the 2005 acidification, based on two EDS

transects of MG06-1B sediment, probably due to the deposition of ARD minerals and elemental S. The scanning electron microscope used for EDS analyses is not practical for measuring entire cores. However, an X-ray fluorescence core logger, such as an Itrax scanning XRF, could be used to develop a high-resolution record of S content in the cores. The concentration of selectively extracted Fe, and most elements estimated by EDS, are influenced by factors including both pH and the degree of oxidation. Because the oxidation/reduction history of Mother Goose Lake sediment and water, both at the time of deposition and post-burial, is not known, chemical species whose aqueous concentrations are strongly influenced by oxidation cannot be used to accurately reconstruct the acidity of the lake.

Slurry pH is an accepted method of measuring the acidity of sediment. Although other methods exist, none are as affordable, fast, precise (measuring pH within 0.05 pH units instead of a proxy for approximate pH), or as feasible (e.g. there are insufficient diatoms for a species-based pH reconstruction), as slurry pH. Slurry pH is primarily controlled by the pH of pore water, which is primarily controlled by the pH of the lake at the time of sediment deposition. Buffering systems lead to a step-wise response of lake water to the input of acid. Carbonate buffering forms a sink of acid in lake water around pH 4.4, silicate weathering in sediment neutralizes a large amount of acidity around pH 4, while the oxidation and reduction of Fe in the sediment adds an uncertainty to the slurry $[H^+]$ needed to overcome the buffers because of the release and sequestration of H^+, respectively.

The oxidization state of the core in the laboratory is different than at the time of sediment deposition. To counter the effects of the oxidation state on the consumption

and release of H^+, caused by the oxidation and reduction of Fe, Al, and S, sediment with a similar ORP to the assumed ORP at the time of deposition should be sampled. The border between oxidized and reduced sediment is visible because Fe which should oxidize before Al and S (Stumm and Morgan, 1996), produced a visible color change when oxidized in the core. The ORP in the laboratory air is known, as is the approximate ORP at the base of well-mixed Mother Goose Lake. The reduction due to burial produced an ORP much lower than the ORP at the time of deposition. Therefore, the slurry pH of approximately equal proportions of oxidized and reduced sediment in the core was assumed to provide the best estimate of the pH of the lake at the time of deposition, since their average ORP is most similar to the ORP at the time of deposition. The exact ratio of oxidized to reduced sediment that should be used is dependent on the form(s) of metal hydroxide produced by oxidation and reduction reactions, and the Fe, Al, and sulfate/sulfide concentrations. Using half oxidized and half reduced sediment brings the average ORP of the samples to close to the ORP at the time of deposition, but similarly averaged samples should not be used for the proxies that are more dependent on the oxidation state.

To quantify how close to exactly half oxidized and half reduced each sample was, fully oxidized and fully reduced subsamples were taken from core MG07-6, and their slurry $[H^+]$ was averaged (Figure 6). The results were compared to the main data set for that interval of sediment. The average plus one standard deviation of the difference between $[H^+]$ in samples from the main slurry pH data set from the $[H^+]$ of 50% fully reduced and 50% fully oxidized samples was used as the oxidation-state uncertainty.

Mother Goose Lake has been periodically acidified as geothermal activity involving sulfuric gasses melted ice and snow on Mt. Chiginagak. Tephra fall can also acidify Mother Goose Lake, but not to the degree geothermal activity can (Figures 24 and 27). I considered intervals with slurry [H^+] minus the oxidation-state uncertainty above the threshold of bicarbonate buffering as representing ~~–v~~ery likely" acidification events. For these events, a large discharge of acidified water from Mt. Chiginagak was needed to overcome the bicarbonate buffer. Based on the slurry pH record, there have been seven ~~–v~~ery likely" and 21 other ~~–li~~kely" or ~~–p~~ossible" acidic events at Mother Goose Lake during the past 3800 years (Table 14; Figure 28). This is a minimum estimate because events might coincide with a gap (~740 years total) in the sediment cores, or the lake water pH could have dropped below 4.4 while the sediment pH stayed above 4.4 because of sulfate reduction. Slurry pH does not correlate with any other likely proxies of geothermal events studied (Figure 28).

This study presents the first estimate of the late Holocene geothermal activity of Mt. Chiginagak. This is also the first time, to my knowledge, that slurry pH has been used to reconstruct the geothermal history of a volcano. This tool may be useful for hazard assessments in other volcanically influenced drainages susceptible to acid discharge.

REFERENCES CITED

Armienta, M.A., Vilaclara, G., De la Cruz-Reyna, S., Ramos, S., Ceniceros, N., Cruz, O., Aguayo, A., Arcega-Cabrera, F., 2008. Water chemistry of lakes related to active and inactive Mexican volcanoes. Journal of Volcanology and Geothermal Research 178 (2), 249-258.

Begét, J., Mason, O., Anderson, P., 1992. Age, extent and climatic significance of the c. 3400 BP Aniakchak tephra, western Alaska, USA. The Holocene 2 (1), 51-56.

Borggaard, O.K., 1988. Phase identification by phase dissolution techniques. In: Stucki, J.W., Goodman, B.A., Schwertmann, U. (eds.). Iron in Soils and Clay Minerals. Reidel, Dordrecht.

Burgner, R.L., DiCostanzo, C.J., Ellis, R.J., Harry, G.Y.,Hartman, W.L., Kerns, O.E., Mathisen, O.A., Royce, W.F., 1969. Biological studies and estimates of optimum escapements of sockeye salmon in the major river systems in southwest Alaska. Fisheries Bulletin 67, 405-459.

Chao, T.T., Zhou, L., 1983. Extraction techniques for dissolution of amorphous iron oxides from soils and sediments. Soil Science of America Journal 47, 225-232.

Charles, D.F., Smol, J.P., 1988. New methods for using diatoms and chrysophytes to infer past pH of low-alkalinity lakes. Limnology and Oceanography 33 (6), 1451-1462.

Christenson, B.W., Wood, C.P., 1993. Evolution of a vent-hosted hydrothermal system beneath Ruapehu Crater Lake, New Zealand. Bulletin of Volcanology 55, 547-565.

Coats, R.R., 1950. Volcanic activity in the Aleutian Arc. U.S. Geological Survey Bulletin B 0974-B, 35-49.

Coleman, N.T., Craig, D., 1961. The spontaneous alteration of hydrogen clay. Soil Science 91, 14-18.

Coleman, N.T., Williams, D.E., Nielsen, T.R., Jenny, H., 1951. On the validity of interpretations of potentiometrically measured soil pH. Soil Science Society of America Journal 15, 106-110.

Conkling, B.L., Blancher, R.W., 1989. Glass microelectrode techniques for in situ pH measurements. Soil Society of America Journal 54, 58-62.

Davis, L.E., 1943. Measurements of pH with the glass electrode as affected by soil moisture. Soil Science 56, 405-422.

Davis, R.B., Anderson, D.S., Berge, F., 1985. Palaeolimnological evidence that lake acidification is accompanied by loss of organic matter. Nature 316 (1), 436-438.

Dean, W.E., 1974. Determination of carbonate and organic matter in calcareous sediments and sedimentary rocks by loss on ignition: comparison with other methods. Journal of Sedimentary Petrology 44, 242-248.

Detterman, R.L., Case, J.E., Wilson, F.H., Yount, M.E., Allaway, Jr., W.H., l983. Generalized geologic map, Ugashik, Bristol Bay, and part of Karluk quadrangless, Alaska. U.S. Geological Survey Miscellaneous Field Studies Map MF-1539-A, 1:250,000 scale.

Detterman, R.L., Wilson, F.H., Yount, M.E., Miller, T.P., 1987. Quaternary geologic map of the Ugashik, Bristal Bay, and western part of the Karluk quadrangles, Alaska. U.S. Geological Survey Miscellaneous Investigations Series Map I-1801, 1:250,000 scale.

Dreher, S.T., Eichelberger, J.C., Larsen, J.F., 2005. The petrology and geochemistry of the Aniakchak caldera-forming Ignimbrite, Aleutian Arc, Alaska. Journal of Petrology 46 (9), 1747-1768.

Drever, J.I., 1997. The geochemistry of natural waters: surface and groundwater environments. Prentice-Hall. Upper Saddle River.

Ewert, J.W., Guffanti, M., Murray, T.L., 2005. An assessment of volcanic threat and monitoring capabilities in the United States: Framework for a national volcano early warning system NVEWS. U.S. Geological Survey Open-File Report OF 2005-1164.

Ferris, F.G., Schultze, S., Witten, T.C., Fyfe, W.S., Beveridge, T.J., 1989. Metal interactions with microbial biofilms in acidic and neutral pH environments. Applied and Environmental Microbiology 55, 1249-1257.

Fillpek, L.H., Nordstrom, D.K., Ficklin, W.H., 1987. Interaction of acid mine drainage with waters and sediments of west squaw creek in the West Shasta mining district, California. Environmental Science and Technology 21, 388-396.

Foscolos, A.E., Barshad, I., 1969. Equilibrium constants between both freshly prepared and aged H Montmorillionites and chloride salt solutions. Soil Society of America Proceedings 33, 242-247.

Fromm, P., 1980. A review of some physiological and toxicological responses of freshwater fish to acid stress. Environmental Biology of Fishes 5 (1), 79-93.

Fulignati, P., Sbtana, A., Luperini, W., Greco, V., 2002. Formation of rock coatings induced by the acid fumarole plume of the passively degassing volcano of La Fossa (Vulcano Island, Italy). Journal of Volcanology and Geothermal Research 115, 397-410.

Giggenbach, W.F., 1974. The chemistry of crater lake, Mt. Ruapehu (New Zealand) during and after the 1971 active period. New Zealand Journal of Science 17, 33-45.

Gilbert, M., Laudelout, H., 1965. Exchange properties of hydrogen ions in clays. Soil Science 100, 157-162.

Guilizzoni, P., Lami, A., Marchetto, A., 1992. Plant pigment ratios from lake sediments as indicators of recent acidification in alpine lakes. Limnology and Oceanography 37 (7), 1565-1569.

Heegaard, E., Birks, H.J.B., Telford, R.J., 2005. Relationships between calibrated ages and depth in stratigraphic sequences: an estimation procedure by mixed-effect regression. The Holocene 15 (4), 612-618.

Herlihy, A.T., Mills, A.L., 1985. Sulfate reduction in freshwater sediments receiving acid mine drainage. Applied and Environmental Microbiology 49, 179-186.

Herlihy, A.T., Mills, A.L., 1986. The pH regime of sediments underlying acidified waters. Biogeochemistry 2 (1), 95-99.

Ikuta, K., Suzuki, Y., Kitamura, S., 2003. Effects of low pH on the reproductive behavior of salmonid fishes. Fish Physiology and Biochemistry 28, 407-410.

Jaggar, T.A., 1932. Aleutian eruptions 1930-1932. The Volcano Letter 375, 1-4.

Jørgensen, B.B., 1977. Bacterial sulfate reduction within reduced microniches of oxidized marine sediments. Marine Biology 41 (1), 1432-1793.

Jørgensen, B.B., Fenchel, T., 1974. The sulfur cycle of a marine sediment model system. Marine Biology 24 (3), 189-201.

Karlin, R.E., Abella, S.E.B., 1992. Paleoearthquakes in the Puget Sound region recorded in sediments from Lake Washington, U.S.A.. Science 258 (5088), 1617-1620.

Kienle, J., Swanson, S. E., and Pulpan, H., 1981. Magmatism and subduction in the eastern Aleutian Arc. In: Shimozuru, D. and Yokoyama, I., (eds.), 1981. Arc volcanism: physics and tectonics. IAVCEI symposium, Proceedings. Terra Scientific Publishing Co., Tokyo.

Ketterer, M.E., Watson, B.R., Matisoff, G., Wilson, C.G., 2002. Rapid dating of recent aquatic sediments using Pu activities and $^{240}Pu/^{239}Pu$ as determined by Quadrupole Inductively Coupled Plasma Mass Spectrometry. Environmental science and technology 36 (6), 1307-1311.

Kisslinger, J.B., 1983. Some volcanoes, volcanic eruptions, and earthquakes in the former Russian America. Peter Doroshin's account of volcanic activity and earthquakes between 1840 and 1866. Pacific Northwest Quarterly 74 (2), 59-68.

Küsel, K., Roth, U., Trinkwalter, T., Peiffer, S., 2001. Effect of pH on the anaerobic microbial cycling of sulfur in mining-impacted freshwater lake sediments. Environmental and Experimental Botany 46, 213-223.

Leduc, L.G., Ferroni, G.D., 1994. The chemolithotrophic bacterium *Thiobacillus ferrooxidans*. Federation of European Microbiological Societies Microbiology Reviews 14, 103-120.

Leonard, E.N., Mattson, V.R., Benoit, D.A., Hoke, R.A., Ankley, G.T., 1993. Seasonal variation of acid volatile sulfide concentration in sediment cores from three northeastern Minnesota lakes. Hydrobiologia 271, 87-95.

Lindsay, W.L., 1979. Chemical equilibria in soils. Wiley-Interscience, New York.

Loeppert, R.H., Inskeep, W.P., 1996. Iron. In: Sparks, D.L., Page, A.L., Helmke, P.A., Loeppert, R.H., Soltampour, P.N., Tabatabai, M.A., Johnston, C.T., Summer, M.E., (eds.), SSSA book series: 5: methods of soil analysis: Part 3—Chemical Methods. Soil science society of America and American Society of Agronomy. Madison.

Major, J.J., Newhall, C.G., 1989. Snow and ice perturbation during historical volcanic eruptions and the formation of lahars and floods. Bulletin of Volcanology 52, 1-27.

Manley, W.F., Kaufman, D.S., 2002, Alaska PaleoGlacier Atlas: Institute of Arctic and Alpine Research (INSTAAR), University of Colorado, http://instaar.colorado.edu/QGISL/ak_paleoglacier_atlas, v. 1.

Marshall, C.E., 1964. The physical chemistry and mineralogy of soils: volume I. John Wiley and Sons Inc., New York.

May, H.M., Kinniburgh, D.G., Helmke, P.A., Jackson, M.L., 1986. Aqueous dissolution, solubilities and thermodynamic stabilities of common aluminosilicate clay minerals: Kaolinite and smectites. Geochimica et Cosmochimica Acta 50, 1667-1677.

McGimsey, R.G., Neal, C.A., Dixon, J.P., and Ushakov, S., 2007. 2005 volcanic activity in Alaska, Kamchatka, and the Kurile Islands: Summary of events and response of the Alaska Volcano Observatory. U.S. Geological Survey Scientific Investigations Report 2007-5269.

McGimsey, R.G., Wallace, K.L., 1999. 1997 volcanic activity in Alaska and Kamchatka: Summary of events and response of the Alaska Volcano Observatory. U.S. Geological Survey Open-File Report OF 99-0448.

Miller, T.P., McGimsey, R.G., Richter, D.H., Riehle, J.R., Nye, C.J., Yount, M.E., Dumoulin, J.A., 1998. Catalog of the historically active volcanoes of Alaska. U.S. Geological Survey Open-File Report 98-582.

Miller, T.P., Smith, R.L., 1987. Late Quaternary caldera-forming eruptions in the eastern Aleutian arc, Alaska. Geology 15, 434-438.

Morel, F.M.M., Hering, J.G., 1993. Principles and applications of aquatic chemistry. John Wiley and Sons, New York.

Neal, C.A., McGimsey, R.G., and Chubarova, O., 2004. 2000 volcanic activity in Alaska and Kamchatka: Summary of events and response of the Alaska Volcano Observatory. U.S. Geological Survey Open-File Report 2004-1034.

Nowaczyk, N.R., 2001. Logging of magnetic susceptibility. In: Last, W.M., Smol, J.P. (eds.), Tracking environmental change using lake sediments, Volume 1: Basin analysis, coring, and chronological techniques. Kluwer Academic Publishers, Dordrecht.

Olsen, R.A., Robbins, J.E., 1971. The cause of the suspension effect in resin-water systems. Soil Science of America Journal 35, 260-265.

Pham, A.N., Rose, A.L., Feitz, A.J., Waite, D., 2006. Kinetics of Fe(III) precipitation in aqueous solutions at pH 6.0-9.5 and 25 °C. Geochimica et Cosmochimica Acta 70, 640-650.

Powers, H.A., 1958. Alaska Peninsula-Aleutian Islands. In: Williams, H. (ed.), Landscapes of Alaska. University of California Press, Los Angeles.

Pyle, D.M., 2000. Sizes of volcanic eruptions. In: Sigurdsson, H., Houghton, B.F., McNutt, S.R., Rymer, H., Stix, J. (eds.), Encyclopedia of volcanoes. Academic Press, San Diego.

Ragland, J.L., Coleman, N.T., 1960. The hydrolysis of aluminum salts in clay and soil systems. Soil Science Society of America Journal 24, 457-460.

Riehle, J.R., Meyer, C.E., Miyaoka, R.T., 1999. Data on Holocene tephra (volcanic ash) deposits in the Alaska Peninsula and lower Cook Inlet region of the Aleutian volcanic arc, Alaska. United States Geological Survey Open-File Report 99-135. http://www.avo.alaska.edu/dbases/akpen_tephra/akpen_tephra.html

Ryan, D.F., Kahler, D.M., 1987. Geochemical and mineralogical indications of pH in lakes and soils in central New Hampshire in the early Holocene. Limnology and Oceanography 32 (3), 751-757.

Scheffer, F., Schanchtschabel, P., 1989. Lehrbuch der Bodenkunde. Enke Verlag, Stuttgart.

Schaefer, J., Nye, C.J., 2002. Historically active volcanoes of the Aleutian Arc. Alaska Division of Geological & Geophysical Surveys Miscellaneous Publication MP 0123.

Schaefer, J.R, Scott, W.E., Evans, W.C., Jorgenson, J., McGimsey, R.G., Wang, B., 2008a. The 2005 catastrophic acid crater lake drainage, lahar, and acidic aerosol formation at Mount Chiginagak volcano, Alaska, USA: Field observations and preliminary water and vegetation chemistry results. Geochemistry Geophysics Geosystems 9 (7), Q07018, doi:10.1029/2007GC001900.

Schaefer, J.R., Wallace, K.L., Kassel, C.M., 2008b. Preliminary bathymetric map of Mother Goose Lake, Alaska Peninsula. Alaska Division of Geological & Geophysical Surveys Raw Data File 2008-3, 1 disk.
http://www.dggs.dnr.state.ak.us/pubs/pubs?reqtype=citation&ID=16301

Schiffman, P., Southard, R.J., 1996. Cation exchange capacity of layer silicates and palagonitized glass in mafic volcanic rocks: a comparative study of bulk extraction and in situ techniques. Clays and Clay Minerals 44 (5), 624-634.

Schiffman, P., Zierenberg, R., Marks, N., Bishop, J.L., Dyar, M.D., 2006. Acid-fog deposition at Kilauea volcano: A possible mechanism for the formation of siliceous-sulfate rock coatings on Mars. Geology 34 (11), 921-924.

Scroth, A.W., Parnell Jr., R.A., 2005. Trace metal retention through the schwertmannite to goethite transformation as observed in a field setting, Alta Mine, MT. Applied Geochemistry (20), 907-917.

Sherlock, E.J., Lawrence, R.W., Poulin, R., 1995. On the neutralization of acid rock drainage by carbonate and silicate minerals. Environmental Geology 25 (1), 43-54.

Siever, R., Garrels, R.M., Kanwisher, J., Berner, R.A., 1961. Interstitial waters of recent marine muds off Cape Cod. Science 134 (3485), 1071-1072.

Sigurdsson, H., 1977. Chemistry of the crater lake during the 1971-72 Soufriere eruption. Journal of Volcanology and Geothermal Research 2, 165-186.

Simkin, T., Siebert, L., 1994. Volcanoes of the world [2nd edition]. Geoscience Press, Tucson.

Sriwana, T., van Bergen, M.J., Sumarti, S., de Hoog, J.C.M., van Os, B.J.H., Wahyuningsih, R., Dam, M.A.C., 1998. Volcanogenic pollution by acid water discharges along Ciwidey River, West Java (Indonesia). Journal of Geochemical Exploration 62, 161-182.

Stewart, C., Johnston, D.M., Leonard, G.S., Horwell, C.J., Thordarson, T., Cronin, S.J., 2006. Contamination of water supplies by volcanic ashfall: A literature review and simple impact modeling. Journal of Volcanology and Geothermal Research 158, 296-306.

Stuiver, M., Reimer, P.J., 1993. Extended ^{14}C data base and revised CALIB 3.0 ^{14}C age calibration program. Radiocarbon 35, 215-230.

Stumm, W., Morgan, J.J., 1996. Aquatic chemistry: chemical equalibria and rates in natural waters [Third edition]. Environmental Science and Technology Series, Wiley-Interscience, New York.

Swoboda, A.R., Kunze, G.W., 1968. Reactivity of montmorillonite surfaces with weak organic bases. Soil Science Society of America Journal 32, 806-811.

Thomas, G.W., 1996. Soil pH and soil acidity. In: Sparks, D.L., Page, A.L., Helmke, P.A., Loeppert, R.H., Soltampour, P.N., Tabatabai, M.A., Johnston, C.T., Summer, M.E., (eds.), SSSA book series: 5: methods of soil analysis: Part 3—Chemical Methods. Soil science society of America and American Society of Agronomy. Madison.

Varekamp, J.C., 2008. The volcanic acidification of glacial Lake Caviahue, Province of Neuquen, Argentina. Journal of Volcanology and Geothermal Research 178 (2), 184-196.

Varekamp, J.C., 2003. Lake contamination models for evolution towards steady state. Journal of Limnology 62 (suppl. 1), 67-72.

Varekamp, J.C., Pasternack, G.B., Rowe Jr., G.L., 2000, Volcanic lake systematics II. Chemical constraints. Journal of Volcanology and Geothermal Research 97, 161-179.

Verosub, K.L., Roberts, A.P., 1995. Environmental magnetism: Past present and future. Journal of Geophysical Research 100 (B2), 2175-2192.

Ward, D.M., Winfrey, M.R., 1985. Interactions between methanogenic and sulfate-reducing bacteria in sediments. Advances in Aquatic Microbiology 3, 141-179.

Waythomas, C.F., Neal, C.A., 1998. Tsunami generation by pyroclastic flow during the 3500-year B.P. caldera-forming eruption of Aniakchak Volcano, Alaska. Bulletin of Volcanology 60, 110-124.

Whiticar, M.J., Faber, E., Schoell, M., 1986. Biogenic methane formation in marine and freshwater environments: CO_2 reduction vs. acetate fermentation-Isotope evidence. Geochimica et Cosmochimica Acta 50 (5), 693-709.

Williamson, M.A., Parnell, R.A., 1994. Partitioning of copper and zinc in the sediments and porewaters of a high-elevation alkaline lake, east-central Arizona, U.S.A.. Applied Geochemistry 9 (5), 597-608.

Witham, C.S., Oppenheimer, C., Horwell, C.J., 2005. Volcanic ash-leachates: a review and recommendations for sampling methods. Journal of Volcanology and Geothermal Research 141, 299-326.

Wolfe, B.B., Hall, R.I., Last, W.M., Edwards, T.W.D., English, M.C., Karst-Riddoch, T.L., Paterson, A., Palmini, R., 2006. Reconstruction of multi-century flood histories from oxbow lake sediments, Peace-Athabasca Delta, Canada. Hydrological Processes 20, 4131-4153.

Young, L.B., Harvey, H.H., 1992. Geochemistry of Mn and Fe in lake sediments in relation to lake acidity. Limnology and Oceanography 37 (3), 603-613.

Table 1. Overview of sediment cores from Mother Goose Lake, 2006 and 2007.

Core (MG)	Location[a]		Water depth (m)	Length (cm)	Tephra (#)	Analyses completed	Notes
	Lat (°)	Long (°)					
06-1A	57.21017	-157.29443	~31	46.0	N/A	MS profile, photographs, and preliminary whole rock Fe, Ni, Mn, Na, and K measurements	Surface core
06-1B	57.21017	-157.29443	~31	100.5	N/A	MS profile, photographs, pu inventory, and preliminary slurry pH measurements	Surface core
07-2	57.20635	-157.29163	31.7	558.5	15	MS profile, photographs, description sheets, and radiocarbon dating	Long core; significantly disturbed sediment
07-2A	57.20635	-157.29163	31.7	49.0	N/A	Photographs	Surface core
07-2B	57.20635	-157.29163	31.7	39.5	N/A	Separated into 0.5 cm depth intervals	Surface core; field sampled into 0.5 cm intervals
07-6	57.18736	-157.30644	33.7	508.0	53	MS profile, photographs, description sheets, radiocarbon dating, preliminary active iron, and slurry pH measurements	Focus of research; long Core, aka MG07-13A
07-6A	57.18736	-157.30644	33.7	N/A	N/A	N/A	Surface core; aka MG07-13B, destroyed in shipping
07-10	57.19658	-157.33096	48.1	62.0	N/A	MS profile, photographs, and description sheets	Long core; mostly disturbed sediment
07-10B	57.19658	-157.33096	48.1	47.0	N/A	Photographs	Surface core; unknown (sub decimeter) amount of sediment lost from top after dropped in field
07-11	57.19691	-157.33174	48.0	280.5	N/A	MS profile, photographs, and description sheets	Long core; mostly disturbed sediment
07-12	57.19679	-157.33127	46.4	150.0	N/A	Photographs and description sheets	Long core; mostly disturbed sediment
07-12B	57.19679	-157.33127	46.4	45.0	4	MS profile, photographs, description sheet, Pu inventory	Surface core

[a]Coordinates based on Alaska NAD 27 datum

Table 2. Summary of radiocarbon samples from MG07-2 and MG07-6.

Lab ID[a]	Centered tube depth (cm)[b]	Mass (mg)	^{14}C age (years BP)	2σ ± (^{14}C years)	Median probability age (cal yr BP)[c]	2σ age range (cal yr BP)	Material type
Core MG07-2							
47688	41.5	6.3	2305	50	2338	2329-2349	Grass, leaves, and twigs
46079	225.0	14.9	385	30	476	334-502	Wood
47689	313.5	24.4	800	30	711	686-733	Leaves and aquatic and terrestrial grass
46080	326.5	3.7	70	320	173	-6-457	Charred grassy plant
46081	385.5	7.1	165	30	189	-2-284	Leaves
46082	482.5	5.1	640	30	590	560-661	Seedpods, aquatic macrofossils, grass, leaf, and wood
46083	511.0	3.3	500	200	526	316-665	Wood and leaf fragments
Core MG07-6							
46073	66.5	2.9	1060	120	978	798-1168	Wood, aquatic macro fossils, and grass
46074	135.0	3.3	1430	30	1323	1300-1348	Grass, aquatic macrofossils, leaves, and seedpods
46075	179.5	7.3	1685	40	1585	1534-1689	Aquatic macrofossils, leaves, wood, and grass
46076	304.5	6.1	2985	40	3177	3078-3250	Charred leaves, aquatic macro fossils, and small amount of wood
47690	365.0	3.9	2480	140	2480	2360-2726	Seedpods, leaf fragments, and aquatic macrofossils
46077	404.5	12.5	2895	30	3027	2960-3077	Leaves
46078	488.5	4.0	3390	160	3639	3451-3837	Charred leaves, aquatic macro fossils, and one twig

[a] Radiocarbon ages analyzed at the Keck Carbon Cycle AMS Facility at the University of California at Irvine.
[b] Each sample = 1 cm thick
[c] Calibrations calculated with Caleb v5.0.1 using the IntCal04 calibration (Stuiver and Reimer, 1993)

Table 3. Water samples collected in 2007.

Sample[a]	Date	Time	Location description	Water temperature (˚C)	pH	Conductivity (µs/cm)	Total Fe (ppm)	Fe (II) (ppm)	Fe (III) (ppm)	Latitude (˚N)[b]	Longitude (˚W)[b]
A-a	8/13/2007	18:08	Between spit and island between Volcano Creek and Indecision Creek inflows	17.8	4.26	215	N/A	N/A	N/A	57.19696	157.26732
B-a	8/13/2007	18:25	Volcano creek inflow, several meters upstream of mixing point	12.8	3.39	466	58.7	56.9	1.8	57.20436	157.27284
C-a	8/13/2007	19:18	Core site MG07-2, 0m depth, 31.7 m of water	14.8	4.42	205	0.2	0.2	0.0	57.20635	157.29163
C-b	8/13/2007	~19:30	Core site MG07-2, 5m depth, 31.7 m of water	13.3	4.33	208	0.2	0.3	0.0	57.20635	157.29163
C-c	8/13/2007	~19:35	Core site MG07-2, 7m depth, 31.7 m of water	13.3	3.68	316	1.9	1.6	0.3	57.20635	157.29163
C-d	8/13/2007	~19.40	Core site MG07-2, 30m depth, 31.7 m of water	9.7	4.27	243	0.2	0.0	0.2	57.20635	157.29163
D-a	8/14/2007	16:23	Rocky shore of island, ~1 m offshore in ~30 cm of water	13.8	4.45	211	0.2	0.2	0.0	57.19858	157.29921
E-a	8/15/2007	12:20	Water profile, 0m depth, 39 m of water	13.2	4.44	204	N/A	N/A	N/A	57.19645	157.32701
F-a	8/15/2007	17:00	Surface water of Volcano Creek sediment plume, off sandbar, weather prevented collecting other data	N/A	N/A	N/A	27.4	17.5	9.9	57.20562	157.27288
F-b	8/22/2007	14:22	Surface water of Volcano Creek sediment plume, off sandbar, plume much smaller than 8/15/2008, ~50 cm of water	9.5	3.51	329	3.4	0.3	3.1	57.20562	157.27288

Sample[a]	Date	Time	Location description	Water temperature (˚C)	pH	Conductivity (µs/cm)	Total Fe (ppm)	Fe (II) (ppm)	Fe (III) (ppm)	Latitude (˚N)[b]	Longitude (˚W)[b]
G-a	8/16/2007	17:20	Core site, water profile, 0m depth, 48.1 m of water	14.3	4.35	184	N/A	N/A	N/A	57.19658	157.33096
G-a1	8/17/2007	18:20	Water from top of short core, just above sediment/water interface, did not collect data due to limited sample size, **split into two samples G-b (surface) and G-c (base))**	N/A	N/A	N/A	N/A	N/A	N/A	57.19658	157.33096
G-b	8/16/2007	19:20	Surface fraction of G-a1	N/A	N/A	N/A	0.3	0.2	0.0	57.19658	157.33096
G-c	8/16/2007	20:20	Bottom fraction of G-a1	N/A	N/A	N/A	0.0	0.0	0.0	57.19658	157.33096
H-c	8/21/2007	16:30	Surface water, site of core MG07-6, 33.7 m of water	13.0	4.22	240	0.2	0.1	0.0	57.18736	157.30644
H-d	8/21/2007	16:30	**(Sample analyzed 3 hr after collection**) 0.4 m above sediment, site of core MG07-6	15.2	4.48	180	0.6	0.6	0.0	57.18736	157.30644
I-a	8/22/2007	12:20	Surface water, water profile at buoy deployment, 32 m of water	13.0	4.27	185	0.2	0.0	0.3	57.20764	157.29756
I-b	8/22/2007	12:20	12.5m depth, water profile at buoy deployment, 32 m of water	12.1	4.15	185	0.2	0.0	0.5	57.20764	157.29756
J-a	8/22/2007	13:20	Surface water, water profile J	13.2	4.35	183	0.2	0.0	0.2	57.20609	157.28904
J-b	8/22/2007	13:20	14 m depth, water profile J	12.1	4.03	203	0.3	0.0	0.5	57.20609	157.28904
K-a	8/22/2007	15:40	~300 m from Volcano Creek inflow, very wavy, measured 15 min after collection	14.6	4.34	188	0.2	0.0	0.2	57.20651	157.22270

Sample[a]	Date	Time	Location description	Water temperature (˚C)	pH	Conductivity (µs/cm)	Total Fe (ppm)	Fe (II) (ppm)	Fe (III) (ppm)	Latitude (˚N)[b]	Longitude (˚W)[b]
L-a	8/22/2007	22:29	Needle Lake near inflow	18.3	7.29	100	0.0	0.0	0.0	57.14960	157.17803

[a]Site location – sample letter
[b]Coordinates based on Alaska NAD-27 datum

Table 4. $^{239+240}$Pu activity for cores MG06-1B and MG07-12.

Depth (cm)	$^{239+240}$Pu (Bq/kg)	± (Bq/kg)
MG06-1B		
0.0-1.0	0	N/A
9.5-10.5	0.15	0.01
14.5-15.5	0.16	0.01
19.5-20.5	0.20	0.02
24.5-25.5	0.40	0.02
29.5-30.5	0.19	0.01
34.5-35.5	1.42	0.08
39.5-40.5	2.23	0.04
44.5-45.5	1.34	0.06
46.5-47.5	1.46	N/A
48.5-49.5	2.48	N/A
49.5-50.5	2.55	0.04
50.5-51.5	2.81	N/A
51.5-52.5	3.13	N/A
53.5-54.5	0.16	N/A
54.5-55.5	0	N/A
MG07-12		
0.0-0.5	0.21	0.03
0.5-1.0	0.05	0.01
1.0-1.5	< 0.03	N/A
1.5-2.0	< 0.03	N/A
2.0-2.5	< 0.03	N/A
2.5-3.0	< 0.03	N/A
3.0-3.5	< 0.03	N/A
3.5-4.0	< 0.03	N/A
4.0-4.5	< 0.03	N/A
4.5-5.0	< 0.03	N/A
5.0-5.5	< 0.03	N/A
5.5-6.0	< 0.03	N/A
6.0-6.5	< 0.03	N/A
6.5-7.0	< 0.03	N/A
8.0-8.5	< 0.03	N/A
10.0-10.5	< 0.03	N/A
19.0-19.5	< 0.03	N/A
19.5-20.0	< 0.03	N/A
20.0-20.5	< 0.03	N/A
21.0-21.5	< 0.03	N/A
27.5-28.0	< 0.03	N/A

Table 5. Munsell colors of beds in cores MG06-1B and MG07-6. Color numbers (1-4) do not reflect any order.

Section	Tube depth (cm)		Color one			Color two			Color three			Color four		
	Start	End	Hue	Value	Chroma	Hue	Value	Chroma	Hue	Value	Chroma	Hue	Value	Chroma
MG06-1B	0	1.5	10YR	2	1	10YR	7	1						
N/A	1.5	5	10YR	8-5	8	10YR	5	4-6						
N/A	5	26	10YR	7	1-2	10YR	8	1	10YR	2	1	10YR	4	2
N/A	26	30	10YR	5	4-6	10YR	3	1						
N/A	30	40.5	5YR	3-2.5	1	5YR	7	1-2						
N/A	40.5	49	5YR	4-5	1									
N/A	49	52.5	10YR	7	3-4									
N/A	52.5	57.5	10YR	6	4	10YR	2-3	1						
N/A	57.5	60	10YR	6-7	4									
N/A	60	63	10YR	5	4-6	5Y	2.5	0						
N/A	63	79	5YR	5-6	1									
N/A	79	82	5YR	3-4	2	5Y	2.5	0						
N/A	82	85	10YR	6-8	2	5Y	2.5	0						
N/A	85	86	5Y	2.5	0									
N/A	86	87	5YR	5	1	5YR	2.5	1						
N/A	87	88	5YR	3	2									
N/A	88	92.5	10YR	8-6	3	10YR	6	1						
N/A	92.5	101	5YR	2.5	1	10YR	7-6	3						
MG07-6														
Top	0	2	5Y	2.5	1	10YR	5-8	1						
Top	2	8	5Y	2.5	1	10 YR	7	4						
Top	8	10.5	5Y	2.5	0-1									
Top	10.5	14	5Y	2.5	1	10 YR	7	4						
Top	14	15	5Y	2.5	0-1									

Section	Tube depth (cm)		Color one			Color two			Color three			Color four		
	Start	End	Hue	Value	Chroma	Hue	Value	Chroma	Hue	Value	Chroma	Hue	Value	Chroma
Top	15	46.5	5Y	2.5	1	10 YR	7	4						
Middle (upper half)	48.5	52.5	5YR	4	2									
Middle (upper half)	52.5	53.5	10YR	8	2									
Middle (upper half)	53.5	98	5Y	2.5	1	10YR	8	1	5YR	4	2			
Middle (upper half)	98	99	10YR	5	6									
Middle (upper half)	99	104	5Y	2.5	1	10YR	8	1	5YR	4	2			
Middle (upper half)	104	105.5	10YR	5	6									
Middle (upper half)	105.5	122.5	5Y	2.5	1	10YR	8	1	5YR	4	2			
Middle (upper half)	122.5	122.6	5Y	2.5	0									
Middle (upper half)	122.6	148.5	5Y	2.5	1	10YR	8	1	5YR	4	2			
Middle (upper half)	148.5	158.5	5YR	5-8	1									
Middle (upper half)	158.5	162.5	10YR	6	1									
Middle (upper half)	162.5	167.5	10YR	7	1									
Middle (upper half)	167.5	168.5	10YR	5	1									

Middle (upper half)	168.5	182.5	10YR	8	1	5YR	4	2				
Middle (upper half)	182.5	182.6	5Y	2.5	0							
Middle (upper half)	182.6	187	10YR	8	1	5YR	4	2				
Middle (lower half)	197	209.5	5Y	2.5	1	10YR	5-8	1				
Middle (lower half)	209.5	210	5Y	2.5	0							
Middle (lower half)	210	232	5Y	2.5	1	10YR	5-8	1				
Middle (lower half)	232	239	10YR	6	3	10YR	6	1	10YR	7	6	
Middle (lower half)	239	248	5Y	2.5	1	10YR	5-8	1				
Middle (lower half)	248	249	5Y	2.5	0							
Middle (lower half)	249	258	5Y	2.5	1	10YR	5-8	1				
Middle (lower half)	258	259	5YR	7	2							
Middle (lower half)	259	278	5Y	2.5	1	10YR	5-8	1				

Section	Tube depth (cm)		Color one			Color two			Color three			Color four		
	Start	End	Hue	Value	Chroma	Hue	Value	Chroma	Hue	Value	Chroma	Hue	Value	Chroma
Lower	289	299	10YR	6	2	10YR	6	4						
Lower	299	301	5Y	2.5	0									
Lower	301	306	10YR	7	6	10YR	6	1						
Lower	306	309	10YR	7	4									
Lower	309	310	5Y	2.5	0									
Lower	310	359	10YR	6	3	10YR	4	1	5Y	5	2	5YR	6	2
Lower	359	361	5Y	2.5	0									
Lower	361	379	5Y	6	2	5YR	7	2	10YR	4	1			
Lower	379	381	5Y	2.5	0									
Lower	381	389	5Y	6	2	5YR	7	2	10YR	4	1			
Lower	389	392	10YR	6	2	10YR	5	3						
Lower	392	400	GAP											
Lower	400	421	10YR	6	4	10YR	7	4	10YR	5	1	5YR	7	3
Lower	421	422	5Y	2.5	0									
Lower	422	463	10YR	6	1	10YR	3	1	10YR	6	3	5YR	6	2
Lower	463	471	5Y	2.5	0									
Lower	471	472	5YR	8	3									
Lower	472	486	5YR	7	1	5YR	5	3	10YR	7	4			
Lower	486	490	5Y	2.5	0	5YR	7	3						
Lower	490	508	10YR	6	1-4	10YR	3	1	5YR	6	1	5YR	5	4

Table 6. Tephra inventory of cores MG06-1B and MG07-6.

Centered depth (cm)	Layer thickness (cm)	Age (years before 2006)	Confidence[a]	Pure tephra
MG06-1B				
81.5	1.0	97.8	A	x
87.5	1.0	105	A	x
MG07-6				
0.5	1.0	678	A	x
9.3	1.5	717	A	x
14.8	0.5	741	A	
18.3	1.5	758	C	
20.8	0.5	771	B	
29.3	0.5	817	C	
30.7	0.3	825	C	
31.3	0.5	828	C	
33.3	1.5	839	C	
41.8	0.5	884	C	
63.3	0.5	999	C	
79.8	0.5	1087	C	
81.3	0.5	1095	C	
93.0	1.0	1159	C	
122.7	0.3	1317	A	
136.3	0.5	1389	C	
148.8	0.5	1457	B	
168.0	1.0	1559	A	
172.8	0.5	1582	C	
173.8	0.5	1587	A	
182.3	0.5	1632	C	
205.2	0.6	1759	A	x
209.6	0.4	1782	C	
210.1	0.6	1784	C	
215.1	0.7	1811	B	
216.3	0.4	1819	B	
231.4	0.3	1905	C	
231.8	0.1	1907	C	
235.8	0.5	1931	C	
236.8	0.5	1936	A	x
239.9	0.2	1954	A	x
247.8	0.6	1997	B	
262.2	0.3	2081	B	
262.8	0.5	2085	B	
273.3	0.5	2149	A	x
299.8	1.5	2310	C	
309.3	0.5	2367	B	
312.3	0.5	2387	C	

Centered depth (cm)	Layer thickness (cm)	Age (years before 2006)	Confidence[a]	Pure tephra
319.8	1.5	2437	A	x
325.0	1.0	2470	A	x
332.8	0.5	2522	A	x
339.5	1.0	2567	C	
378.8	0.5	2850	C	
380.3	0.5	2861	A	x
388.0	1.0	2920	B	
415.5	1.5	3135	A	x
421.8	0.5	3184	A	x
425.9	0.2	3214	A	x
426.5	0.2	3217	B	
449.8	0.5	3408	A	x
466.3	8.5	3510	C	
493.3	0.5	3702	A	x

[a]„A', 'B', and 'C' were qualitatively used to indicate: certain, probable, and possible tephras, respectively, based on high magnetic susceptibility, the presence of apparent grains (~medium ash to fine lapillus), and color shifts.

Table 7. Active iron concentrations, bulk density, and loss on ignition for cores MG06-1B and MG07-6.

Centered depth (cm)[a]	Mass wet sediment (mg)	Solid content (%)	Loss on Ignition (%)	Mass of dry sample (mg)	Active iron sediment (mg/kg)	Average active iron (mg/kg)	Standard deviation (mg/kg)	Standard deviation plus bulk density error (25%)[b]
MG06-1B								
0.8	500			Unknown	12570			
0.8	500	Unknown	Unknown	Unknown	11800	11740	860	3060
0.8	500			Unknown	10860			
2.3	500			Unknown	13410			
2.3	500	Unknown	Unknown	Unknown	12280	13290	960	3460
2.3	500			Unknown	14190			
3.8	498			Unknown	13460			
3.8	538	Unknown	Unknown	Unknown	13970	13510	440	3410
3.8	482			Unknown	13090			
5.3	451			Unknown	13180			
5.3	470	Unknown	Unknown	Unknown	14610	14090	790	3610
5.3	502			Unknown	14480			
6.8	572			Unknown	12240			
6.8	508	Unknown	Unknown	Unknown	12200	12570	610	3200
6.8	485			Unknown	13270			
9.8	500			Unknown	11980			
9.8	500	Unknown	Unknown	Unknown	12380	11960	440	3020
9.8	500			Unknown	11510			
20.3	466			Unknown	12090			
20.3	588	Unknown	Unknown	Unknown	12120	12470	630	3180
20.3	547			Unknown	13190			
57.8	490			Unknown	18710			
57.8	486	Unknown	Unknown	Unknown	17850	18010	640	4550

Centered depth (cm)[a]	Mass wet sediment (mg)	Solid content (%)	Loss on Ignition (%)	Mass of dry sample (mg)	Active iron sediment (mg/kg)	Average active iron (mg/kg)	Standard deviation (mg/kg)	Standard deviation plus bulk density error (25%)[b]
57.8	500			Unknown	17470			
MG07-6								
0.25	396			228	44110			
0.25	419	57.5	7.1	241	37070	38720	4790	N/A
0.25	630			362	34970			
20.25	634			235	73100			
20.25	528	37.1	8.8	196	72160	73340	1310	N/A
20.25	400			149	74750			
40.25	630			270	74480			
40.25	585	42.9	8.1	251	88420	78090	9080	N/A
40.25	842			361	71380			
65.25	592			243	75330			
65.25	699	41.1	8.2	287	69270	69450	5800	N/A
65.25	395			162	63740			
70.75	508			200	101790			
70.75	572	39.5	9.0	226	108230	91750	23190	N/A
70.75	666			263	65230			
78.25	469			184	78340			
78.25	506	39.3	8.5	199	67880	64890	15170	N/A
78.25	831			326	48450			
99.75	658			258	52240			
99.75	564	39.2	8.6	221	54140	50230	5210	N/A
99.75	750			294	44310			
109.75	465			167	76660			
109.75	637	36	8.7	229	79850	68980	16150	N/A
109.75	770			277	50410			

Centered depth (cm)[a]	Mass wet sediment (mg)	Solid content (%)	Loss on Ignition (%)	Mass of dry sample (mg)	Active iron sediment (mg/kg)	Average active iron (mg/kg)	Standard deviation (mg/kg)	Standard deviation plus bulk density error (25%)[b]
127.75	601			261	89510			
127.75	546	43.4	8.2	237	86960	82110	10690	N/A
127.75	505			219	69850			
160.75	644			381	40500			
160.75	476	59.1	6.7	281	44870	42370	2250	N/A
160.75	645			381	41740			
202.25	513			178	40650			
202.25	509	34.7	8.4	177	37410	44310	9290	N/A
202.25	524			182	54870			
217.25	543			217	44870			
217.25	476	40	8.7	190	44020	45340	1620	N/A
217.25	536			214	47140			
222.75	478			193	55230			
222.75	556	40.3	7.9	224	57290	53420	5020	N/A
222.75	527			212	47750			
225.75	504			195	81970			
225.75	558	38.8	7.5	216	81610	78510	5690	N/A
225.75	531			206	71940			
227.25	640			265	38870			
227.25	536	41.4	8.2	222	37600	38230	640	N/A
227.25	601			249	38220			
257.75	561			245	62090			
257.75	530	43.6	7.7	231	74110	65870	7150	N/A
257.75	558			244	61410			
267.25	508			223	70630			
267.25	687	43.9	8.0	301	49520	55620	13080	N/A

Centered depth (cm)[a]	Mass wet sediment (mg)	Solid content (%)	Loss on Ignition (%)	Mass of dry sample (mg)	Active iron sediment (mg/kg)	Average active iron (mg/kg)	Standard deviation (mg/kg)	Standard deviation plus bulk density error (25%)[b]
267.25	542			238	46700			
299.25	616			327	31730			
299.25	544	53	6.9	289	28920	30850	1670	N/A
299.25	568			301	31900			
352.25	758			304	41870			
352.25	403	40.1	7.7	162	36840	39900	2690	N/A
352.25	663			266	41000			
363.75	527			197	72470			
363.75	524	37.3	8.7	196	68260	67390	5560	N/A
363.75	573			214	61450			
379.25	646			269	46230			
379.25	571	41.6	8.3	237	47880	47520	1150	N/A
379.25	541			225	48450			
429.25	470			167	60640			
429.25	530	35.6	8.9	188	64800	61340	3160	N/A
429.25	699			249	58590			
494.25	491			186	46520			
494.25	547	37.9	8.2	208	40670	43160	3020	N/A
494.25	506			192	42300			
Blank				0	0			
Blank	N/A	N/A	N/A	0	0	0	0	N/A
Blank				0	0			

[a]Sample thicknesses = 1.6 cm (MG06-1B); 0.5 cm (MG07-6)

[b]Because there was not enough material to measure bulk density in core MG06-1B, an additional 25% error was added to the standard deviation to account for the uncorrected sample mass, using the sum of the squares method.

Table 8. Bulk sediment chemistry of MG06-1B.

Sample depth (cm)		Fe (mg/ kg)	Ni (mg/ kg)	Mn (mg/ kg))	Na (mg/ kg))	K (mg/ kg)	Mg (mg/ kg)	Zn (mg/ kg)
Top	Bottom							
MG06-1B								
0.0	0.3	64	0	0	15	12	8	0
1.0	1.8	43	0	0	17	13	8	0
2.0	2.3	54	0	1	17	14	9	0
4.0	4.3	58	0	1	16	12	9	0
8.0	9.0	59	0	1	20	23	10	0
14.0	15.0	53	0	1	18	13	10	0
18.0	19.0	63	0	1	17	11	10	0
22.0	22.5	56	0	1	17	12	10	0
26.5	27.5	59	0	2	15	12	9	0
30.5	31.0	64	0	1	13	10	9	0
32.0	32.5	64	0	1	17	12	10	0
38.0	39.0	59	0	1	19	14	11	0
40.0	41.0	52	0	1	20	13	11	0
47.0	48.0	48	0	1	22	13	13	0
52.5	53.0	62	0	1	19	12	11	0
57.0	57.5	54	0	1	17	11	10	0
61.5	61.8	64	0	1	18	12	11	0
66.0	67.0	48	0	1	20	14	11	0
75.0	76.0	47	0	1	21	14	13	0
81.0	82.0	44	0	1	24	10	15	0
84.0	84.5	55	0	1	20	14	13	0
93.5	94.0	50	0	1	19	13	11	0
Replicates								
18	19	54	0	0	16	11	10	0
38	39	58	0	1	19	13	11	0
40	41	56	0	1	18	12	11	0
66	67	46	0	1	21	18	11	0
81	82	43	0	1	25	11	16	0
Standards								
Centerville Diabase W2		1	0	1	19	7	35	0
Peridotite PCC-1		1	2	1	0	0	279	0
Icelandic Basalt BIR1		2	0	1	15	0	67	0
Granodiorite GSP-1		29	0	0	21	46	5	0
Andesite AGV-1		1	0	1	34	28	9	0
2709		1	0	1	13	22	15	0
SDO-1		1	0	0	4	30	9	0
Blanks								
Blank A	Blank A	0	0	0	0	0	0	0
Blank B	Blank B	0	0	0	0	0	0	0
Blank C	Blank C	0	0	0	0	0	0	0
Blank D	Blank D	0	0	0	0	0	0	0

Table 9. Errors for replicate and standard bulk sediment chemistry analyses.

Sample depth (cm) Top	Bottom	Fe (%)	Ni (%)	Mn (%)	Na (%)	K (%)	Mg (%)	Zn (%)	Average (%)	Average (No Ni) (%)
Replicates										
18	19	14.2	1.8	55.7	5.0	2.9	1.6	7.3	**13.5**	**14.4**
38	39	1.2	0.0	0.0	1.7	3.1	0.0	11.2	**1.0**	**2.9**
40	41	7.7	45.3	7.4	8.2	11.7	5.5	23.4	**14.3**	**10.6**
66	67	4.6	78.4	1.0	8.6	31.5	2.8	2.0	**21.1**	**8.4**
81	82	3.7	41.0	0.1	4.6	10.9	6.9	10.3	**11.2**	**6.1**
	Average:	**6.3**	**33.3**	**12.8**	**5.6**	**12.0**	**3.4**	**10.8**	**12.2**	**8.5**
Standards										
STD W2		98.0	68.6	1.0	16.3	42.8	9.2	10.4	**35.2**	**29.6**
STD PCC1		98.2	3.9	2.3	61.9	22.4	6.6	14.8	**30.0**	**34.4**
STD BIR1		97.8	33.5	1.6	13.8	22.9	14.3	21.7	**29.4**	**28.7**
STD GSP1		3.9	420.9	20.2	2.4	0.8	7.0	9.6	**66.4**	**7.3**
STD AGV1		97.3	204.2	3.7	8.7	16.6	0.0	15.0	**49.4**	**23.6**
STD 2709		97.8	41.4	4.3	13.2	7.3	2.9	7.6	**24.9**	**22.2**
STD SDO1		98.2	17.4	14.1	48.6	8.3	7.1	0.6	**27.8**	**29.5**
	Average:	**84.5**	**112.9**	**6.7**	**23.5**	**17.3**	**6.7**	**11.4**	**37.6**	**25.0**

Table 10. Approximate elemental determined by energy dispersive spectrometry for core MG06-1B.

Centered sample depth (cm)	Si (weight %)	S (weight %)	Al (weight %)	Fe (weight %)	Na (weight %)	Ca (weight %)	K (weight %)	Mg (weight %)	Ti (weight %)	P (weight %)	Mn (weight %)
0.00- 2.16 cm											
0.00	20.62	1.35	7.01	3.51	1.46	1.06	0.42	0.97	0.20	0.14	0.17
0.12	19.96	1.51	6.64	5.07	1.10	0.92	0.72	0.70	0.24	0.23	0.03
0.24	19.33	1.52	6.10	6.46	1.55	1.13	0.73	0.61	0.15	0.12	0.00
0.36	21.49	1.22	6.88	2.75	1.30	1.28	0.77	0.50	0.14	0.19	0.07
0.48	21.58	1.15	6.60	2.66	1.04	1.31	0.76	0.76	0.44	0.16	0.08
0.60	21.45	1.35	6.60	3.27	1.09	1.15	0.81	0.73	0.18	0.00	0.06
0.72	21.08	1.30	6.15	4.41	1.21	1.07	0.61	0.86	0.11	0.04	0.16
0.84	19.79	1.60	5.72	6.61	1.12	0.80	0.69	0.50	0.22	0.12	0.09
0.96	21.57	1.73	6.37	2.43	1.51	0.81	0.65	0.79	0.22	0.29	0.06
1.08	21.18	1.84	6.49	3.10	0.94	0.59	0.63	0.38	0.16	0.54	0.00
1.20	21.04	2.29	6.14	2.62	1.02	0.59	0.64	0.59	0.39	0.29	0.03
1.32	21.64	2.29	6.54	2.00	0.68	0.51	0.70	0.50	0.28	0.18	0.00
1.44	21.08	2.55	6.33	2.60	1.04	0.51	0.58	0.41	0.35	0.06	0.06
1.56	20.57	2.57	6.53	2.81	0.80	0.47	0.64	0.51	0.23	0.30	0.03
1.68	20.86	2.19	6.56	2.57	1.10	0.52	0.56	0.63	0.35	0.28	0.20
1.80	21.18	2.15	6.72	2.18	1.13	0.67	0.68	0.52	0.19	0.25	0.02
1.92	21.37	2.00	6.49	2.40	0.92	0.61	0.68	0.62	0.27	0.32	0.03
2.04	20.92	2.13	6.76	2.76	0.99	0.60	0.64	0.72	0.33	0.13	0.01
2.16	20.74	2.10	6.54	2.62	1.17	0.63	0.64	0.54	0.32	0.39	0.21
Average:	**20.92**	**1.83**	**6.48**	**3.31**	**1.11**	**0.80**	**0.66**	**0.62**	**0.25**	**0.21**	**0.07**
Standard deviation:	**0.64**	**0.46**	**0.30**	**1.36**	**0.22**	**0.28**	**0.09**	**0.15**	**0.09**	**0.13**	**0.07**
21.50- 23.18 cm											
21.50	21.22	0.44	7.80	3.74	1.45	1.03	0.84	0.90	0.24	0.00	0.00
21.62	21.11	0.52	7.38	4.19	1.40	1.30	0.73	0.61	0.25	0.00	0.04
21.74	20.77	0.47	7.18	4.38	1.46	1.29	0.68	0.88	0.19	0.13	0.04
21.86	20.45	0.68	7.16	5.21	0.96	1.31	0.81	0.86	0.21	0.01	0.00
21.98	19.79	0.58	8.07	4.98	1.27	1.13	0.72	0.64	0.23	0.19	0.10
22.10	21.21	0.34	7.12	4.47	1.47	1.27	0.91	0.84	0.11	0.00	0.04

Centered sample depth (cm)	Si (weight %)	S (weight %)	Al (weight %)	Fe (weight %)	Na (weight %)	Ca (weight %)	K (weight %)	Mg (weight %)	Ti (weight %)	P (weight %)	Mn (weight %)
22.22	20.72	0.42	7.38	4.28	1.41	1.35	0.74	0.82	0.30	0.18	0.05
22.34	20.95	0.37	7.36	4.49	1.42	1.46	0.79	0.77	0.22	0.01	0.00
22.46	21.13	0.32	7.16	4.42	1.31	1.40	0.82	0.72	0.26	0.04	0.15
22.58	20.50	0.57	6.93	5.15	1.53	1.42	0.88	0.47	0.10	0.16	0.04
22.70	20.97	0.27	7.29	4.56	1.31	1.41	0.86	0.72	0.18	0.12	0.09
22.82	20.95	0.37	7.23	4.34	1.81	1.39	0.69	0.82	0.10	0.04	0.00
22.94	20.62	0.53	7.30	4.80	1.02	1.49	0.69	1.18	0.26	0.00	0.02
23.06	20.85	0.43	7.19	4.48	1.65	1.34	0.71	0.52	0.20	0.24	0.05
23.18	20.25	0.75	7.27	5.00	1.21	1.33	0.82	0.62	0.23	0.07	0.03
Average:	**20.77**	**0.47**	**7.32**	**4.57**	**1.38**	**1.33**	**0.78**	**0.76**	**0.21**	**0.08**	**0.04**
Standard deviation:	**0.39**	**0.13**	**0.28**	**0.40**	**0.22**	**0.12**	**0.08**	**0.18**	**0.06**	**0.08**	**0.04**

Table 11. Oxidation-state uncertainty for slurry pH measurements.

Core MG07-6 Centered depth (cm)	Mixture of oxidized and reduced sediment $[H^+]^a$	100% Reduced $[H^+]$	100% Oxidized $[H^+]$	Average of 100% oxidized and 100% reduced $[H^+]$	Absolute difference between two combined averages $[H^+]$
27	2.51E-06	5.13E-07	4.79E-05	2.42E-05	2.17E-05
29	2.95E-06	5.01E-07	1.70E-05	8.74E-06	5.79E-06
31	2.95E-06	4.90E-07	9.77E-06	5.13E-06	2.18E-06
33	5.69E-06	5.25E-07	1.05E-05	5.50E-06	1.90E-07
35	9.33E-06	6.46E-07	1.12E-05	5.93E-06	3.40E-06
37	5.62E-06	5.50E-07	3.02E-05	1.54E-05	9.75E-06
39	6.31E-06	5.25E-07	5.89E-05	2.97E-05	2.34E-05
41	7.00E-06	7.76E-07	5.89E-05	2.98E-05	2.28E-05
				Average:	**1.11E-05**
				Standard deviation:	**9.91E-06**
				Average plus one standard deviation:	**2.10E-05**

[a]Sediment in mixtures was typical of all sediment in main data set, based on degree of visual oxidation and reduction. Each value is the average of two samples than span the thickness of the subsamples used for separate oxidized and reduced analyses. See Figure 5 for sampling scheme.

Table 12. Slurry pH values by depth and age in MG06-1B and MG07-6.

Centered tube depth (cm)	Tephra-free depth (cm)	Centered age (years before 2006)	1/2 95% confidence interval	pH[a]	[H+][a]	Upper error [H^+]	Lower error [H^+]	Lake Acidification cutoff criteria[b]		
								Highly Likely	Likely	Possible
MG06-1B			NA							
0.75	0.75	0.9	NA	3.24	5.75E-04	5.97E-04	5.54E-04	Yes	Yes	Yes
2.25	2.25	2.7	NA	3.90	1.26E-04	1.47E-04	1.05E-04	Yes	Yes	Yes
3.75	3.75	4.5	NA	4.78	1.66E-05	3.79E-05	-4.70E-06			
5.25	5.25	6.3	NA	5.43	3.72E-06	2.50E-05	-1.76E-05			
6.75	6.75	8.1	NA	5.63	2.34E-06	2.36E-05	-1.90E-05			
8.25	8.25	9.9	NA	5.46	3.47E-06	2.48E-05	-1.78E-05			
9.75	9.75	11.7	NA	5.76	1.74E-06	2.30E-05	-1.96E-05			
11.25	11.25	13.5	NA	5.82	1.51E-06	2.28E-05	-1.98E-05			
12.75	12.75	15.3	NA	6.02	9.55E-07	2.23E-05	-2.03E-05			
14.25	14.25	17.1	NA	5.85	1.41E-06	2.27E-05	-1.99E-05			
15.75	15.75	18.9	NA	5.80	1.58E-06	2.29E-05	-1.97E-05			
17.25	17.25	20.7	NA	5.64	2.29E-06	2.36E-05	-1.90E-05			
18.75	18.75	22.5	NA	5.60	2.51E-06	2.38E-05	-1.88E-05			
20.25	20.25	24.3	NA	6.14	7.24E-07	2.20E-05	-2.06E-05			
24.75	24.75	29.7	NA	5.95	1.12E-06	2.24E-05	-2.02E-05			
29.25	29.25	35.1	NA	5.50	3.16E-06	2.45E-05	-1.81E-05			
36.75	36.75	44.1	NA	5.44	3.63E-06	2.49E-05	-1.77E-05			
57.75	57.75	69.3	NA	5.70	2.00E-06	2.33E-05	-1.93E-05			
66.75	66.75	80.1	NA	4.79	1.62E-05	3.75E-05	-5.08E-06			
78.75	78.75	94.5	NA	4.95	1.12E-05	3.25E-05	-1.01E-05			
90.75	88.75	106.5	NA	5.39	4.07E-06	2.54E-05	-1.72E-05			
MG07-6										
0.5	0	678	154	5.32	4.79E-06	2.61E-05	-1.65E-05			
1.5	0.4	680	154	5.74	1.82E-06	2.31E-05	-1.95E-05			
2.5	1.4	685	154	5.95	1.12E-06	2.24E-05	-2.02E-05			
3.5	2.4	691	154	5.87	1.35E-06	2.26E-05	-2.00E-05			
4.5	3.5	697	154	5.89	1.29E-06	2.26E-05	-2.00E-05			

Centered tube depth (cm)	Tephra-free depth (cm)	Centered age (years before 2006)	1/2 95% confidence interval	pH[a]	[H+][a]	Upper error [H^+]	Lower error [H^+]	Lake Acidification cutoff criteria[b]		
								Highly Likely	Likely	Possible
5.5	4.5	702	154	5.93	1.17E-06	2.25E-05	-2.01E-05			
6.5	5.5	707	154	5.46	3.47E-06	2.48E-05	-1.78E-05			
7.5	6.5	712	154	5.35	4.47E-06	2.58E-05	-1.68E-05			
8.5	7.4	717	154	5.26	5.50E-06	2.68E-05	-1.58E-05			
9.5	7.4	717	154	5.56	2.75E-06	2.41E-05	-1.85E-05			
10.5	7.9	720	154	5.38	4.17E-06	2.55E-05	-1.71E-05			
11.5	8.9	725	154	5.42	3.80E-06	2.51E-05	-1.75E-05			
12.5	9.9	730	154	5.48	3.31E-06	2.46E-05	-1.80E-05			
13.5	10.9	736	154	5.41	3.89E-06	2.52E-05	-1.74E-05			
14.5	11.8	741	154	5.33	4.68E-06	2.60E-05	-1.66E-05			
15.5	12.3	743	154	5.72	1.91E-06	2.32E-05	-1.94E-05			
16.5	13.3	749	154	5.58	2.63E-06	2.39E-05	-1.87E-05			
17.5	14.3	754	154	5.16	6.92E-06	2.82E-05	-1.44E-05			
18.5	15.3	759	154	5.18	6.61E-06	2.79E-05	-1.47E-05			
19.5	16.2	764	154	5.00	1.00E-05	3.13E-05	-1.13E-05			
20.5	17.2	769	154	5.85	1.41E-06	2.27E-05	-1.99E-05			
21.5	18.2	775	154	5.18	6.61E-06	2.79E-05	-1.47E-05			
22.5	19.2	781	154	5.64	2.29E-06	2.36E-05	-1.90E-05			
23.5	20.2	786	154	5.55	2.82E-06	2.41E-05	-1.85E-05			
24.5	21.2	791	154	5.64	2.29E-06	2.36E-05	-1.90E-05			
25.5	22.2	797	154	5.43	3.72E-06	2.50E-05	-1.76E-05			
26.5	23.2	802	154	5.60	2.51E-06	2.38E-05	-1.88E-05			
27.5	24.2	808	154	5.60	2.51E-06	2.38E-05	-1.88E-05			
28.5	25.2	813	154	5.50	3.16E-06	2.45E-05	-1.81E-05			
29.5	26.2	818	154	5.56	2.75E-06	2.41E-05	-1.85E-05			
30.5	27.2	824	154	5.60	2.51E-06	2.38E-05	-1.88E-05			
31.5	28.2	829	154	5.46	3.47E-06	2.48E-05	-1.78E-05			
32.5	29.2	834	154	5.38	4.17E-06	2.55E-05	-1.71E-05			
33.5	30.2	840	154	5.11	7.76E-06	2.91E-05	-1.35E-05			
34.5	31.2	845	154	5.14	7.24E-06	2.85E-05	-1.41E-05			

Centered tube depth (cm)	Tephra-free depth (cm)	Centered age (years before 2006)	1/2 95% confidence interval	pH[a]	[H+][a]	Upper error [H^+]	Lower error [H^+]	Lake Acidification cutoff criteria[b]		
								Highly Likely	Likely	Possible
35.5	32.2	850	154	4.92	1.20E-05	3.33E-05	-9.28E-06			
36.5	33.2	856	154	5.33	4.68E-06	2.60E-05	-1.66E-05			
37.5	34.2	861	154	5.17	6.76E-06	2.81E-05	-1.45E-05			
38.5	35.2	867	154	5.37	4.27E-06	2.56E-05	-1.70E-05			
39.5	36.2	872	154	5.03	9.33E-06	3.06E-05	-1.20E-05			
40.5	37.2	877	154	5.36	4.37E-06	2.57E-05	-1.69E-05			
41.5	38.2	883	154	4.95	1.12E-05	3.25E-05	-1.01E-05			
42.5	39.2	888	154	5.58	2.63E-06	2.39E-05	-1.87E-05			
43.5	40.2	893	154	5.65	2.24E-06	2.35E-05	-1.91E-05			
44.5	41.2	899	154	5.50	3.16E-06	2.45E-05	-1.81E-05			
45.5	42.2	904	154	5.43	3.72E-06	2.50E-05	-1.76E-05			
49	45.7	923	154	5.12	7.59E-06	2.89E-05	-1.37E-05			
50	46.7	928	154	5.17	6.76E-06	2.81E-05	-1.45E-05			
51	47.7	934	154	5.05	8.91E-06	3.02E-05	-1.24E-05			
52	48.7	939	154	5.14	7.24E-06	2.85E-05	-1.41E-05			
53	49.7	944	154	5.11	7.76E-06	2.91E-05	-1.35E-05			
54	50.7	950	154	5.08	8.32E-06	2.96E-05	-1.30E-05			
55	51.7	955	154	5.50	3.16E-06	2.45E-05	-1.81E-05			
56	52.7	960	154	5.46	3.47E-06	2.48E-05	-1.78E-05			
57	53.7	966	154	5.54	2.88E-06	2.42E-05	-1.84E-05			
58	54.7	971	154	5.23	5.89E-06	2.72E-05	-1.54E-05			
59	55.7	976	154	5.44	3.63E-06	2.49E-05	-1.77E-05			
60	56.7	982	153	5.45	3.55E-06	2.48E-05	-1.78E-05			
61	57.7	987	151	5.48	3.31E-06	2.46E-05	-1.80E-05			
62	58.7	993	149	5.38	4.17E-06	2.55E-05	-1.71E-05			
63	59.7	998	148	5.44	3.63E-06	2.49E-05	-1.77E-05			
64	60.7	1003	146	4.40	3.98E-05	6.11E-05	1.85E-05		Yes	Yes
65	61.7	1009	145	5.58	2.63E-06	2.39E-05	-1.87E-05			
66	62.7	1014	143	4.09	8.13E-05	1.03E-04	6.00E-05	Yes	Yes	Yes
68	64.7	1025	140	5.47	3.39E-06	2.47E-05	-1.79E-05			

Centered tube depth (cm)	Tephra-free depth (cm)	Centered age (years before 2006)	1/2 95% confidence interval	pH[a]	[H+][a]	Upper error [H^+]	Lower error [H^+]	Lake Acidification cutoff criteria[b]		
								Highly Likely	Likely	Possible
69	65.7	1030	138	5.59	2.57E-06	2.39E-05	-1.87E-05			
70	66.7	1035	136	4.97	1.07E-05	3.20E-05	-1.06E-05			
71	67.7	1041	135	5.88	1.32E-06	2.26E-05	-2.00E-05			
72	68.7	1046	133	5.25	5.62E-06	2.69E-05	-1.57E-05			
73	69.7	1052	132	5.46	3.47E-06	2.48E-05	-1.78E-05			
74	70.7	1057	130	5.24	5.75E-06	2.71E-05	-1.55E-05			
75	71.7	1062	128	5.29	5.13E-06	2.64E-05	-1.62E-05			
76	72.8	1068	127	5.54	2.88E-06	2.42E-05	-1.84E-05			
77	73.8	1073	125	4.78	1.66E-05	3.79E-05	-4.70E-06			
78	74.8	1079	123	5.50	3.16E-06	2.45E-05	-1.81E-05			
79	75.8	1084	122	4.31	4.90E-05	7.03E-05	2.77E-05		Yes	Yes
80	76.8	1089	120	5.20	6.31E-06	2.76E-05	-1.50E-05			
81	77.8	1094	119	5.03	9.33E-06	3.06E-05	-1.20E-05			
82	78.8	1100	117	5.45	3.55E-06	2.48E-05	-1.78E-05			
83	79.8	1105	115	5.76	1.74E-06	2.30E-05	-1.96E-05			
84	80.8	1110	114	5.61	2.45E-06	2.38E-05	-1.88E-05			
85	81.8	1116	112	5.93	1.17E-06	2.25E-05	-2.01E-05			
86	82.8	1121	111	5.38	4.17E-06	2.55E-05	-1.71E-05			
87	83.8	1127	109	5.96	1.10E-06	2.24E-05	-2.02E-05			
88	84.8	1132	107	5.76	1.74E-06	2.30E-05	-1.96E-05			
89	85.8	1137	106	5.92	1.20E-06	2.25E-05	-2.01E-05			
90	86.8	1143	104	6.04	9.12E-07	2.22E-05	-2.04E-05			
91	87.8	1148	103	5.90	1.26E-06	2.26E-05	-2.00E-05			
92	88.8	1153	101	5.94	1.15E-06	2.24E-05	-2.02E-05			
93	89.8	1159	99	6.06	8.71E-07	2.22E-05	-2.04E-05			
94	90.8	1164	98	5.93	1.17E-06	2.25E-05	-2.01E-05			
95	91.8	1170	96	5.70	2.00E-06	2.33E-05	-1.93E-05			
96	92.8	1175	95	5.54	2.88E-06	2.42E-05	-1.84E-05			
97	93.8	1180	93	5.93	1.17E-06	2.25E-05	-2.01E-05			
98	94.8	1186	91	5.81	1.55E-06	2.28E-05	-1.98E-05			

Centered tube depth (cm)	Tephra-free depth (cm)	Centered age (years before 2006)	1/2 95% confidence interval	pH[a]	[H+][a]	Upper error [H^+]	Lower error [H^+]	Lake Acidification cutoff criteria[b]		
								Highly Likely	Likely	Possible
99	95.8	1191	90	5.73	1.86E-06	2.32E-05	-1.94E-05			
100	96.8	1196	88	5.34	4.57E-06	2.59E-05	-1.67E-05			
101	97.8	1202	86	5.60	2.51E-06	2.38E-05	-1.88E-05			
102	98.8	1207	85	6.00	1.00E-06	2.23E-05	-2.03E-05			
103	99.8	1212	83	5.59	2.57E-06	2.39E-05	-1.87E-05			
104	100.8	1218	82	5.73	1.86E-06	2.32E-05	-1.94E-05			
105	101.8	1223	80	5.53	2.95E-06	2.43E-05	-1.83E-05			
106	102.8	1229	78	5.58	2.63E-06	2.39E-05	-1.87E-05			
107	103.8	1234	77	5.53	2.95E-06	2.43E-05	-1.83E-05			
108	104.8	1239	75	5.48	3.31E-06	2.46E-05	-1.80E-05			
109	105.8	1245	74	4.98	1.05E-05	3.18E-05	-1.08E-05			
110	106.8	1250	72	5.46	3.47E-06	2.48E-05	-1.78E-05			
111	107.8	1255	70	5.75	1.78E-06	2.31E-05	-1.95E-05			
112	108.8	1261	69	5.82	1.51E-06	2.28E-05	-1.98E-05			
113	109.8	1266	67	5.96	1.10E-06	2.24E-05	-2.02E-05			
114	110.8	1272	66	5.99	1.02E-06	2.23E-05	-2.03E-05			
115	111.8	1277	64	5.83	1.48E-06	2.28E-05	-1.98E-05			
116	112.8	1282	62	5.98	1.05E-06	2.23E-05	-2.03E-05			
117	113.8	1288	61	6.26	5.50E-07	2.18E-05	-2.08E-05			
118	114.8	1293	59	5.94	1.15E-06	2.24E-05	-2.02E-05			
119	115.8	1299	58	5.89	1.29E-06	2.26E-05	-2.00E-05			
120	116.8	1304	56	5.79	1.62E-06	2.29E-05	-1.97E-05			
121	117.8	1309	54	5.70	2.00E-06	2.33E-05	-1.93E-05			
122	118.8	1315	53	5.91	1.23E-06	2.25E-05	-2.01E-05			
123	119.4	1318	52	5.80	1.58E-06	2.29E-05	-1.97E-05			
124	120.4	1323	50	5.67	2.14E-06	2.34E-05	-1.92E-05			
125	121.4	1329	49	5.77	1.70E-06	2.30E-05	-1.96E-05			
126	122.4	1334	50	6.26	5.50E-07	2.18E-05	-2.08E-05			
127	123.4	1340	50	5.39	4.07E-06	2.54E-05	-1.72E-05			
128	124.4	1345	51	5.69	2.04E-06	2.33E-05	-1.93E-05			

Centered tube depth (cm)	Tephra-free depth (cm)	Centered age (years before 2006)	1/2 95% confidence interval	pH[a]	[H+][a]	Upper error [H^+]	Lower error [H^+]	Lake Acidification cutoff criteria[b]		
								Highly Likely	Likely	Possible
128	124.4	1345	51	5.33	4.68E-06	2.60E-05	-1.66E-05			
129	125.4	1350	52	5.60	2.51E-06	2.38E-05	-1.88E-05			
130	126.4	1356	52	5.88	1.32E-06	2.26E-05	-2.00E-05			
131	127.4	1361	53	5.82	1.51E-06	2.28E-05	-1.98E-05			
132	128.4	1366	54	5.66	2.19E-06	2.35E-05	-1.91E-05			
133	129.4	1372	54	5.89	1.29E-06	2.26E-05	-2.00E-05			
134	130.4	1377	55	5.77	1.70E-06	2.30E-05	-1.96E-05			
135	131.4	1383	55	5.87	1.35E-06	2.26E-05	-2.00E-05			
136	132.4	1388	56	5.75	1.78E-06	2.31E-05	-1.95E-05			
137	133.4	1394	57	5.74	1.82E-06	2.31E-05	-1.95E-05			
138	134.4	1399	57	5.72	1.91E-06	2.32E-05	-1.94E-05			
139	135.4	1404	58	5.82	1.51E-06	2.28E-05	-1.98E-05			
140	136.4	1410	59	5.71	1.95E-06	2.32E-05	-1.94E-05			
141	137.4	1415	59	4.85	1.41E-05	3.54E-05	-7.17E-06			
142	138.4	1421	60	5.03	9.33E-06	3.06E-05	-1.20E-05			
143	139.4	1426	61	5.06	8.71E-06	3.00E-05	-1.26E-05			
144	140.4	1431	61	4.99	1.02E-05	3.15E-05	-1.11E-05			
145	141.4	1437	62	4.50	3.16E-05	5.29E-05	1.03E-05			Yes
146	142.4	1442	63	5.30	5.01E-06	2.63E-05	-1.63E-05			
147	143.4	1448	63	5.84	1.45E-06	2.27E-05	-1.99E-05			
148	144.4	1453	64	6.00	1.00E-06	2.23E-05	-2.03E-05			
149	145.4	1459	64	6.08	8.32E-07	2.21E-05	-2.05E-05			
150	146.4	1464	65	5.63	2.34E-06	2.36E-05	-1.90E-05			
151	147.4	1469	66	5.80	1.58E-06	2.29E-05	-1.97E-05			
152	148.4	1475	66	5.58	2.63E-06	2.39E-05	-1.87E-05			
153	149.4	1480	67	5.58	2.63E-06	2.39E-05	-1.87E-05			
154	150.4	1486	68	5.46	3.47E-06	2.48E-05	-1.78E-05			
155	151.4	1491	68	5.68	2.09E-06	2.34E-05	-1.92E-05			
156	152.4	1497	69	5.21	6.17E-06	2.75E-05	-1.51E-05			
157	153.4	1502	70	5.58	2.63E-06	2.39E-05	-1.87E-05			

Centered tube depth (cm)	Tephra-free depth (cm)	Centered age (years before 2006)	1/2 95% confidence interval	pH[a]	[H+][a]	Upper error [H^+]	Lower error [H^+]	Lake Acidification cutoff criteria[b]		
								Highly Likely	Likely	Possible
158	154.4	1507	70	5.36	4.37E-06	2.57E-05	-1.69E-05			
159	155.4	1513	71	5.10	7.94E-06	2.92E-05	-1.34E-05			
160	156.4	1518	72	4.77	1.70E-05	3.83E-05	-4.32E-06			
161	157.4	1524	72	5.08	8.32E-06	2.96E-05	-1.30E-05			
162	158.4	1529	73	5.34	4.57E-06	2.59E-05	-1.67E-05			
163	159.4	1535	74	6.09	8.13E-07	2.21E-05	-2.05E-05			
164	160.4	1540	74	5.91	1.23E-06	2.25E-05	-2.01E-05			
165	161.4	1546	75	6.31	4.90E-07	2.18E-05	-2.08E-05			
166	162.4	1551	75	6.07	8.51E-07	2.22E-05	-2.04E-05			
167	163.4	1557	76	6.12	7.59E-07	2.21E-05	-2.05E-05			
168	163.8	1559	76	5.93	1.17E-06	2.25E-05	-2.01E-05			
169	164.3	1562	77	6.17	6.76E-07	2.20E-05	-2.06E-05			
170	165.3	1567	77	5.95	1.12E-06	2.24E-05	-2.02E-05			
171	166.3	1572	78	6.16	6.92E-07	2.20E-05	-2.06E-05			
172	167.3	1578	79	6.16	6.92E-07	2.20E-05	-2.06E-05			
173	168.3	1583	80	5.88	1.32E-06	2.26E-05	-2.00E-05			
174	169.3	1589	81	6.21	6.17E-07	2.19E-05	-2.07E-05			
175	170.3	1594	82	5.78	1.66E-06	2.30E-05	-1.96E-05			
176	171.3	1600	83	5.71	1.95E-06	2.32E-05	-1.94E-05			
177	172.3	1605	84	5.41	3.89E-06	2.52E-05	-1.74E-05			
178	173.3	1611	85	5.02	9.55E-06	3.08E-05	-1.18E-05			
179	174.3	1616	86	5.04	9.12E-06	3.04E-05	-1.22E-05			
180	175.3	1622	87	5.74	1.82E-06	2.31E-05	-1.95E-05			
181	176.3	1627	88	5.77	1.70E-06	2.30E-05	-1.96E-05			
182	177.2	1632	89	5.70	2.00E-06	2.33E-05	-1.93E-05			
183	177.7	1635	90	5.52	3.02E-06	2.43E-05	-1.83E-05			
184	178.7	1641	90	5.75	1.78E-06	2.31E-05	-1.95E-05			
185	179.7	1646	91	5.53	2.95E-06	2.43E-05	-1.83E-05			
186	180.7	1652	92	5.73	1.86E-06	2.32E-05	-1.94E-05			
197.5	192.2	1716	104	4.27	5.37E-05	7.50E-05	3.24E-05		Yes	Yes

Centered tube depth (cm)	Tephra-free depth (cm)	Centered age (years before 2006)	1/2 95% confidence interval	pH[a]	[H+][a]	Upper error [H^+]	Lower error [H^+]	Lake Acidification cutoff criteria[b]		
								Highly Likely	Likely	Possible
198.5	193.2	1721	104	4.55	2.82E-05	4.95E-05	6.88E-06			Yes
199.5	194.2	1727	105	4.78	1.66E-05	3.79E-05	-4.70E-06			
200.5	195.2	1733	106	5.54	2.88E-06	2.42E-05	-1.84E-05			
201.5	196.2	1738	107	5.30	5.01E-06	2.63E-05	-1.63E-05			
202.5	197.2	1744	108	5.32	4.79E-06	2.61E-05	-1.65E-05			
203.5	198.2	1749	109	5.48	3.31E-06	2.46E-05	-1.80E-05			
204.5	199.2	1755	110	5.98	1.05E-06	2.23E-05	-2.03E-05			
205.5	200.2	1761	111	5.83	1.48E-06	2.28E-05	-1.98E-05			
206.5	201.2	1766	112	6.03	9.33E-07	2.22E-05	-2.04E-05			
207.5	202.2	1772	113	5.94	1.15E-06	2.24E-05	-2.02E-05			
208.5	203.2	1778	114	6.03	9.33E-07	2.22E-05	-2.04E-05			
209.5	204	1782	115	5.76	1.74E-06	2.30E-05	-1.96E-05			
210.5	204.7	1786	116	6.07	8.51E-07	2.22E-05	-2.04E-05			
211.5	205.7	1792	117	6.07	8.51E-07	2.22E-05	-2.04E-05			
212.5	206.7	1797	118	6.22	6.03E-07	2.19E-05	-2.07E-05			
213.5	207.7	1803	119	6.04	9.12E-07	2.22E-05	-2.04E-05			
214.5	208.7	1809	120	5.04	9.12E-06	3.04E-05	-1.22E-05			
215.5	209.7	1814	120	4.75	1.78E-05	3.91E-05	-3.52E-06			
216.5	210.7	1820	121	5.05	8.91E-06	3.02E-05	-1.24E-05			
217.5	211.7	1826	122	5.00	1.00E-05	3.13E-05	-1.13E-05			
218.5	212.7	1831	123	5.22	6.03E-06	2.73E-05	-1.53E-05			
219.5	213.7	1837	124	5.30	5.01E-06	2.63E-05	-1.63E-05			
220.5	214.7	1843	125	6.34	4.57E-07	2.18E-05	-2.08E-05			
221.5	215.7	1849	126	5.60	2.51E-06	2.38E-05	-1.88E-05			
222.5	216.7	1854	127	5.33	4.68E-06	2.60E-05	-1.66E-05			
223.5	217.7	1860	128	5.12	7.59E-06	2.89E-05	-1.37E-05			
224.5	218.7	1866	129	5.84	1.45E-06	2.27E-05	-1.99E-05			
225.5	219.7	1871	130	5.33	4.68E-06	2.60E-05	-1.66E-05			
226.5	220.7	1877	131	5.08	8.32E-06	2.96E-05	-1.30E-05			
227.5	221.7	1883	132	4.76	1.74E-05	3.87E-05	-3.92E-06			

Centered tube depth (cm)	Tephra-free depth (cm)	Centered age (years before 2006)	1/2 95% confidence interval	pH[a]	[H+][a]	Upper error [H^+]	Lower error [H^+]	Lake Acidification cutoff criteria[b]		
								Highly Likely	Likely	Possible
228.5	222.7	1889	133	5.81	1.55E-06	2.28E-05	-1.98E-05			
229.5	223.7	1895	134	6.06	8.71E-07	2.22E-05	-2.04E-05			
230.5	224.7	1900	135	6.08	8.32E-07	2.21E-05	-2.05E-05			
231.5	225.7	1906	136	5.93	1.17E-06	2.25E-05	-2.01E-05			
232.5	226.7	1912	137	6.19	6.46E-07	2.19E-05	-2.07E-05			
233.5	227.7	1918	138	5.95	1.12E-06	2.24E-05	-2.02E-05			
234.5	228.7	1924	139	6.37	4.27E-07	2.17E-05	-2.09E-05			
235.5	229.7	1929	140	6.17	6.76E-07	2.20E-05	-2.06E-05			
236.5	230.7	1935	141	6.11	7.76E-07	2.21E-05	-2.05E-05			
237.5	231.7	1941	142	5.64	2.29E-06	2.36E-05	-1.90E-05			
238.5	232.7	1947	143	5.51	3.09E-06	2.44E-05	-1.82E-05			
239.5	233.7	1953	144	5.75	1.78E-06	2.31E-05	-1.95E-05			
240.5	234.4	1957	144	5.86	1.38E-06	2.27E-05	-1.99E-05			
241.5	235.4	1963	145	5.47	3.39E-06	2.47E-05	-1.79E-05			
242.5	236.4	1969	146	5.74	1.82E-06	2.31E-05	-1.95E-05			
243.5	237.4	1974	147	5.49	3.24E-06	2.45E-05	-1.81E-05			
244.5	238.4	1980	148	6.05	8.91E-07	2.22E-05	-2.04E-05			
245.5	239.4	1986	149	5.74	1.82E-06	2.31E-05	-1.95E-05			
246.5	240.4	1992	150	6.08	8.32E-07	2.21E-05	-2.05E-05			
247.5	241.3	1997	151	6.67	2.14E-07	2.15E-05	-2.11E-05			
248.5	241.7	2000	151	6.10	7.94E-07	2.21E-05	-2.05E-05			
249.5	242.7	2006	152	5.92	1.20E-06	2.25E-05	-2.01E-05			
250.5	243.7	2012	153	6.30	5.01E-07	2.18E-05	-2.08E-05			
251.5	244.7	2018	154	5.73	1.86E-06	2.32E-05	-1.94E-05			
252.5	245.7	2024	155	5.95	1.12E-06	2.24E-05	-2.02E-05			
253.5	246.7	2029	156	5.88	1.32E-06	2.26E-05	-2.00E-05			
254.5	247.7	2035	157	5.92	1.20E-06	2.25E-05	-2.01E-05			
255.5	248.7	2041	158	6.16	6.92E-07	2.20E-05	-2.06E-05			
256.5	249.7	2047	159	5.76	1.74E-06	2.30E-05	-1.96E-05			
257.5	250.7	2053	160	5.94	1.15E-06	2.24E-05	-2.02E-05			

Centered tube depth (cm)	Tephra-free depth (cm)	Centered age (years before 2006)	1/2 95% confidence interval	pH[a]	[H+][a]	Upper error [H^+]	Lower error [H^+]	Lake Acidification cutoff criteria[b]		
								Highly Likely	Likely	Possible
258.5	251.7	2059	161	5.28	5.25E-06	2.65E-05	-1.61E-05			
259.5	252.7	2065	162	5.79	1.62E-06	2.29E-05	-1.97E-05			
260.5	253.7	2071	163	5.75	1.78E-06	2.31E-05	-1.95E-05			
261.5	254.7	2077	164	5.37	4.27E-06	2.56E-05	-1.70E-05			
262.5	255.7	2084	165	5.42	3.80E-06	2.51E-05	-1.75E-05			
264.5	257.7	2096	167	5.95	1.12E-06	2.24E-05	-2.02E-05			
265.5	258.7	2102	168	6.07	8.51E-07	2.22E-05	-2.04E-05			
266.5	259.7	2108	169	5.55	2.82E-06	2.41E-05	-1.85E-05			
267.5	260.7	2114	170	5.46	3.47E-06	2.48E-05	-1.78E-05			
267.5	260.7	2114	170	5.20	6.31E-06	2.76E-05	-1.50E-05			
268.5	261.7	2120	171	5.62	2.40E-06	2.37E-05	-1.89E-05			
269.5	262.7	2126	171	5.72	1.91E-06	2.32E-05	-1.94E-05			
270.5	263.7	2132	172	5.83	1.48E-06	2.28E-05	-1.98E-05			
271.5	264.7	2138	173	5.64	2.29E-06	2.36E-05	-1.90E-05			
272.5	265.7	2144	174	5.80	1.58E-06	2.29E-05	-1.97E-05			
273.5	266.7	2151	175	5.45	3.55E-06	2.48E-05	-1.78E-05			
274.5	267.7	2157	176	5.38	4.17E-06	2.55E-05	-1.71E-05			
275.5	268.7	2163	177	5.67	2.14E-06	2.34E-05	-1.92E-05			
276.5	269.7	2169	178	5.42	3.80E-06	2.51E-05	-1.75E-05			
277.5	270.7	2175	179	5.59	2.57E-06	2.39E-05	-1.87E-05			
289.5	282.7	2250	191	5.27	5.37E-06	2.67E-05	-1.59E-05			
290.5	283.7	2257	192	4.98	1.05E-05	3.18E-05	-1.08E-05			
291.5	284.7	2263	193	4.95	1.12E-05	3.25E-05	-1.01E-05			
292.5	285.7	2269	194	5.16	6.92E-06	2.82E-05	-1.44E-05			
293.5	286.7	2276	195	5.35	4.47E-06	2.58E-05	-1.68E-05			
294.5	287.7	2282	196	4.89	1.29E-05	3.42E-05	-8.42E-06			
295.5	288.7	2289	197	5.03	9.33E-06	3.06E-05	-1.20E-05			
296.5	289.7	2295	197	4.92	1.20E-05	3.33E-05	-9.28E-06			
297.5	290.7	2301	198	5.56	2.75E-06	2.41E-05	-1.85E-05			
298.5	291.7	2308	199	5.06	8.71E-06	3.00E-05	-1.26E-05			

Centered tube depth (cm)	Tephra-free depth (cm)	Centered age (years before 2006)	1/2 95% confidence interval	pH[a]	[H+][a]	Upper error [H+]	Lower error [H+]	Lake Acidification cutoff criteria[b]		
								Highly Likely	Likely	Possible
299.5	292.1	2310	200	4.82	1.51E-05	3.64E-05	-6.16E-06			
300.5	292.1	2310	200	5.00	1.00E-05	3.13E-05	-1.13E-05			
301.5	293	2316	201	5.16	6.92E-06	2.82E-05	-1.44E-05			
302.5	294	2323	202	4.74	1.82E-05	3.95E-05	-3.10E-06			
303.5	295	2329	203	5.58	2.63E-06	2.39E-05	-1.87E-05			
304.5	296	2336	204	5.09	8.13E-06	2.94E-05	-1.32E-05			
305.5	297	2342	205	4.97	1.07E-05	3.20E-05	-1.06E-05			
306.5	298	2349	205	4.62	2.40E-05	4.53E-05	2.69E-06			Yes
307.5	299	2355	206	5.29	5.13E-06	2.64E-05	-1.62E-05			
308.5	300	2362	207	4.70	2.00E-05	4.13E-05	-1.35E-06			Yes
309.5	301	2368	208	4.77	1.70E-05	3.83E-05	-4.32E-06			
310.5	302	2375	209	4.69	2.04E-05	4.17E-05	-8.83E-07			Yes
311.5	303	2382	210	4.80	1.58E-05	3.71E-05	-5.45E-06			
312.5	304	2389	211	4.65	2.24E-05	4.37E-05	1.09E-06			Yes
313.5	305	2395	212	4.77	1.70E-05	3.83E-05	-4.32E-06			
314.5	306	2402	213	4.85	1.41E-05	3.54E-05	-7.17E-06			
315.5	307	2408	214	4.79	1.62E-05	3.75E-05	-5.08E-06			
316.5	308	2415	215	4.76	1.74E-05	3.87E-05	-3.92E-06			
317.5	309	2422	216	4.76	1.74E-05	3.87E-05	-3.92E-06			
318.5	310	2428	217	4.61	2.45E-05	4.58E-05	3.25E-06			Yes
319.5	311	2435	218	5.09	8.13E-06	2.94E-05	-1.32E-05			
320.5	312	2442	219	4.94	1.15E-05	3.28E-05	-9.82E-06			
321.5	313	2448	220	5.44	3.63E-06	2.49E-05	-1.77E-05			
322.5	314	2455	221	4.87	1.35E-05	3.48E-05	-7.81E-06			
323.5	315	2462	222	5.28	5.25E-06	2.65E-05	-1.61E-05			
324.5	316	2469	223	4.77	1.70E-05	3.83E-05	-4.32E-06			
325.5	316.7	2473	224	4.69	2.04E-05	4.17E-05	-8.83E-07			Yes
326.5	317.7	2480	224	4.78	1.66E-05	3.79E-05	-4.70E-06			
327.5	318.7	2487	225	5.30	5.01E-06	2.63E-05	-1.63E-05			
328.5	319.7	2494	226	5.18	6.61E-06	2.79E-05	-1.47E-05			

Centered tube depth (cm)	Tephra-free depth (cm)	Centered age (years before 2006)	1/2 95% confidence interval	pH[a]	[H+][a]	Upper error [H^+]	Lower error [H^+]	Lake Acidification cutoff criteria[b]		
								Highly Likely	Likely	Possible
329.5	320.7	2501	227	4.98	1.05E-05	3.18E-05	-1.08E-05			
330.5	321.7	2507	228	4.98	1.05E-05	3.18E-05	-1.08E-05			
331.5	322.7	2514	229	5.20	6.31E-06	2.76E-05	-1.50E-05			
332.5	323.7	2521	230	5.24	5.75E-06	2.71E-05	-1.55E-05			
333.5	324.3	2525	231	5.10	7.94E-06	2.92E-05	-1.34E-05			
334.5	325.3	2532	232	5.15	7.08E-06	2.84E-05	-1.42E-05			
335.5	326.3	2539	233	4.68	2.09E-05	4.22E-05	-4.07E-07			Yes
336.5	327.3	2546	234	5.72	1.91E-06	2.32E-05	-1.94E-05			
337.5	328.3	2553	235	5.67	2.14E-06	2.34E-05	-1.92E-05			
338.5	329.3	2560	236	5.62	2.40E-06	2.37E-05	-1.89E-05			
339.5	330.3	2567	237	5.05	8.91E-06	3.02E-05	-1.24E-05			
340.5	331	2572	237	4.83	1.48E-05	3.61E-05	-6.51E-06			
341.5	332	2578	238	5.53	2.95E-06	2.43E-05	-1.83E-05			
342.5	333	2585	239	5.21	6.17E-06	2.75E-05	-1.51E-05			
343.5	334	2592	240	5.07	8.51E-06	2.98E-05	-1.28E-05			
344.5	335	2600	241	4.73	1.86E-05	3.99E-05	-2.68E-06			Yes
345.5	336	2607	242	4.87	1.35E-05	3.48E-05	-7.81E-06			
346.5	337	2614	243	4.66	2.19E-05	4.32E-05	5.78E-07			Yes
347.5	338	2621	244	4.88	1.32E-05	3.45E-05	-8.12E-06			
348.5	339	2628	245	4.71	1.95E-05	4.08E-05	-1.80E-06			Yes
349.5	340	2635	246	5.32	4.79E-06	2.61E-05	-1.65E-05			
350.5	341	2642	247	5.06	8.71E-06	3.00E-05	-1.26E-05			
351.5	342	2649	248	4.83	1.48E-05	3.61E-05	-6.51E-06			
352.5	343	2656	249	5.65	2.24E-06	2.35E-05	-1.91E-05			
353.5	344	2663	250	4.58	2.63E-05	4.76E-05	5.00E-06			Yes
354.5	345	2671	251	4.52	3.02E-05	5.15E-05	8.90E-06			Yes
355.5	346	2678	252	5.31	4.90E-06	2.62E-05	-1.64E-05			
356.5	347	2685	253	4.65	2.24E-05	4.37E-05	1.09E-06			Yes
357.5	348	2692	254	5.45	3.55E-06	2.48E-05	-1.78E-05			
358.5	349	2699	250	4.93	1.17E-05	3.30E-05	-9.55E-06			

Centered tube depth (cm)	Tephra-free depth (cm)	Centered age (years before 2006)	1/2 95% confidence interval	pH[a]	[H+][a]	Upper error [H+]	Lower error [H+]	Lake Acidification cutoff criteria[b]		
								Highly Likely	Likely	Possible
359.5	350	2707	246	5.26	5.50E-06	2.68E-05	-1.58E-05			
360.5	351	2714	242	5.80	1.58E-06	2.29E-05	-1.97E-05			
361.5	352	2721	238	5.13	7.41E-06	2.87E-05	-1.39E-05			
362.5	353	2729	235	4.36	4.37E-05	6.50E-05	2.24E-05		Yes	Yes
363.5	354	2736	231	4.37	4.27E-05	6.40E-05	2.14E-05		Yes	Yes
364.5	355	2743	228	4.13	7.41E-05	9.54E-05	5.28E-05	Yes	Yes	Yes
365.5	356	2751	224	4.37	4.27E-05	6.40E-05	2.14E-05		Yes	Yes
366.5	357	2758	220	5.49	3.24E-06	2.45E-05	-1.81E-05			
367.5	358	2765	216	5.06	8.71E-06	3.00E-05	-1.26E-05			
368.5	359	2773	213	4.97	1.07E-05	3.20E-05	-1.06E-05			
369.5	360	2780	209	4.84	1.45E-05	3.58E-05	-6.85E-06			
370.5	361	2788	205	4.91	1.23E-05	3.36E-05	-9.00E-06			
371.5	362	2795	202	5.12	7.59E-06	2.89E-05	-1.37E-05			
372.5	363	2803	198	5.06	8.71E-06	3.00E-05	-1.26E-05			
373.5	364	2810	194	4.91	1.23E-05	3.36E-05	-9.00E-06			
374.5	365	2817	191	4.83	1.48E-05	3.61E-05	-6.51E-06			
375.5	366	2825	187	5.05	8.91E-06	3.02E-05	-1.24E-05			
376.5	367	2833	183	5.75	1.78E-06	2.31E-05	-1.95E-05			
377.5	368	2840	179	4.67	2.14E-05	4.27E-05	7.96E-08			Yes
378.5	369	2848	176	4.97	1.07E-05	3.20E-05	-1.06E-05			
379.5	370	2855	172	5.08	8.32E-06	2.96E-05	-1.30E-05			
380.5	371	2863	168	5.03	9.33E-06	3.06E-05	-1.20E-05			
381.5	372	2870	165	5.27	5.37E-06	2.67E-05	-1.59E-05			
382.5	373	2878	161	4.63	2.34E-05	4.47E-05	2.14E-06			Yes
383.5	374	2886	157	4.68	2.09E-05	4.22E-05	-4.07E-07			Yes
384.5	375	2893	153	4.78	1.66E-05	3.79E-05	-4.70E-06			
385.5	376	2901	150	4.73	1.86E-05	3.99E-05	-2.68E-06			Yes
386.5	377	2909	146	4.74	1.82E-05	3.95E-05	-3.10E-06			
387.5	378	2916	142	4.74	1.82E-05	3.95E-05	-3.10E-06			
388.5	378.7	2922	139	4.91	1.23E-05	3.36E-05	-9.00E-06			

Centered tube depth (cm)	Tephra-free depth (cm)	Centered age (years before 2006)	1/2 95% confidence interval	pH[a]	[H+][a]	Upper error [H+]	Lower error [H+]	Lake Acidification cutoff criteria[b]		
								Highly Likely	Likely	Possible
389.5	379.7	2930	136	4.75	1.78E-05	3.91E-05	-3.52E-06			
390.5	380.7	2937	132	4.77	1.70E-05	3.83E-05	-4.32E-06			
391.5	381.7	2945	128	4.74	1.82E-05	3.95E-05	-3.10E-06			
392.5	382.7	2953	125	4.64	2.29E-05	4.42E-05	1.61E-06			Yes
402.5	392.7	3031	97	3.99	1.02E-04	1.24E-04	8.10E-05	Yes	Yes	Yes
403.5	393.7	3039	101	3.93	1.17E-04	1.39E-04	9.62E-05	Yes	Yes	Yes
404.5	394.7	3047	104	3.95	1.12E-04	1.34E-04	9.09E-05	Yes	Yes	Yes
405.5	395.7	3055	107	3.89	1.29E-04	1.50E-04	1.08E-04	Yes	Yes	Yes
406.5	396.7	3063	111	4.09	8.13E-05	1.03E-04	6.00E-05	Yes	Yes	Yes
407.5	397.7	3071	115	4.55	2.82E-05	4.95E-05	6.88E-06			Yes
408.5	398.7	3079	118	4.27	5.37E-05	7.50E-05	3.24E-05		Yes	Yes
409.5	399.7	3087	122	4.26	5.50E-05	7.63E-05	3.37E-05		Yes	Yes
410.5	400.7	3095	126	4.57	2.69E-05	4.82E-05	5.62E-06			Yes
411.5	401.7	3103	129	4.02	9.55E-05	1.17E-04	7.42E-05	Yes	Yes	Yes
412.5	402.7	3111	133	4.02	9.55E-05	1.17E-04	7.42E-05	Yes	Yes	Yes
413.5	403.7	3119	137	4.31	4.90E-05	7.03E-05	2.77E-05		Yes	Yes
414.5	404.7	3127	140	4.16	6.92E-05	9.05E-05	4.79E-05	Yes	Yes	Yes
415.5	405.7	3135	143	4.42	3.80E-05	5.93E-05	1.67E-05			Yes
416.5	406.7	3143	147	4.43	3.72E-05	5.85E-05	1.59E-05			Yes
417.5	407.7	3151	151	4.49	3.24E-05	5.37E-05	1.11E-05			Yes
418.5	408.7	3160	154	4.35	4.47E-05	6.60E-05	2.34E-05		Yes	Yes
419.5	409.7	3168	158	4.33	4.68E-05	6.81E-05	2.55E-05		Yes	Yes
420.5	410.7	3176	162	4.26	5.50E-05	7.63E-05	3.37E-05		Yes	Yes
421.5	411.7	3184	165	4.35	4.47E-05	6.60E-05	2.34E-05		Yes	Yes
422.5	412.1	3187	167	4.51	3.09E-05	5.22E-05	9.60E-06			Yes
423.5	413.1	3195	170	4.46	3.47E-05	5.60E-05	1.34E-05			Yes
424.5	414.1	3204	174	4.69	2.04E-05	4.17E-05	-8.83E-07			Yes
425.5	415.1	3212	178	4.69	2.04E-05	4.17E-05	-8.83E-07			Yes
426.5	415.7	3217	180	4.71	1.95E-05	4.08E-05	-1.80E-06			Yes
427.5	416.5	3223	183	4.67	2.14E-05	4.27E-05	7.96E-08			Yes

Centered tube depth (cm)	Tephra-free depth (cm)	Centered age (years before 2006)	1/2 95% confidence interval	pH[a]	[H+][a]	Upper error [H+]	Lower error [H+]	Lake Acidification cutoff criteria[b]		
								Highly Likely	Likely	Possible
428.5	417.5	3231	186	4.23	5.89E-05	8.02E-05	3.76E-05		Yes	Yes
430.5	419.5	3248	193	4.08	8.32E-05	1.04E-04	6.19E-05	Yes	Yes	Yes
431.5	420.5	3256	197	4.66	2.19E-05	4.32E-05	5.78E-07			Yes
432.5	421.5	3264	200	4.53	2.95E-05	5.08E-05	8.21E-06			Yes
433.5	422.5	3273	204	4.94	1.15E-05	3.28E-05	-9.82E-06			
434.5	423.5	3281	208	4.45	3.55E-05	5.68E-05	1.42E-05			Yes
435.5	424.5	3289	211	4.42	3.80E-05	5.93E-05	1.67E-05			Yes
436.5	425.5	3297	215	4.92	1.20E-05	3.33E-05	-9.28E-06			
437.5	426.5	3306	219	4.86	1.38E-05	3.51E-05	-7.50E-06			
438.5	427.5	3314	222	4.68	2.09E-05	4.22E-05	-4.07E-07			Yes
439.5	428.5	3322	226	4.67	2.14E-05	4.27E-05	7.96E-08			Yes
440.5	429.5	3330	229	4.83	1.48E-05	3.61E-05	-6.51E-06			
441.5	430.5	3339	233	4.79	1.62E-05	3.75E-05	-5.08E-06			
442.5	431.5	3347	237	4.75	1.78E-05	3.91E-05	-3.52E-06			
443.5	432.5	3355	240	4.65	2.24E-05	4.37E-05	1.09E-06			Yes
444.5	433.5	3364	244	4.94	1.15E-05	3.28E-05	-9.82E-06			
445.5	434.5	3372	248	4.60	2.51E-05	4.64E-05	3.82E-06			Yes
446.5	435.5	3380	251	4.57	2.69E-05	4.82E-05	5.62E-06			Yes
447.5	436.5	3389	255	4.42	3.80E-05	5.93E-05	1.67E-05			Yes
448.5	437.5	3397	258	4.38	4.17E-05	6.30E-05	2.04E-05		Yes	Yes
449.5	438.5	3405	262	4.66	2.19E-05	4.32E-05	5.78E-07			Yes
450.5	439.5	3414	265	4.67	2.14E-05	4.27E-05	7.96E-08			Yes
451.5	440.5	3422	269	4.86	1.38E-05	3.51E-05	-7.50E-06			
452.5	441.5	3431	273	4.66	2.19E-05	4.32E-05	5.78E-07			Yes
453.5	442.5	3439	276	4.51	3.09E-05	5.22E-05	9.60E-06			Yes
454.5	443.5	3447	280	4.61	2.45E-05	4.58E-05	3.25E-06			Yes
455.5	444.5	3456	284	4.56	2.75E-05	4.88E-05	6.24E-06			Yes
456.5	445.5	3464	287	4.61	2.45E-05	4.58E-05	3.25E-06			Yes
457.5	446.5	3473	291	4.64	2.29E-05	4.42E-05	1.61E-06			Yes
458.5	447.5	3481	294	4.85	1.41E-05	3.54E-05	-7.17E-06			

Centered tube depth (cm)	Tephra-free depth (cm)	Centered age (years before 2006)	1/2 95% confidence interval	pH[a]	[H+][a]	Upper error [H+]	Lower error [H+]	Lake Acidification cutoff criteria[b]		
								Highly Likely	Likely	Possible
459.5	448.5	3489	298	4.96	1.10E-05	3.23E-05	-1.03E-05			
460.5	449.5	3498	302	5.02	9.55E-06	3.08E-05	-1.18E-05			
461.5	450.5	3506	305	5.08	8.32E-06	2.96E-05	-1.30E-05			
462.5	451	3510	307	5.22	6.03E-06	2.73E-05	-1.53E-05			
463.5	451	3510	307	5.21	6.17E-06	2.75E-05	-1.51E-05			
464.5	451	3510	307	5.36	4.37E-06	2.57E-05	-1.69E-05			
465.5	451	3510	307	5.63	2.34E-06	2.36E-05	-1.90E-05			
466.5	451	3510	307	5.69	2.04E-06	2.33E-05	-1.93E-05			
467.5	451	3510	307	5.34	4.57E-06	2.59E-05	-1.67E-05			
468.5	451	3510	307	5.06	8.71E-06	3.00E-05	-1.26E-05			
469.5	451	3510	307	4.96	1.10E-05	3.23E-05	-1.03E-05			
470.5	451	3510	307	4.84	1.45E-05	3.58E-05	-6.85E-06			
471.5	451.9	3518	310	4.67	2.14E-05	4.27E-05	7.96E-08			Yes
472.5	452.9	3526	314	4.57	2.69E-05	4.82E-05	5.62E-06			Yes
473.5	453.9	3535	318	4.46	3.47E-05	5.60E-05	1.34E-05			Yes
474.5	454.9	3543	321	4.46	3.47E-05	5.60E-05	1.34E-05			Yes
475.5	455.9	3552	325	4.73	1.86E-05	3.99E-05	-2.68E-06			Yes
476.5	456.9	3560	329	4.92	1.20E-05	3.33E-05	-9.28E-06			
477.5	457.9	3569	332	4.80	1.58E-05	3.71E-05	-5.45E-06			
478.5	458.9	3577	336	4.65	2.24E-05	4.37E-05	1.09E-06			Yes
479.5	459.9	3585	339	4.91	1.23E-05	3.36E-05	-9.00E-06			
480.5	460.9	3594	343	4.76	1.74E-05	3.87E-05	-3.92E-06			
481.5	461.9	3602	347	4.54	2.88E-05	5.01E-05	7.54E-06			Yes
482.5	462.9	3611	349	4.90	1.26E-05	3.39E-05	-8.71E-06			
483.5	463.9	3619	349	4.95	1.12E-05	3.25E-05	-1.01E-05			
484.5	464.9	3628	349	4.69	2.04E-05	4.17E-05	-8.83E-07			Yes
485.5	465.9	3636	349	4.62	2.40E-05	4.53E-05	2.69E-06			Yes
486.5	466.9	3645	349	4.71	1.95E-05	4.08E-05	-1.80E-06			Yes
487.5	467.9	3653	349	4.52	3.02E-05	5.15E-05	8.90E-06			Yes
488.5	468.9	3661	349	5.12	7.59E-06	2.89E-05	-1.37E-05			

Centered tube depth (cm)	Tephra-free depth (cm)	Centered age (years before 2006)	1/2 95% confidence interval	pH[a]	[H+][a]	Upper error [H^+]	Lower error [H^+]	Lake Acidification cutoff criteria[b]		
								Highly Likely	Likely	Possible
489.5	469.9	3670	349	4.44	3.63E-05	5.76E-05	1.50E-05			Yes
490.5	470.9	3678	349	4.77	1.70E-05	3.83E-05	-4.32E-06			
491.5	471.9	3687	349	5.09	8.13E-06	2.94E-05	-1.32E-05			
492.5	472.9	3695	349	5.04	9.12E-06	3.04E-05	-1.22E-05			
493.5	473.9	3704	349	4.85	1.41E-05	3.54E-05	-7.17E-06			
494.5	474.9	3712	349	4.39	4.07E-05	6.20E-05	1.94E-05		Yes	Yes
495.5	475.9	3721	349	4.73	1.86E-05	3.99E-05	-2.68E-06			Yes
496.5	476.9	3729	349	5.33	4.68E-06	2.60E-05	-1.66E-05			
497.5	477.9	3737	349	4.82	1.51E-05	3.64E-05	-6.16E-06			
498.5	478.7	3744	349	5.07	8.51E-06	2.98E-05	-1.28E-05			
499.5	479.7	3753	349	4.84	1.45E-05	3.58E-05	-6.85E-06			
500.5	480.7	3761	349	5.56	2.75E-06	2.41E-05	-1.85E-05			
501.5	481.7	3770	349	5.31	4.90E-06	2.62E-05	-1.64E-05			
502.5	482.7	3778	349	4.96	1.10E-05	3.23E-05	-1.03E-05			
503.5	483.7	3786	349	4.61	2.45E-05	4.58E-05	3.25E-06			Yes
504.5	484.7	3795	349	4.89	1.29E-05	3.42E-05	-8.42E-06			
505.5	485.7	3803	349	5.00	1.00E-05	3.13E-05	-1.13E-05			
506.5	486.7	3812	349	4.63	2.34E-05	4.47E-05	2.14E-06			Yes

[a]Sediment slurry pH (and thus calculated [H+]) were in a slurry of equal parts wet sediment and distilled deionized water.
[b]Inferred from slurry [H^+] values according to "Highly likely," "Likely," and "Possible" criteria ([H^+] greater than 0.0000609, 0.0000398, or 0.0000187, respectively)

Table 13. Values used to estimate residence time of Mother Goose Lake.

Total average annual rainfall in Port Heiden (cm)[a]:	39.4
Mother Goose Drainage area (km^2)[b]:	406
Volume of precipitation (km^3/yr):	0.160
Volume of Mother Goose Lake (km^3)[b]:	0.429
Residence time of Mother Goose Lake (yr):	2.7
Years to be chemically refreshed (residence time x 6)[c]:	16.1

[a]Based on National Climatic Data Center data (http://www.ncdc.noaa.gov/oa/ncdc.html)
[b]Based on a triangular irregular network model of Mother Goose Lake created in ESRI^{R} ArcGIS^{TM}
[c]Based on Varekamp (2003)

Table 14. Number and timing of large hydrogeothermal discharge events based on the definitions of an acidification in Table 12.

Highly likely			Likely			Possible		
Initiation (years before 2006)	Duration (yr)	Associated tephras (number)	Initiation (years before 2006)	Duration (yr)	Associated tephras (number)	Initiation (years before 2006)	Duration (yr)	Associated tephras (number)
3	2		3	2		3	2	
1014	1	1	1014	11	1	1014	11	1
2743	1		1084	1		1084	1	
3063	32		1716	1		1437	1	
3111	8		2751	22		1721	6	
3127	1		3063	32		2389	40	2
3248	1		3087	8		2428	1	
			3127	24	1	2473	1	1
			3184	24		2539	1	
			3248	16	1	2628	28	
			3397	1		2685	22	
			3712	1	1	2751	22	
						2840	1	
						2901	23	
						3264	311	4
						3289	8	
						3322	8	
						3355	1	
						3414	42	1
						3473	42	
						3552	34	1
						3577	1	
						3602	1	
						3653	25	
						3670	1	
						3721	8	1
						3786	1	
						3812	1	

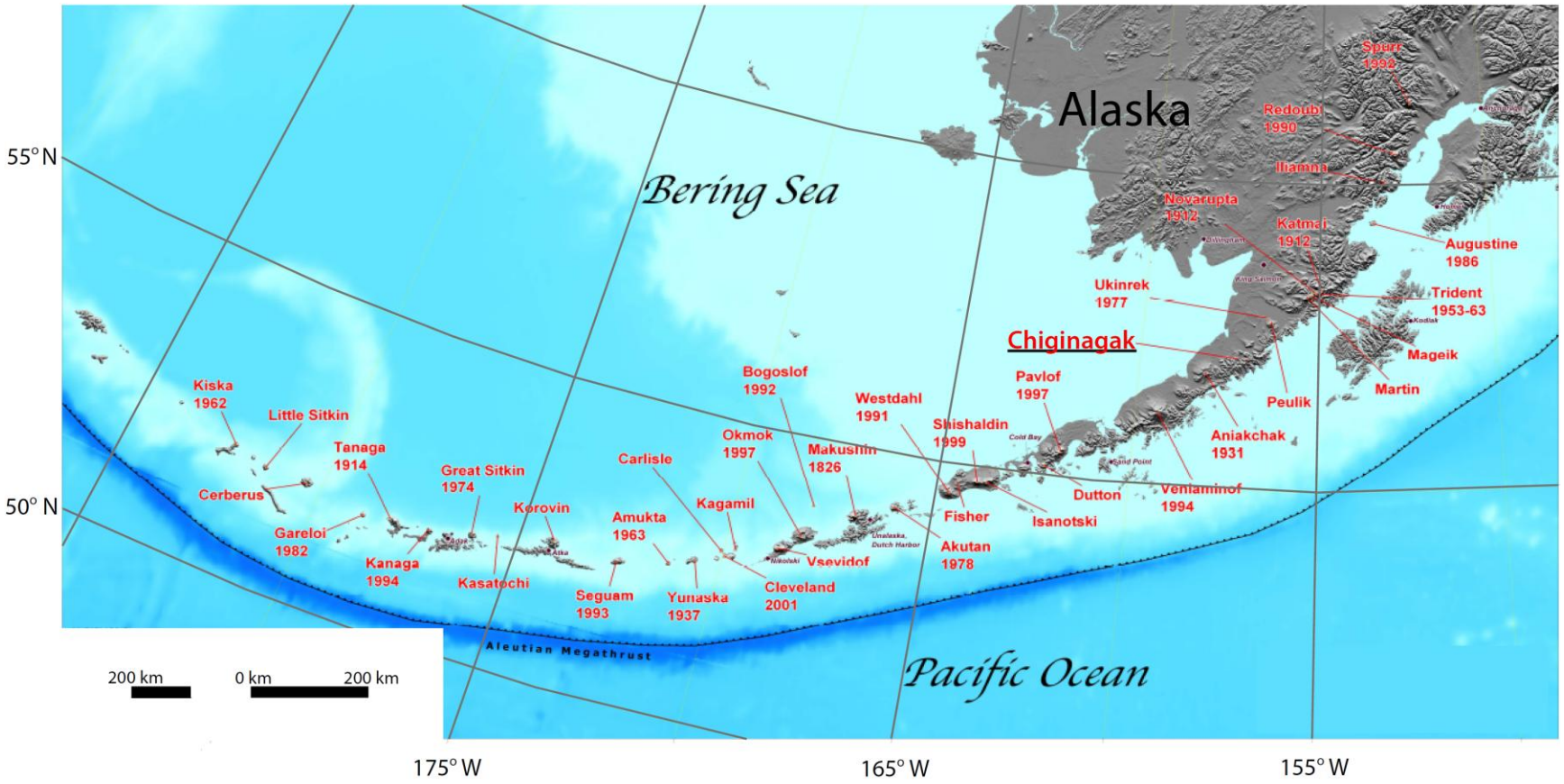

Figure 1. Historically active volcanoes of the Aleutian Arc. Most recent eruption is listed when known. Modified from Schaefer and Nye (2000).

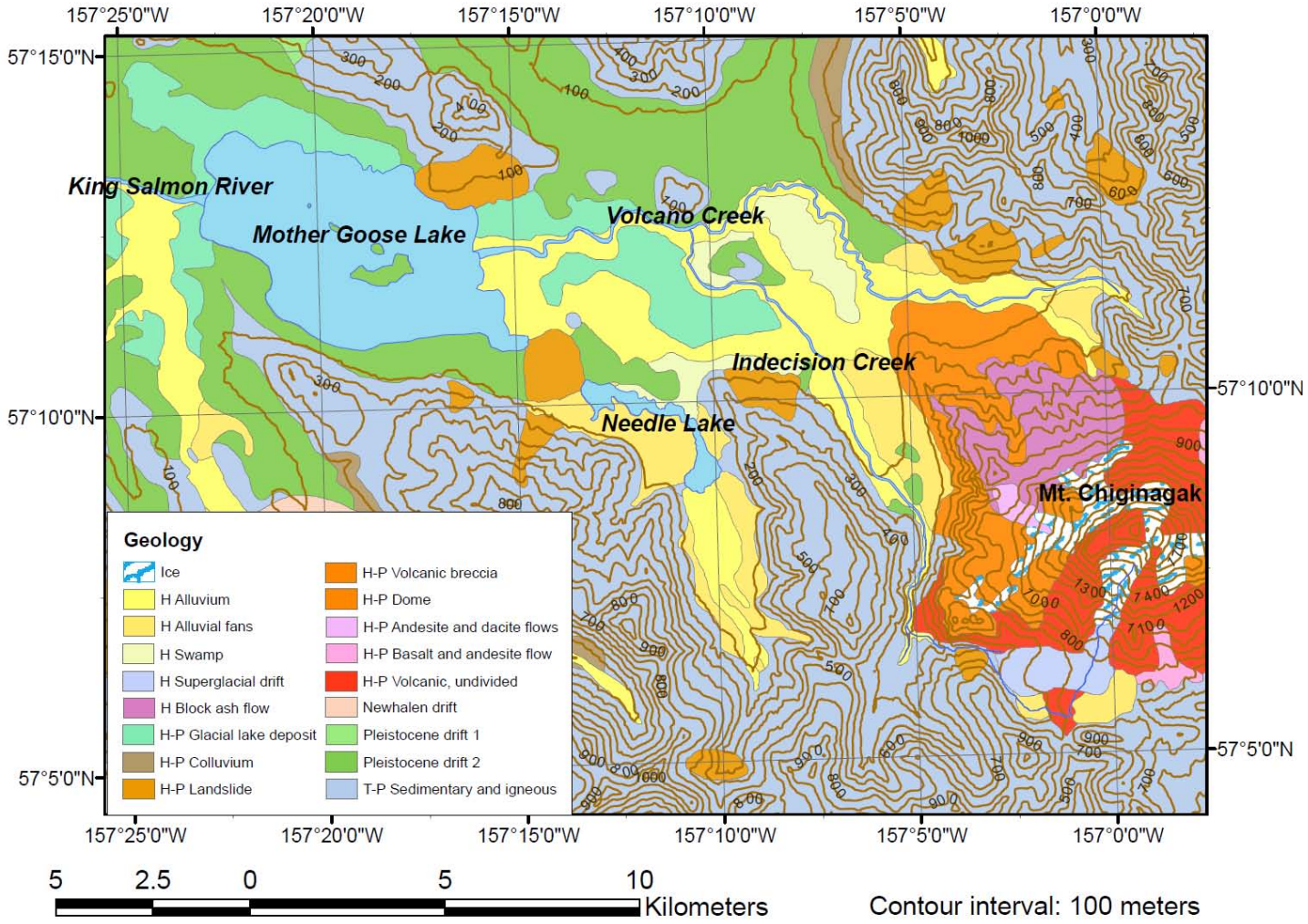

Figure 2. Surficial geology map of Mother Goose Lake's drainage area with major rivers and creeks. Rivers and creeks that do not drain into or out of Mother Goose Lake have been omitted for clarity. "T-P" denotes Tertiary to Permian, "H" Holocene, and "P" Pleistocene. After Detterman et al., (1987).

Figure 3. Photograph of Mt. Chiginagak's crater lake in August 2006. The 2005 event drained through the outlet channel outlined by the black box. The channel flowes through the summit glacer, which fills a notch in the crater rim. This configuration allows the lake to drain catestrophically once the glacier in the notch is melted through. Photo credit: McGimsey, Game; Alaska Volcano Observatory/U.S. Geological Survey.

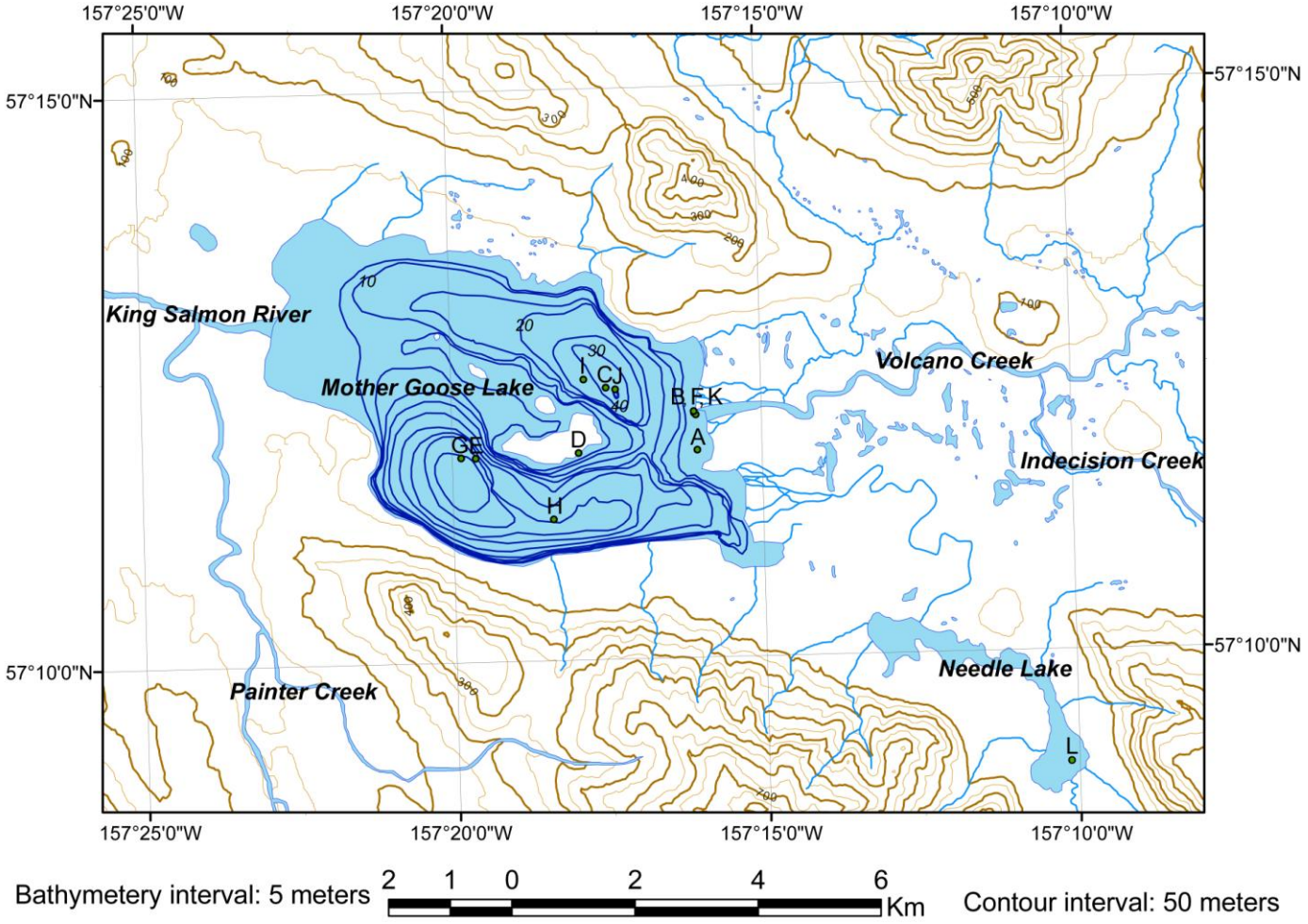

Figure 4. Water sample sites from the summer of 2007. Sample sites are described in Table 3.

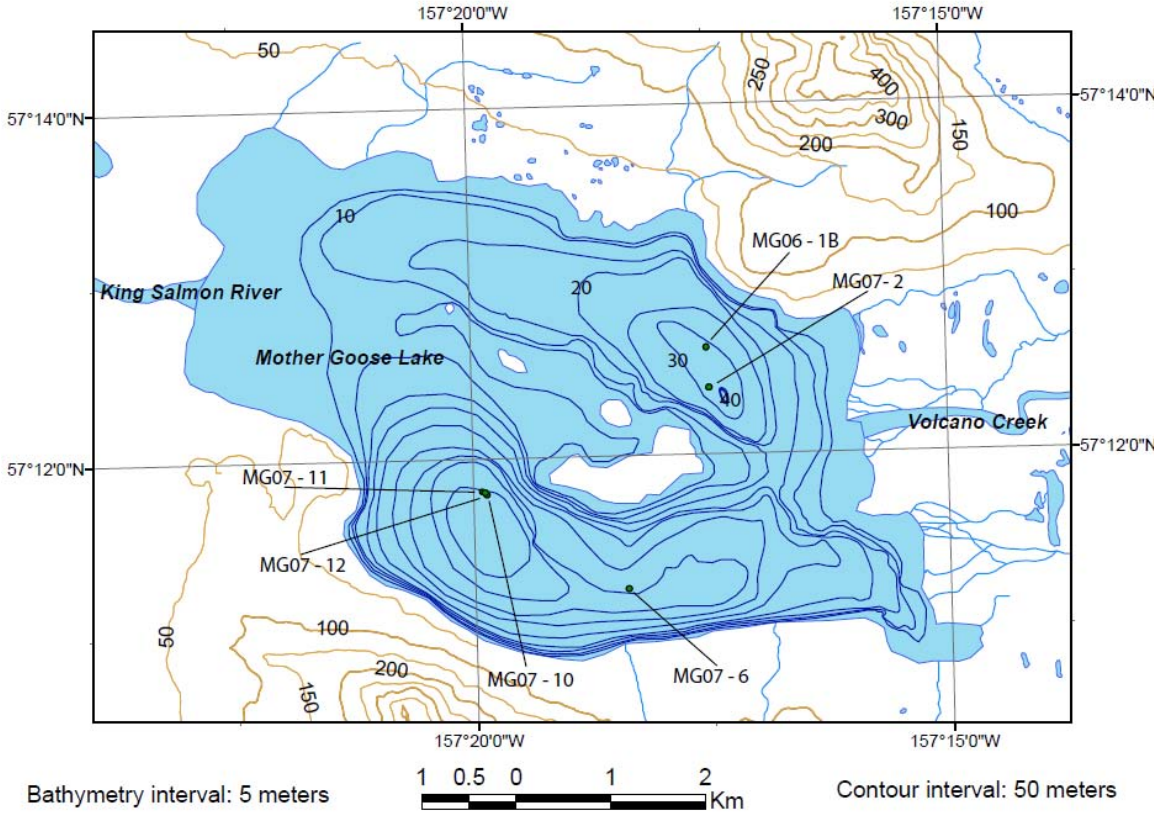

Figure 5. Locations of the core sites in Mother Goose Lake.

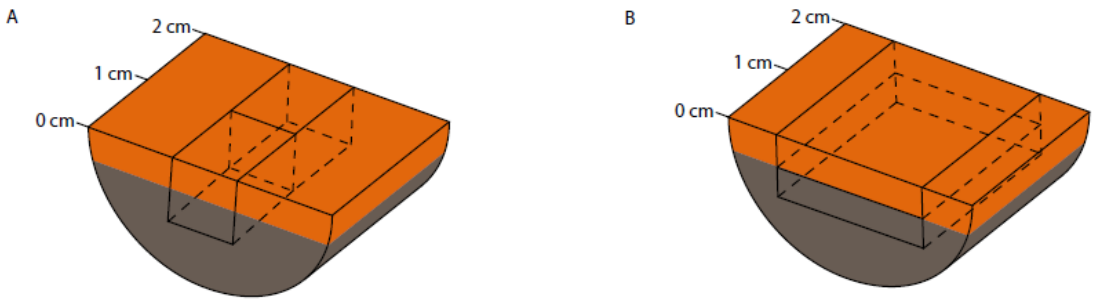

Figure 6. Illustration of the sampling scheme for (A) the main slurry pH data set and (B) the 100% oxidized (orange sediment) and reduced (grey sediment) subsamples (B). The difference between the oxidized and reduced sediment was used to determine the oxidation-state uncertainty using Equation 4.

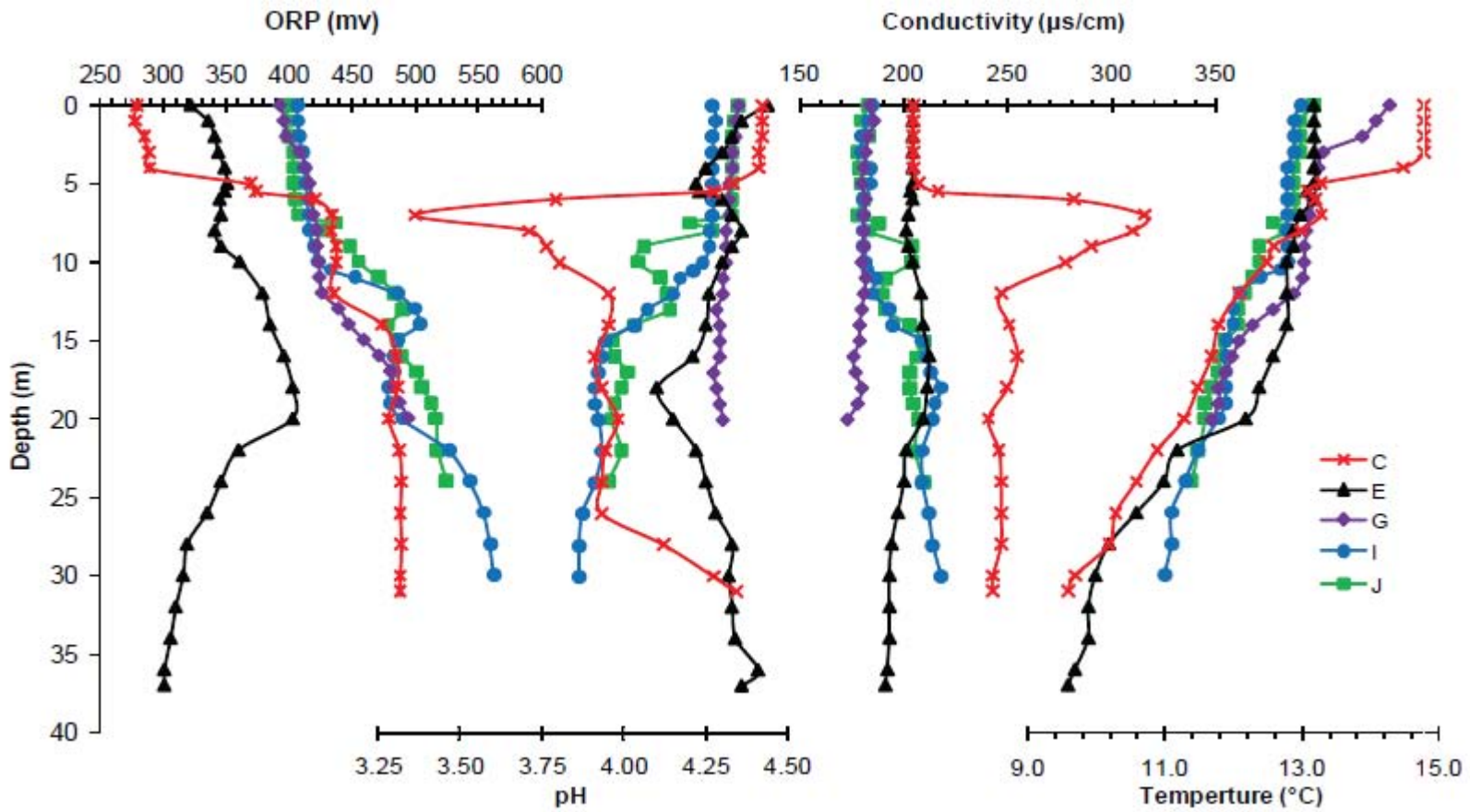

Figure 7**.** Physical and chemical profiles of Mother Goose Lake measured in 2007, including oxidation/reduction potential (ORP), pH, conductivity, and temperature. Letters indicate the site location (Figure 4). Site C had a reduced, acidic, saline, slightly cold interflow that was accompanied by pronounced sedimentation. The sedimentation was probably from flocculation of a species that entered the lake, reduced and acidified, and then neutralized and oxidized, consuming the oxygen in the overlying waters, and precipitating. Site J had a weaker interflow than site C when measured. The rest of the lake was fresh and well mixed, with only a slight thermocline in some areas.

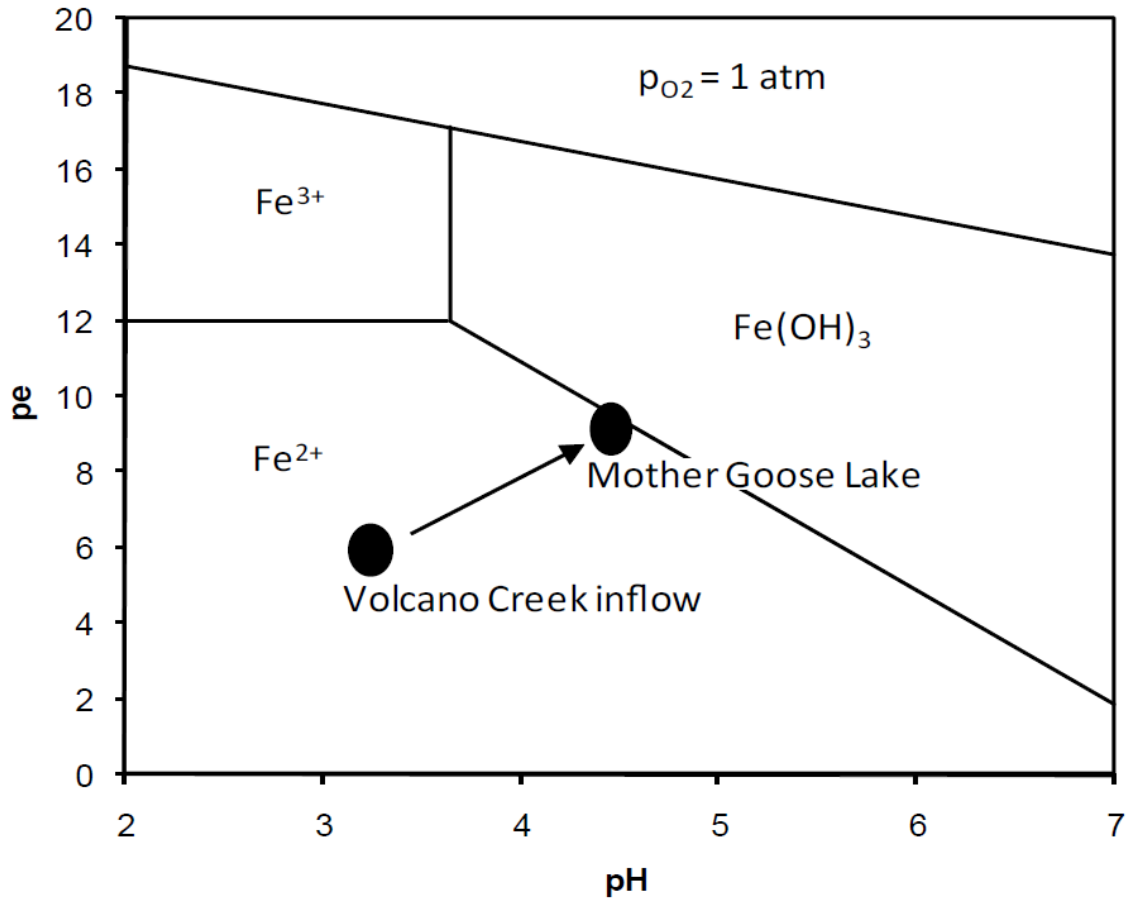

Figure 8. pe-pH diagram of the system O_2, H_2O, Fe^{2+}, Fe^{3+}, and $Fe(OH)_3$ at standard conditions for iron concentrations in Mother Goose Lake. The approximate pH and pe values for Volcano Creek where it enters Mother Goose Lake, and Mother Goose Lake are shown. As water enters Mother Goose Lake, ferrihydrite ($Fe(OH)_3$) should start to precipitate.

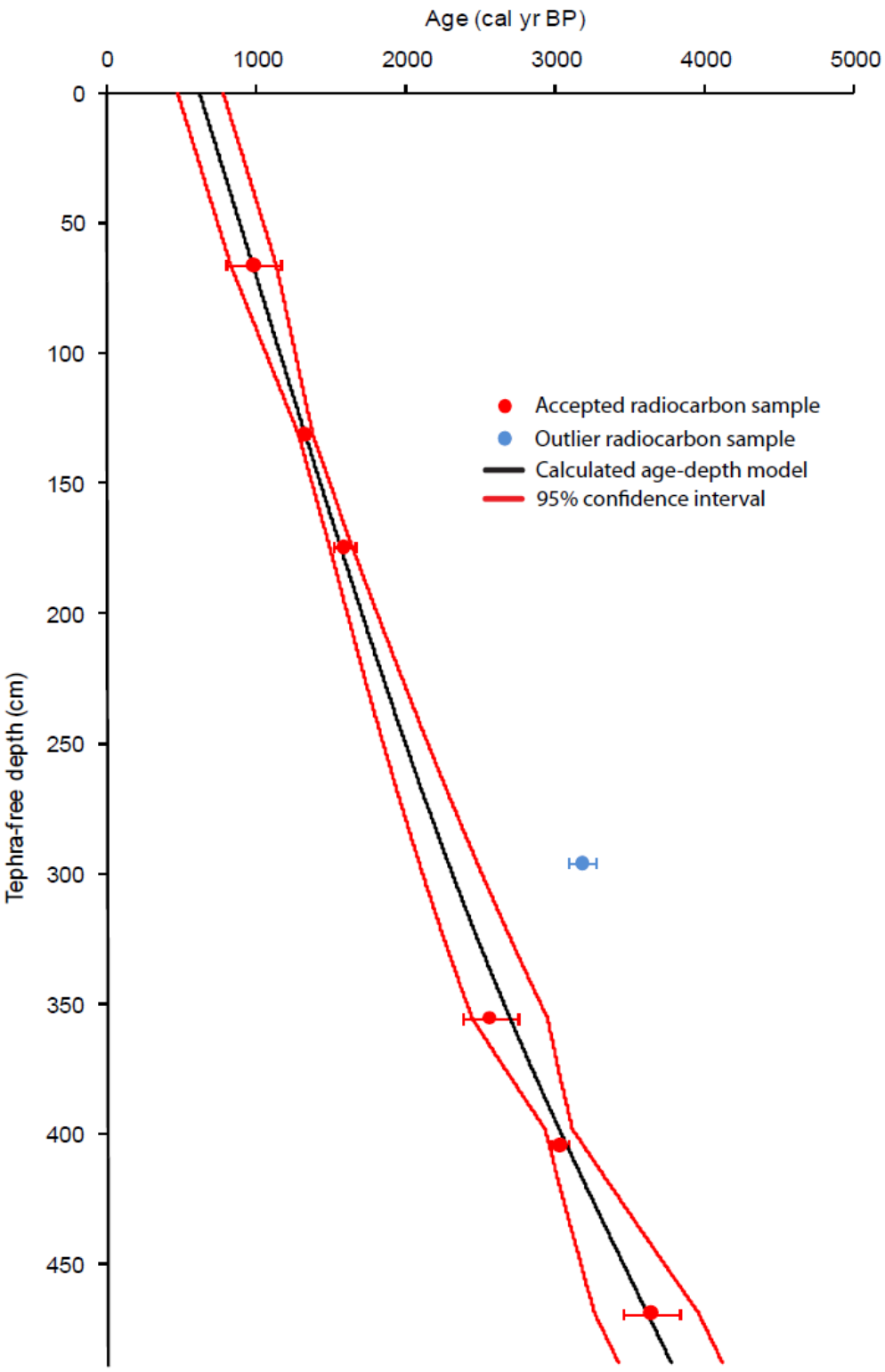

Figure 9. Age-depth model for core MG07-6 calculated according to the procedure of Heegaard et al. (2005) with a k of 5. Error bars are the two-sigma range. Gaps in cores from lost sediment were included in the depth. Data in Tables 2 and 12.

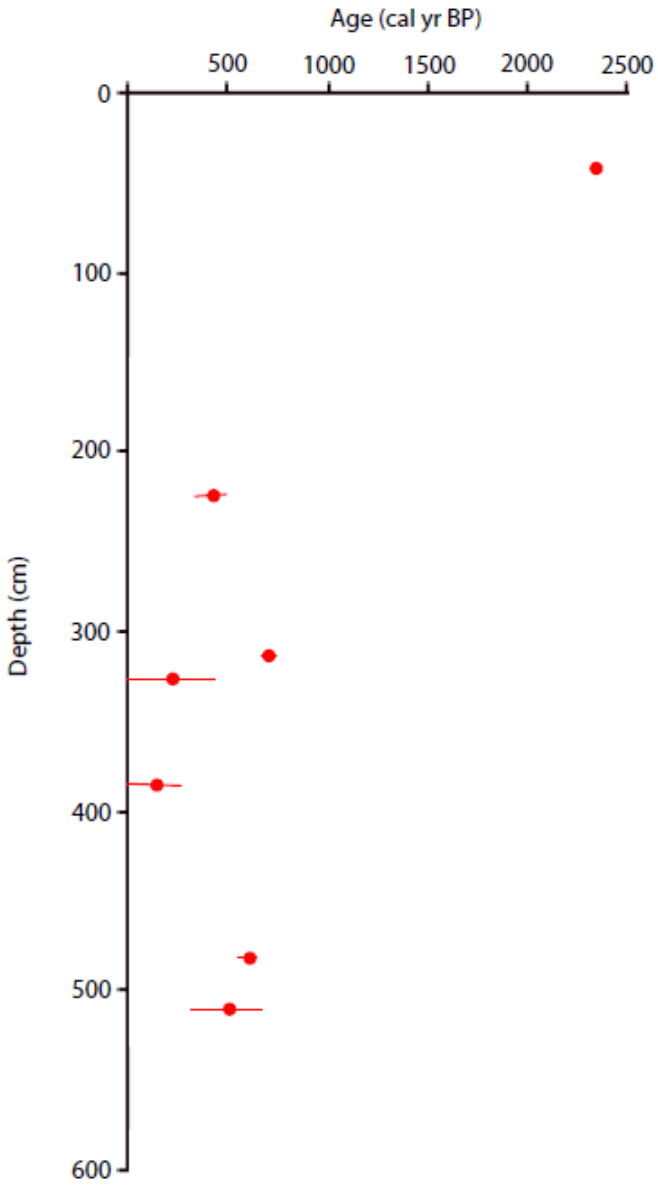

Figure 10. Age-depth relationship for core MG07-2. The ages overlap and most are stratagraphically reversed. Error bars are the two-sigma range. Data in Table 2.

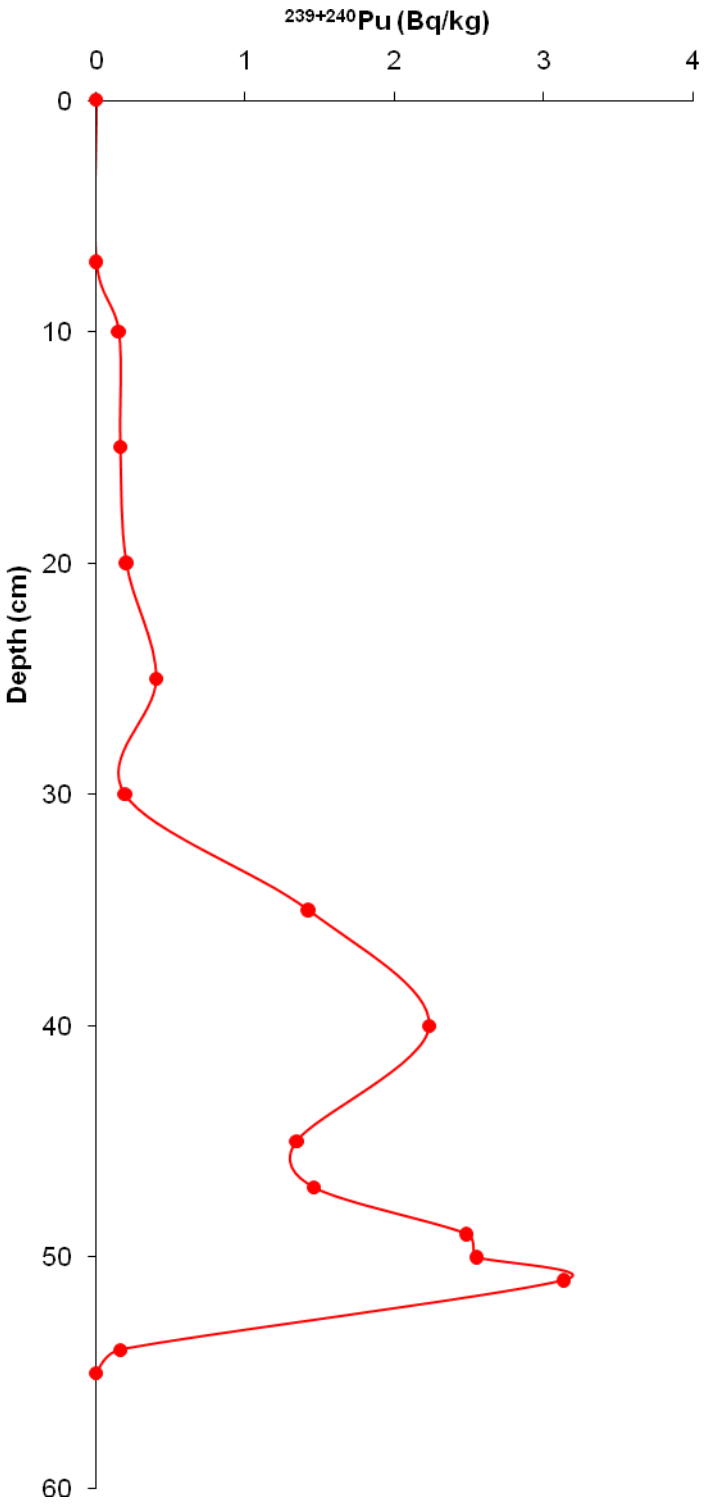

Figure 11. $^{239+240}$Pu activities in MG06-1B. The peak [Pu] corresponds to 1963/1964. Data in Table 4.

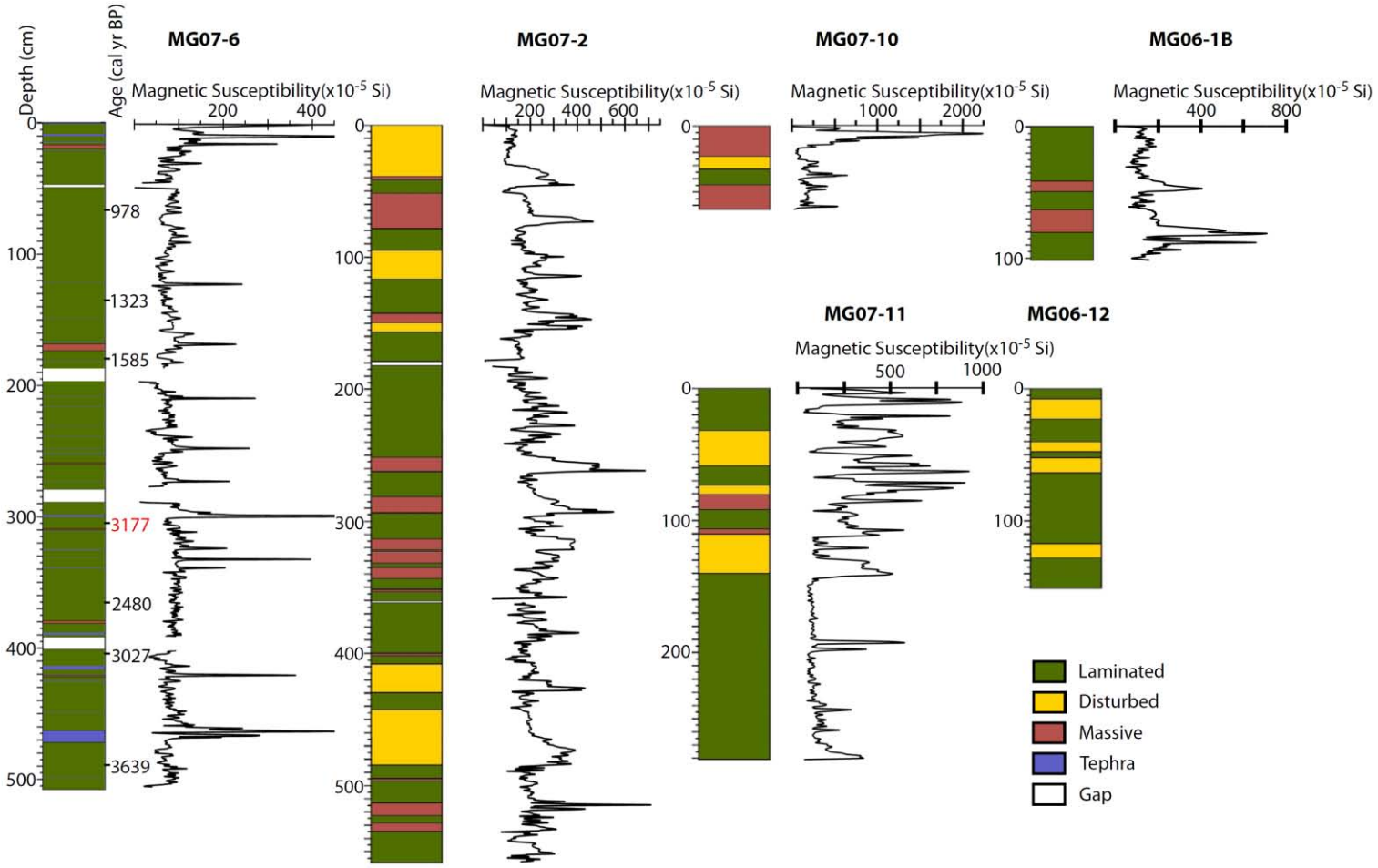

Figure 12. Major sediment properties and magnetic susceptibility measurements of all analyzed cores. Radiocarbon ages are listed to the right of MG07-6; the red age is an outlier excluded from the age model. „A' and 'B' tephras are indicated in MG07-6 by blue (Table 6). Cores MG07-6 and MG06-1B exhibit little evidence of post-depositional modification and are the focus of this study. All other cores contain a significant proportion of disturbed sediment. Massive layers could be disturbed. MS data in Appendix 1.

Figure 13. Example of disturbed sediment from core MG07-11. The contorted and broken bedding contacts indicate zones of disturbed sediment. The stratigraphy in this image is most disturbed in the top and middle sections, decreasing to mostly pronounced bowing of the sediment, from coring, near the base (white lines). Red lines are 1 cm apart.

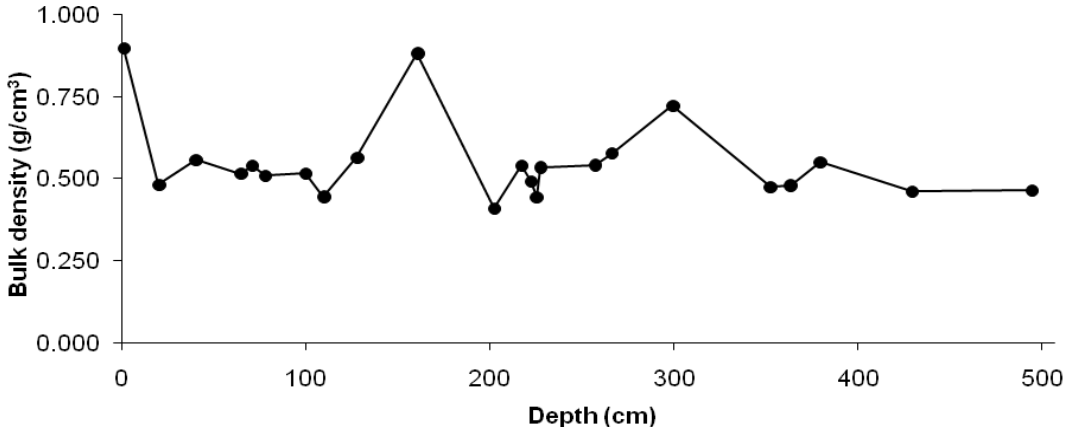

Figure 14. Bulk density by depth in MG07-6. Data in Table 7.

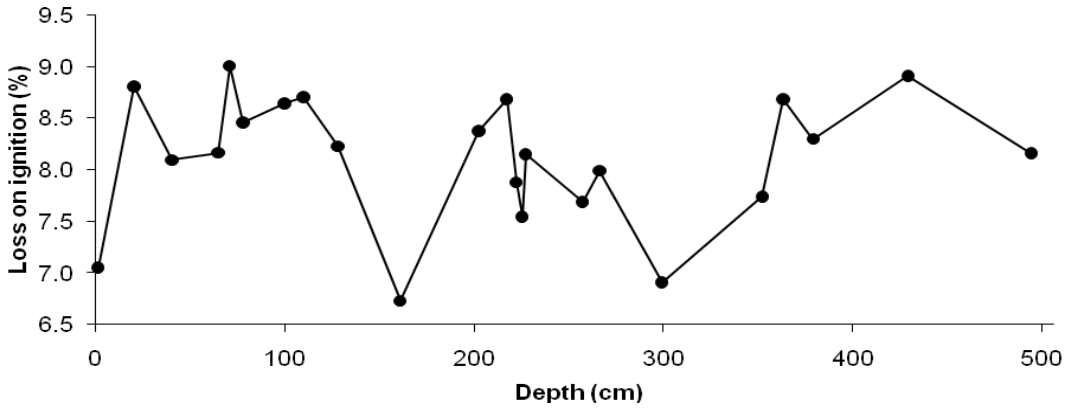

Figure 15. Loss on ignition by depth in MG07-6. Data in Table 7.

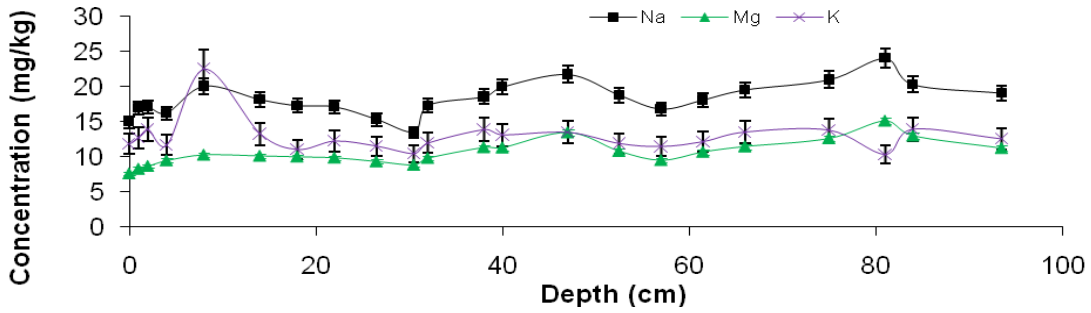

Figure 16. Base cations Na, Mg, and K by depth in core MG06-1B. All base cations exhibit a similar trend. The upper sample was deposited during acidified conditions. Error bars are the average error in measuring each element. Data in Table 8.

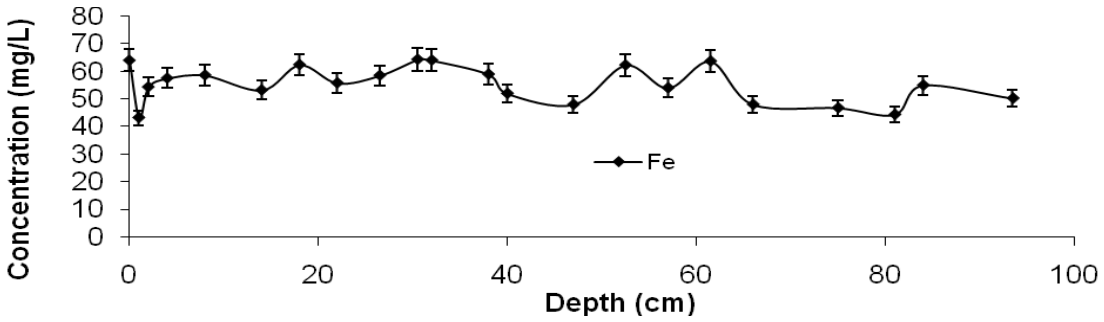

Figure 17. Acid cation (Fe) concentration by depth in MG06-1B. The upper sample was deposited during acidified conditions. Error bars are the average error in measuring Fe. Data in Table 8.

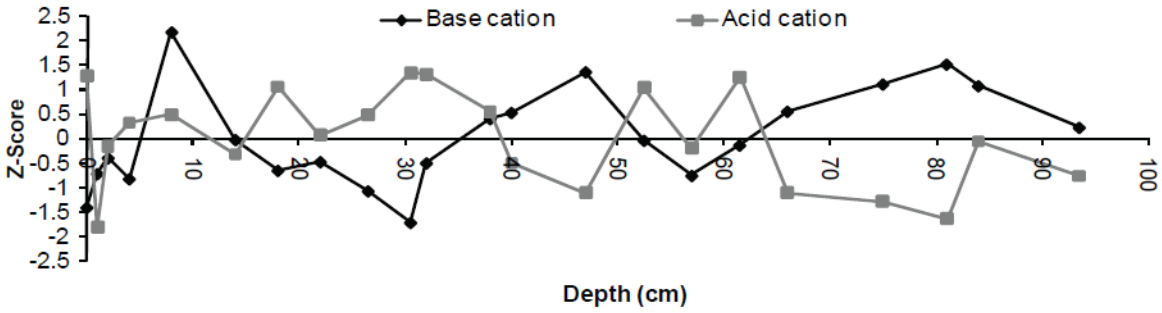

Figure 18. Plot of base cation (average of Na, Mg, and K) versus acid cation (Fe) Z-score by depth in MG06-1B. The Z-scores have an inverse relationship ($r^2 = 0.24$; $p = 0.02$; $n = 22$).

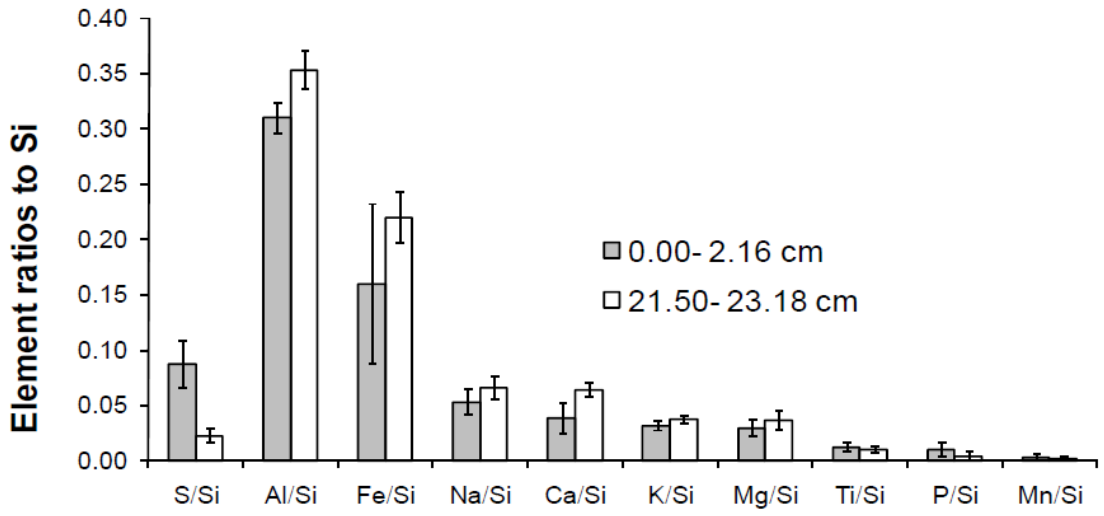

Figure 19. Average element ratios of the elements analyzed by EDS for MG06-1B. 0.00-2.16 cm was deposited during the 2005 acidification event; 21.50-23.18 cm was deposited during an acid-free period. Only S, Al and Ca do not overlap within one standard deviation between the upper and lower transects. Error bars are one standard deviation. Data in Table 10.

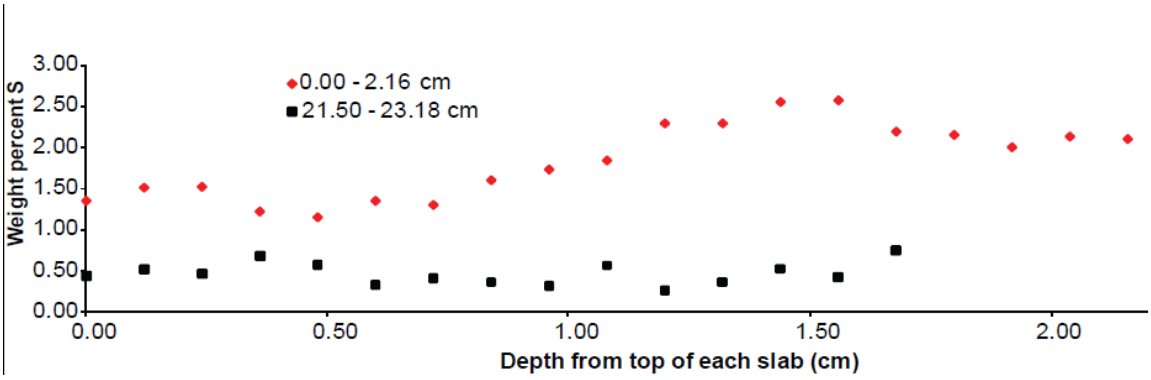

Figure 20. S concentration with distance from the top of each EDS transect from MG06-1B. S decreases toward the top of the upper slab, but remains higher than the lower slab. Data in Table 10.

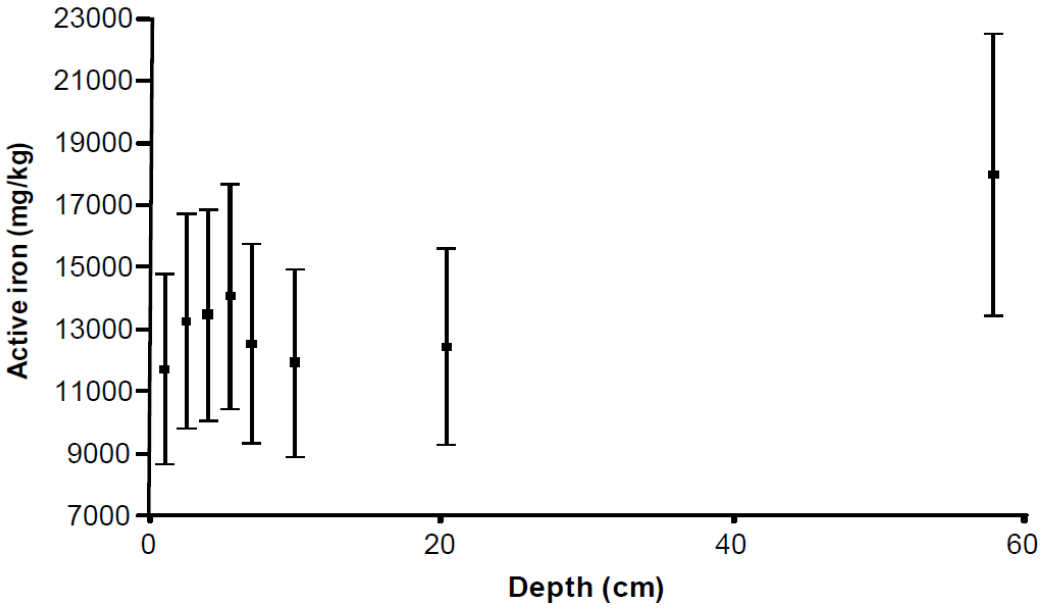

Figure 21. Active-iron concentration by depth in core MG06-1B. Error bars are one standard deviation of the three replicates for each depth plus 25% error in bulk density (There was not enough sediment to measure bulk density so the error in not incorporating bulk density, estimated at 25%, was incorporated into the error using the sum of the squares method). Data in Table 7.

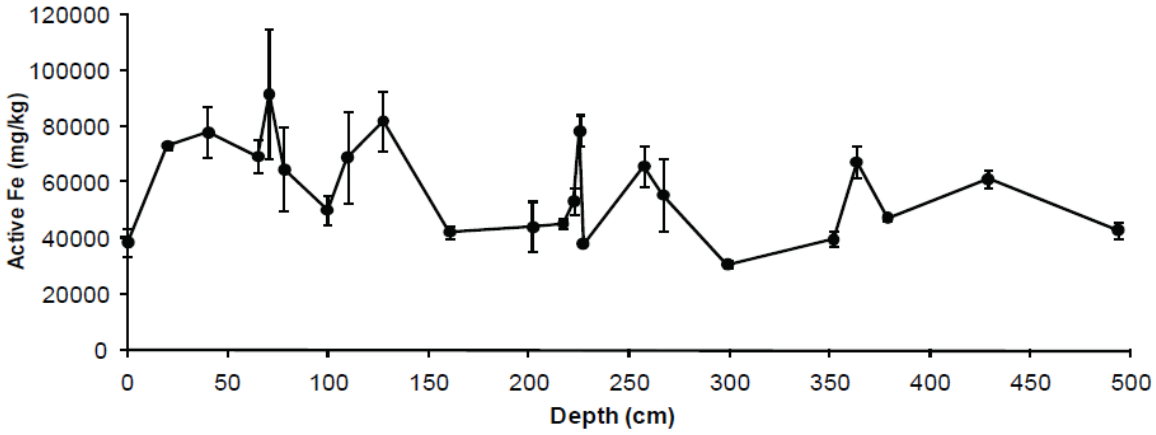

Figure 22. Active-iron concentration by depth in MG07-6. Error bars are one standard deviation of the three measurements averaged into each data point. Data in Table 7.

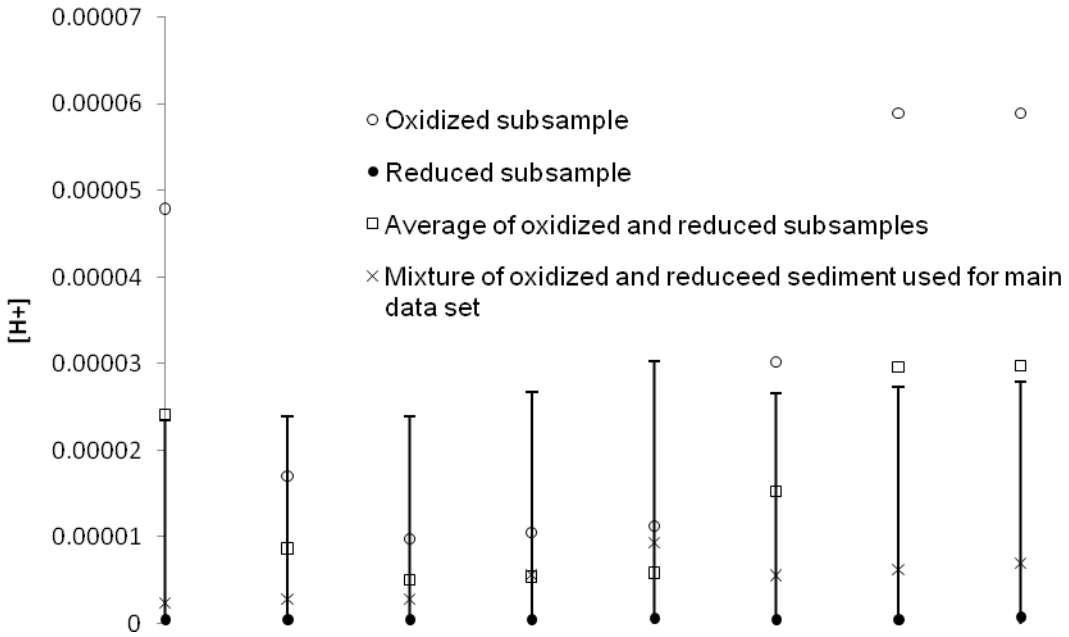

Figure 23. Comparison between slurry pH of oxidized and reduced subsamples from eight levels in core MG07-6. Also shown are the slurry pH values of samples taken as a mixture of the two and used for the primary data set. Error bars are the average absolute difference between the main data set pH values and the pH values of the average of the 100% oxidized and reduced samples plus one standard deviation. Most of the error is positive. Figure 6 illustrates the sampling scheme. Data in Table 11.

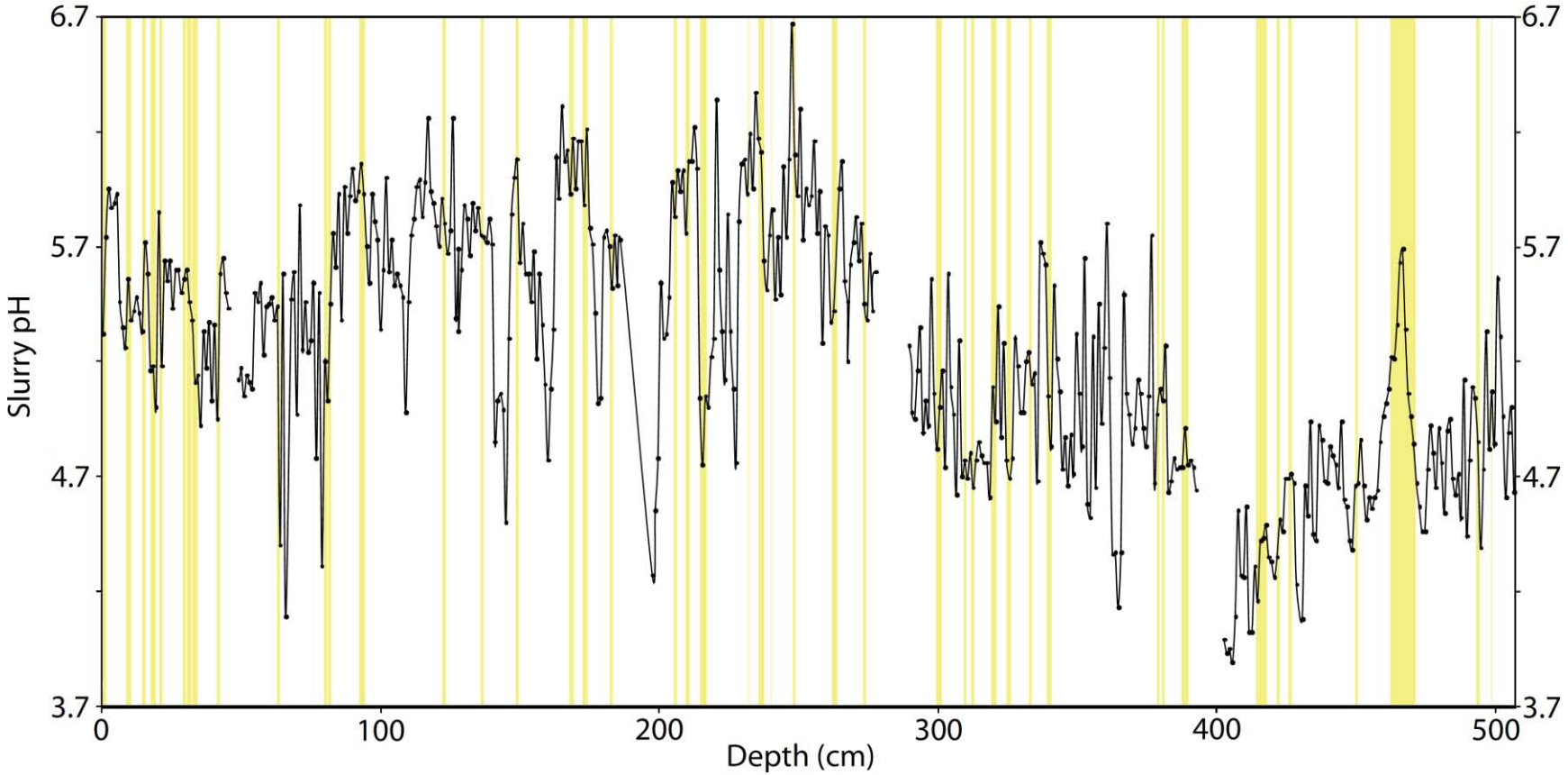

Figure 24. Slurry pH measurements on MG07-6 sediment by depth. Data in Table 11. Tephra (Table 6) are indicated by vertical yellow bars. The thickness of the bars are the thickness of the tephra. Most tephra coincide with decreased slurry pH values.

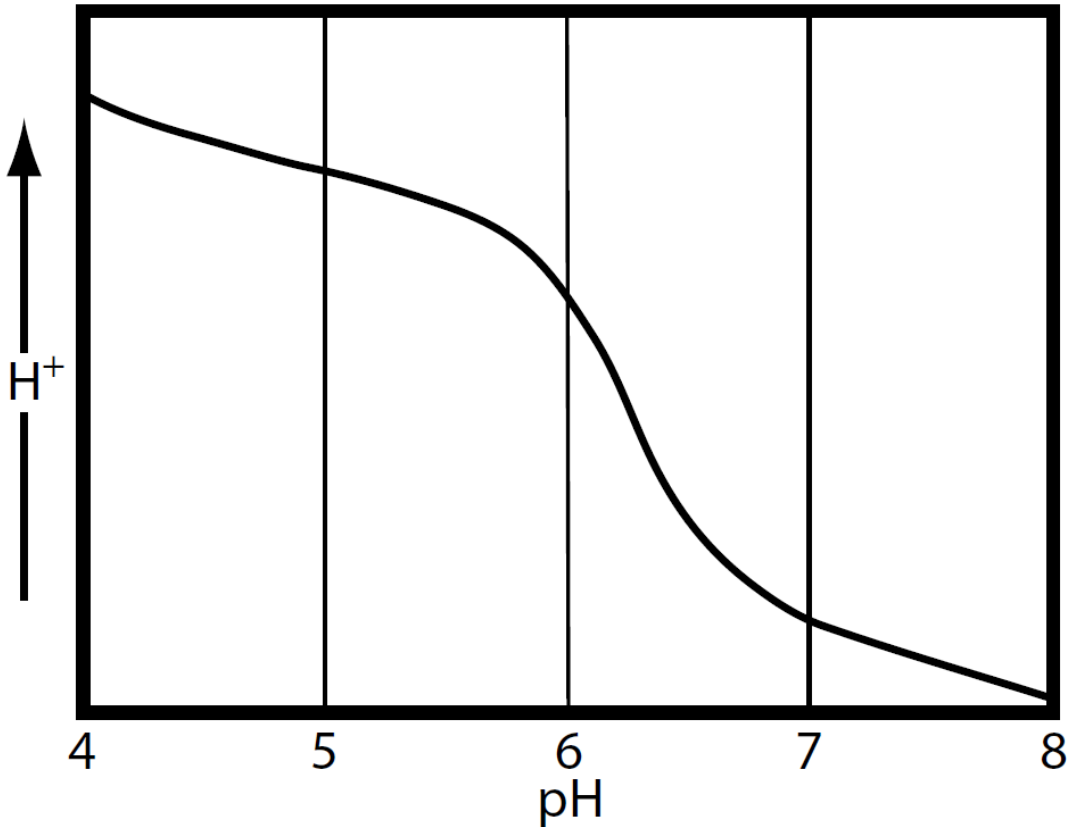

Figure 25. The effect of linear addition of an acid to a solution buffered by carbonate and bicarbonate starting at pH 8. The effect of bicarbonate buffering is centered around pH 5 and ends at pH 4.4. After Stumm and Morgan (1996).

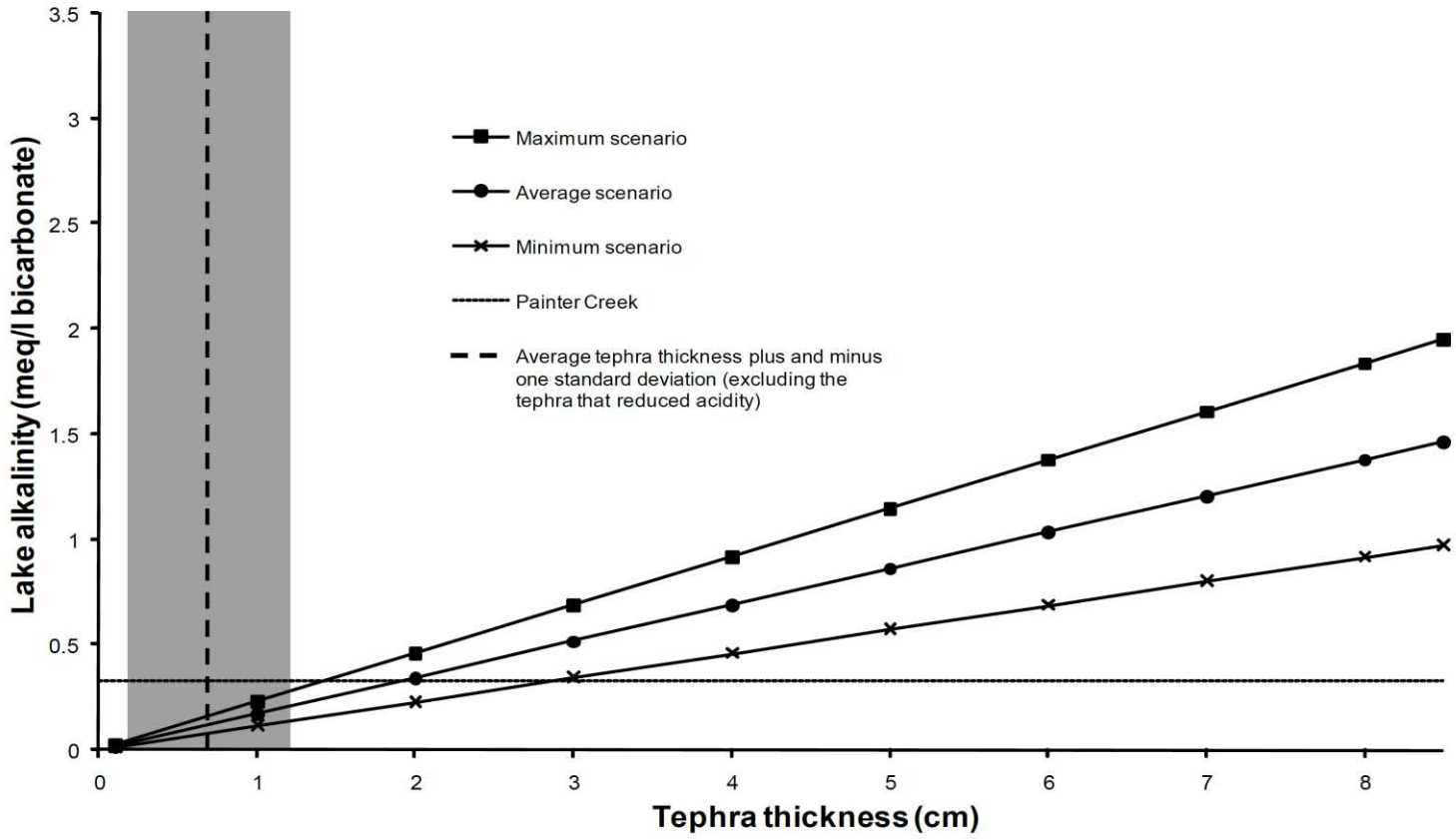

Figure 26. Amount of bicarbonate needed to buffer the maximum possible flux of H^+ from pure palagonitized glass of various thicknesses. The thickest tephra in core MG07-6 (besides the one that reduced acidity) is 1.5 cm thick. The bicarbonate-buffering capacity of Painter Creek is sufficient to almost buffer the maximum modeled input of H^+ (highest density, largest cation-exchange capacity, minimum volume estimate for Mother Goose Lake), while the buffering capacity is enough to neutralize the average and minimum models. The true buffering capacity of Mother Goose Lake is probably somewhere between Chiginagak hot springs (>3.5 meq/l) and Painter Creek, making it unlikely that any tephra in MG07-6 could have overcome the bicarbonate buffering of the lake, by itself.

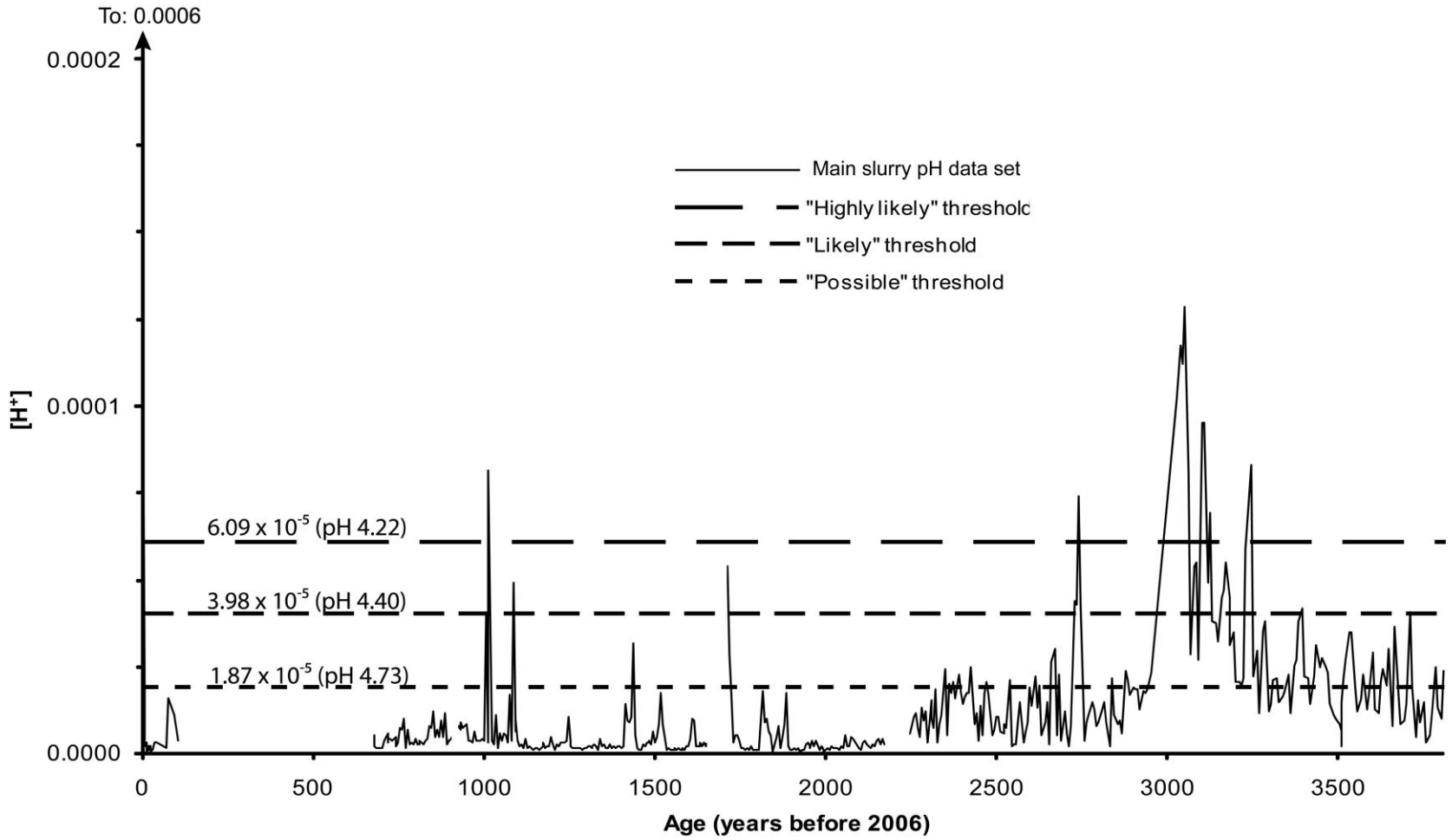

Figure 27. Slurry [H^+] by age (in years before 2006). The 2005 event is the most acidic in the record. Data in Table 12.

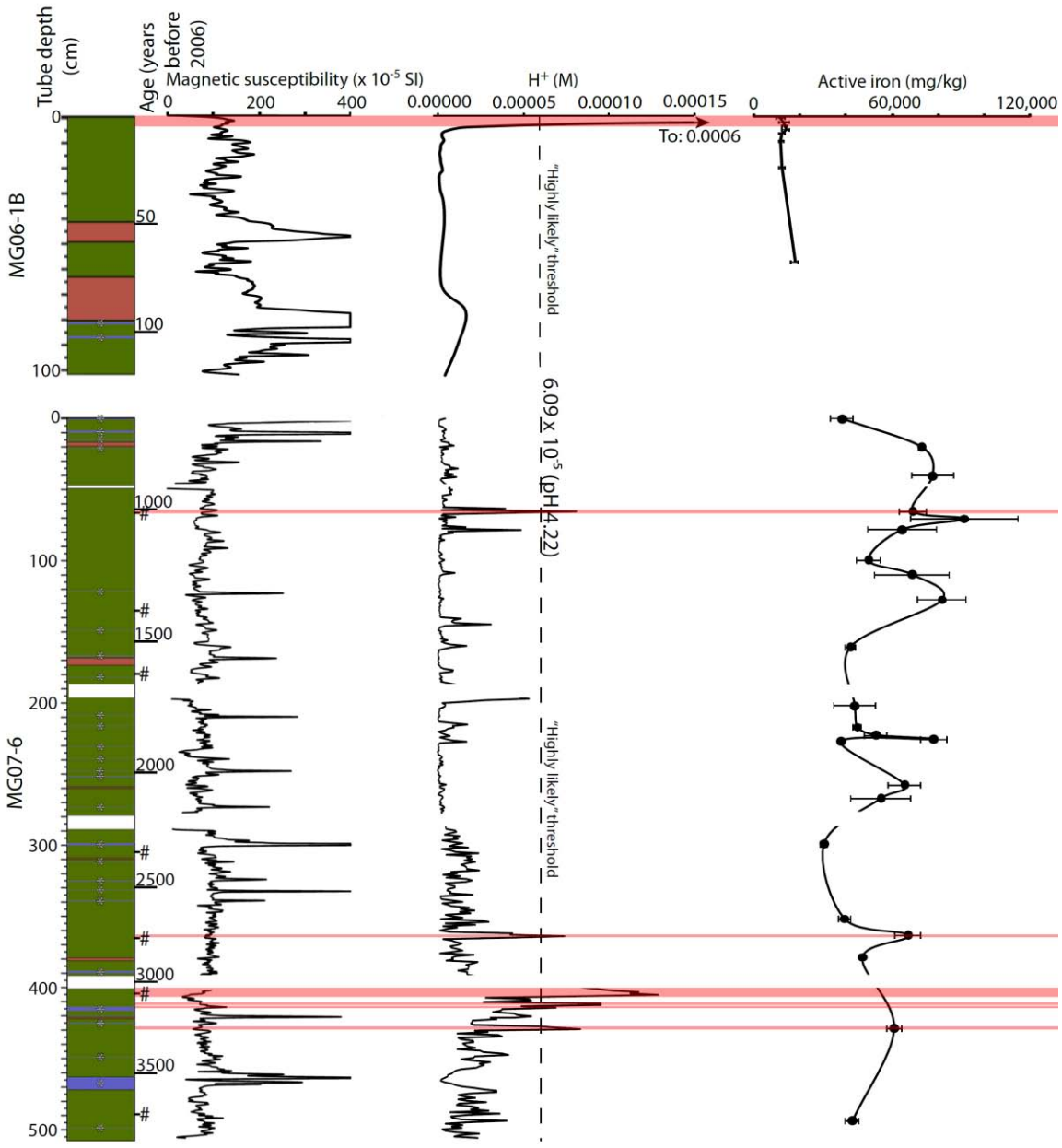

Figure 28. Summary of stratigraphy, age, magnetic susceptibility, main slurry [H^+] data set, and active iron in cores MG06-1B and MG07-6. In the stratgraphic columns, green denotes laminated sediment, red denotes massive sediment, white denotes gaps, and blue denotes tephra in MG07-6. Many tephra are very thin and are difficult to discern at this scale and are indicated by black and white asterisks. Pink horizontal bars denote "Highly likely" geothermal